Alma Mater Studiorum – Università di Bologna

PhD program in **Cellular Molecular and Industrial Biology**
Program n°1: **Cell Biology and Physiology**

XXIII cycle-Scientific area code **BIO/18 Genetics**

Roles of Ecdysone signaling in cell survival and epithelium morphogenesis during *Drosophila melanogaster* development

PhD candidate: **Patrizia ROMANI**

PhD program coordinator

Prof.ssa **Michela RUGOLO**

Supervisor

Prof. **Giuseppe GARGIULO**

Final exam year 2011

In *Drosophila* the steroid hormone ecdysone regulates a wide range of developmental and physiological responses, including reproduction, embryogenesis, postembryonic development and metamorphosis. *Drosophila* provides an excellent system to address some fundamental questions linked to hormone actions. In fact, the apparent relative simplicity of its hormone signaling pathways taken together with well-established genetic and genomic tools developed to this purpose, defines this insect as an ideal model system for studying the molecular mechanisms through which steroid hormones act.

During my PhD research program I've analyzed the role of ecdysone signaling to gain insight into the molecular mechanisms through which the hormone fulfills its pleiotropic functions in two different developmental stages: the oogenesis and the imaginal wing disc morphogenesis. To this purpose, I performed a reverse genetic analysis to silence the function of two different genes involved in ecdysone signaling pathway, *EcR* and *ecd*.

1-Introduction

Drosophila melanogaster has played a fundamental role in the understanding of genetic mechanism from the beginning of the last century, due to the relative simplicity of its genome, the shortness of life cycle and the abundance of progeny.

From the pioneering studies of T. H. Morgan and members of his laboratory, the fruit fly has early become the most characterized model organism for genetic studies.

With the development of molecular biology techniques and genome sequencing, this animal represents today an excellent model to understand the genetic mechanisms at the basis of almost all metazoan development.

The life cycle of *Drosophila* includes a period of embryogenesis, completed within the eggshell, followed by three larval instars (L1, L2 and L3), during which the larva increases its dimensions.

At the end of the third instar, at the pupal stage, a catastrophic metamorphosis occurs characterized by histolysis of larval tissues and imaginal tissue differentiation, responsible for the adult appendages definition. At the end of this stage the adult insect ecloses. The life cycle of a wild type organism lasts about ten days at 25°C.

1.1 Overview of *Drosophila melanogaster* oogenesis

Drosophila oogenesis is one of the most intensively studied processes of development of this model organism and it has become a powerful system for investigating many aspects of cell and developmental biology. The development of a single cell into a mature egg requires almost every cellular processes that can occur during development, from cell cycle control and fate specification to cell polarization and epithelial morphogenesis. Hence a system that appears relatively simple on the surface can provide insights applicable to more complex processes, such as vertebrate development and disease progression. The ovary is the single largest organ in the female fly and it is not essential for survival, allowing for extensive manipulation.

Each adult ovary is composed of 14-16 ovarioles, which contain strings of developing oocytes at progressive ages that could be considered an egg production line. The ovariole is considered the morphological and functional unit of the ovary with a

structure called *germarium* at its anterior end containing somatic and germline stem cells. Egg chambers bud off and mature as they pass down the ovariole, reaching the posterior end, called *vitellarium*, as mature eggs competent for fertilization. Based on the morphology of the maturing egg chamber, oogenesis has been divided into 14 stages temporally well determined (Figure 1) (*King, 1970; Spradling, 1993; Cavaliere et al., 2009*).

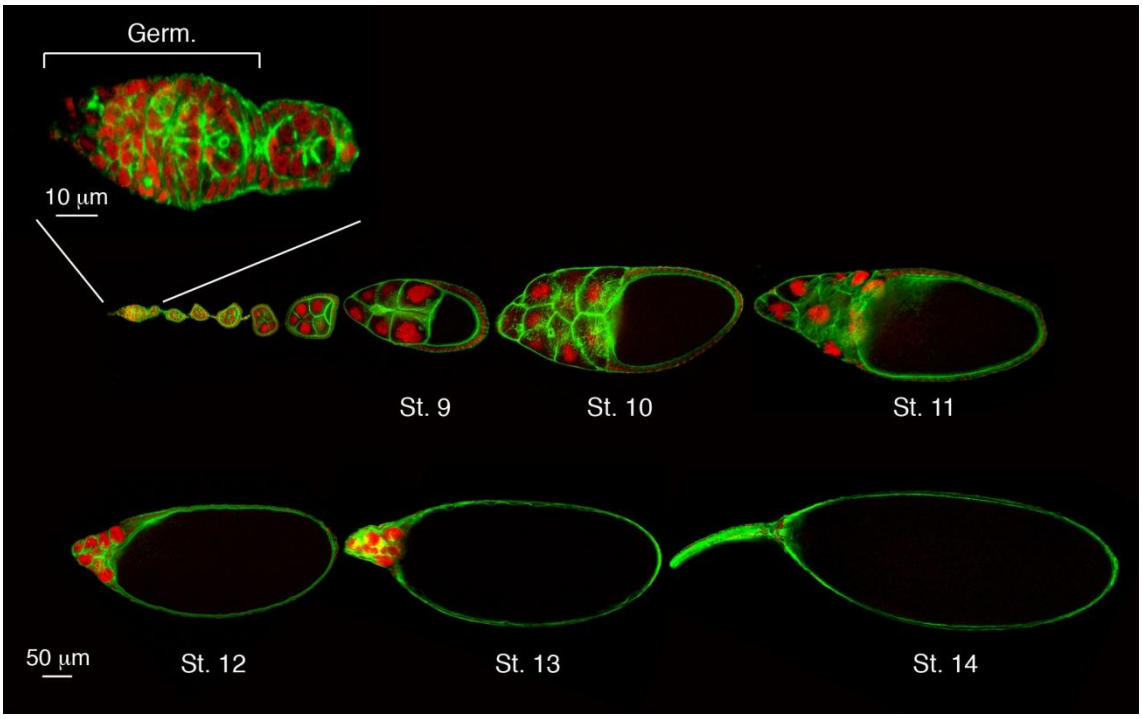

Figure 1: **Stages of egg chamber development.** Confocal cross-sections of wild-type egg chambers. Staining of *Drosophila* egg chambers is facilitated by labelling with FITC-phalloidin (green) that reveals F-actin cytoskeleton and by the nuclear dye propidium iodide (red). A high magnification of the germarium and of a stage-1 egg chamber are shown (top left). During mid-oogenesis (stages 9-11), the rearrangement of follicle cells and the increasing size of the oocyte become evident. In the late stages (stages 12-14), oocyte growth continues and the nurse cells, after carrying out their function, undergo death. Germ., germarium; St., stage. (*Cavaliere et al.*, 2008).

In the germarium each germline stem cell divides asymmetrically to renew itself and to produce a cystoblast that undergoes four synchronized mitotic divisions, each with incomplete cytokinesis, to produce a germline cyst of 16 cystocytes interconnected by ring canals. The orientation of these divisions is controlled by the fusome, a branched

structure composed of a continuous endoplasmic reticulum surrounded by cortical cytoskeletal components and microtubules. One of the two cells originating from the first mitotic division, characterized by the presence of four ring canals, will develop as the oocyte, while the other 15 will develop as accessory nurse cells whose function is to synthesize materials to supply the growing oocyte (*Lin and Spradling,* 1993; *de Cuevas et al.,* 1997). The oocyte is the only cell within the cyst that will progress through meiosis and it arrests during prophase I before exiting the germarium and does not continue until the mature egg is laid and activated.

Nearby, somatic stem cells give rise to precursor follicle cells and about 16 of them invade between adjoining cysts, cease division and become pre-polar cells, which ultimately become polar cells and stalk cells. Inward migration of polar, stalk and epithelial cells separate individual germline cysts into discrete egg chambers (*Horne-Badovinac and Bilder,* 2005). As the cyst exits the germarium, the other somatic cells covering each chamber, the epithelial follicle cells, remain undifferentiated. Follicle cells that surround the egg chamber undergo mitotic divisions to follow the increase in size of the germline cells (Figure 1).

The relative simplicity of the *Drosophila* germarium makes it straightforward to identify and study the behavior of ovarian stem cells in their niche. Work in this system has also shown how dynamic the stem cell population can be. If one stem cell is lost, a neighbor can change its axis of division producing an extra stem cell. Recent work on follicle stem cells has shown that anchoring to the extracellular matrix by integrins is critical for their maintenance (*Fuller and Spradling,* 2007; *Morrison and Spradling,* 2008).

1.2 Follicular epithelium

1.2.1 Follicular epithelium formation and development

Epithelia perform essential functions in all animals, acting as barriers between different compartments and undergoing complex cell movements to drive morphogenesis. The function of epithelial cells depends on their polarization along the apico-basal axis, loss of this polarity has been implicated in tumor development.

The initial encapsulation of germline cysts by precursors of follicle cells (FCs) involves a mesenchymal-to-epithelial transition. Mesenchymal precursor FCs divide a few more times, then encapsulate the egg chamber in the follicular epithelium. As the encapsulated cyst exits germarium, approximately 10-14 of the somatic cells cease proliferation and differentiate, mainly thanks to Notch signaling activation (*Keller Larkin et al.*, 1999). This induces the adjacent anterior follicle cells to differentiate in polar cells, which express the JAK/STAT ligand Unpaired, and the neighbors to become stalk cells, which intercalate and pinch off the egg chambers from the germarium.

The other somatic cells covering each chamber remain undifferentiated and proliferate to form a uniform epithelium of about 1000 cells. FCs stop dividing at the end of stage 6, switch to endoreplicative cycles and become competent to respond to subsequent inductive signals. The anterior and posterior cells continue to secrete Unpaired, that induces terminal fate in the surrounding cells. Afterwards, they begin to differentiate and show morphological and molecular peculiarity of the five main epithelial fates: border, stretched, centripetal, posterior and main body follicle cells (Figure 2).

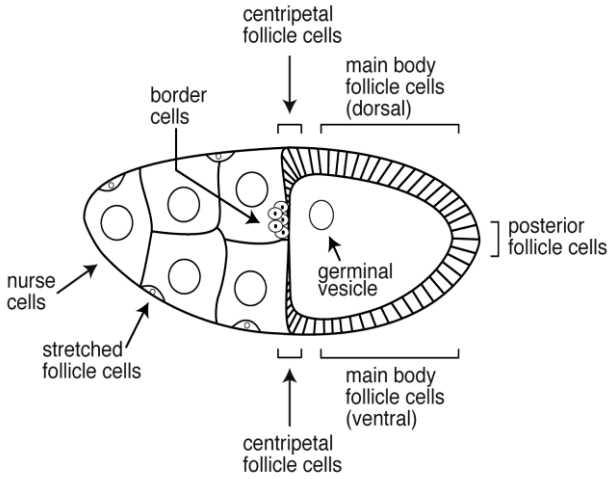

Figure 2: **Schematic view of different cell populations in a stage 10B egg chamber** (*Cavaliere et al.*, 2008).

Each of these populations has a specific function with respect to the production of a mature egg, such as the correct number and position of each type which is critical to accomplish egg morphogenesis. These functions influence the production of structures that are essential to the egg, such as the dorsal appendages and the micropyle and are also critical for proper anterior-posterior organization of the oocyte and, therefore, also for the resulting embryo (*Xi et al.*, 2003).

Follicle cells form a cuboidal epithelium until stage 8, but at the beginning of stage 9 they reorganize in a series of migrations. The 6-10 anterior-most follicle cells, the border cells, migrate through the nurse cells towards the oocyte anterior end. Other 50 anterior cells, the stretched cells, form a flattened epithelium overlying the nurse cells. Signaling events between follicular cells and the oocyte are indeed at the bases of the anterior-posterior and dorsal-ventral embryonic axes determination (*Ray and Schupbach*, 1996; *Beccari et al.*, 2002; *Grammont and Irvine*, 2002; *Xi et al.*, 2003).

Coincidently with these events in the soma, the oocyte itself is busily re-arranging its polarity. Microtubule minus ends, which nucleate from a diffuse microtubule organizing centre, along with the nucleus, gurken RNA and Gurken (Grk) protein are all localized to the posterior end of the oocyte. Grk signals to the closest follicle cells inducing posterior identity. These cells then send back an unidentified signal, which triggers repolarization of the oocyte. Microtubule minus ends are lost from the posterior and

nucleate instead along the lateral and anterior cortex. Plus ends initially accumulate in the middle of the oocyte, but later become focused at the posterior.

Accompanying this process is a movement of the germinal vesicle away from the posterior pole to localize at the anterior corner of the oocyte, where it activates the Epidermal Growth Factor Receptor (EGFR) once more to establish the polarity of the dorsal-ventral axis (*Lopez-Schier,* 2003). During oogenesis, nurse cells also undergo nuclear changes, which involve a series of endoreplication cycles increasing their polyploid values (from 512 to 2048). Nurse cells develop a complex microtubular apparatus organized in ring canals through which they transfer mRNAs, proteins, organelles and lipidic droplets to the oocyte, important for the correct development of the future embryo. During early stages of oogenesis this transfer is slow but continuous and increases strongly at stage 10B. From stage 10B to stage 12, nurse cells transfer all their cytoplasmic contents to the oocyte and finally undergo apoptosis (*Cavaliere et al.,* 1998; *Foley and Cooley,* 1998). At stage 14 of oogenesis, after the construction of eggshell, also the follicle cells die by apoptosis (*Nezis et al.,* 2002).

1.2.2 Follicular epithelium morphology

The follicular epithelium surrounding the germline cyst is a simple monolayer tissue with a pronounced apico-basal polarity. The follicle cell membrane is partitioned into apical and baso-lateral domains that accumulate different sets of membrane proteins, which become separated by the formation of a series of cell junctions along the apico-basal axis of the lateral membrane (*Müller,* 2000; *Wu et al.,* 2008; *Horne-Badovinac and Bilder,* 2005; *Knust,* 2000; *Knust and Bossinger,* 2002; *Tepass et al.,* 2001).

Each *Drosophila* epithelial follicle cell is characterized by five types of junctions (Figure 3) (*Szafranski and Goode,* 2007). The apical junction connects follicle cells to the germ cells; the three conserved lateral junctions, the apico-lateral, adherens and baso-lateral junctions interconnect follicle cells to each other, while a basal junction connects the epithelial cells to the basement membrane. These five domains contain

different protein complexes and genetic studies have revealed that these protein complexes function in a sequential yet interdependent manner to regulate the establishment, elaboration and maintenance of cellular polarity (*Tepass et al.*, 2001; *Bilder et al.*, 2003; *Tanentzapf and Tepass*, 2003).

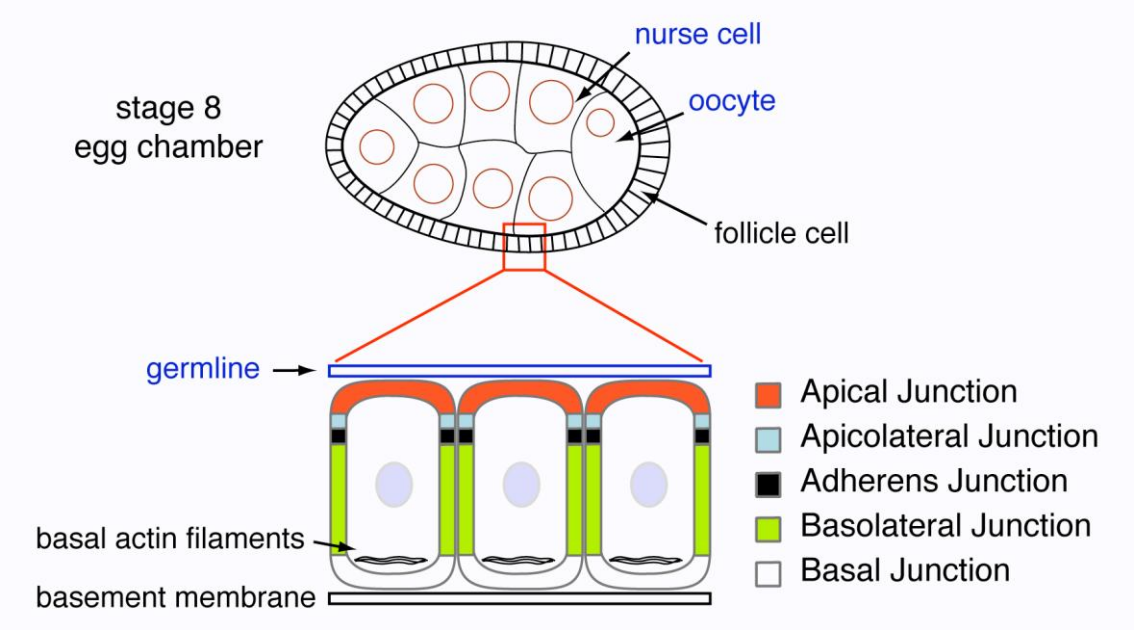

Figure 3: **Apico-basal polarity in the follicle cell epithelium.** The magnified view of three follicle cells shows the localization of certain cellular junctions in the different subdomains of the plasma membrane. The proximity of the apical surface to the germline and basal surface to a basement membrane as well as the position of the basal actin filament are shown.

Apical Junction

The apical membrane domains of the follicle cells are lining the germ cells and presumably adhere to the oocyte plasma membrane via DE-Cadherin (Figure 4) (*Oda et al.*, 1997; *Godt and Tepass*, 1998; *Gonzalez-Reyes and St Johnston*, 1998).

Three genes *shotgun (shg)*, *egghead* (*egh*) and *brainiac* (*brn*), appear to be required for the interaction of the apical membrane of the follicle cells and the oocyte membrane. Mutations in these genes lead to loss of epithelial polarity and multilayering of the follicle cell sheet (*Goode et al.*, 1996; *Rübsam et al.*, 1998). Both *egh* and *brn* encode for putative secreted or transmembrane proteins, suggesting that the germline sends out a signal via Egh and Brn that is received by the follicle cells and is required for the maintenance of epithelial polarity in these cells. It has been proposed that Notch (N) is

the receptor for this signal because N mutant follicle cells exhibit a similar multilayering phenotype as seen in *brn* and *egh* germline clones (*Goode et al.*, 1996; *Ruohola et al.*, 1991).

The apical domain presents high levels of filamentous proteins such as α- and β-Spectrin which are part of the cytoskeleton of the follicle cells. The filamentous protein α-Spectrin forms a network with actin cytoskeleton that regulates and stabilizes the membrane shape. By using mosaic analysis, *Lee et al.*, (1997) showed that β-Spectrin is required for the proper localization of the α - and β heavy chains and mutations resulted in multilayering and loss of apico-basal polarity of the epithelium.

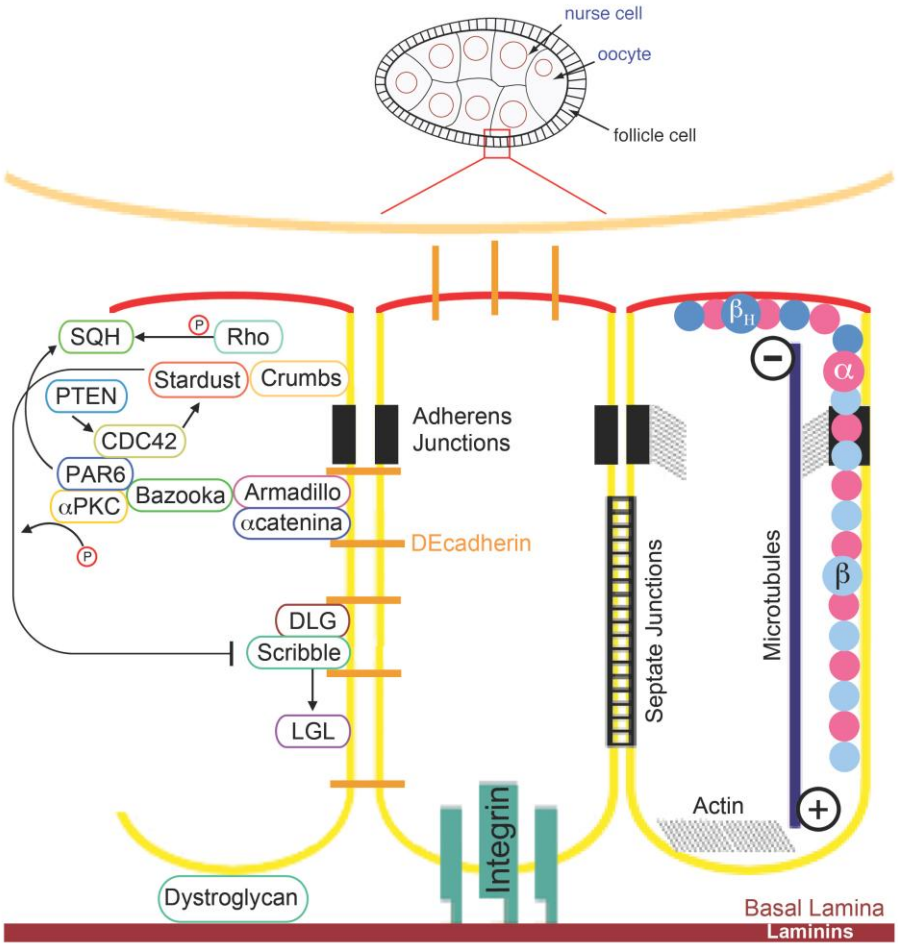

Figure 4: **Detailed scheme of a polarized follicular epithelium.** The magnified view of three follicle cells shows the localization of the different polarity markers at the apical domain (red) and at the latero-basal membrane domain (yellow) (Modified from *Muller*, 2000).

Apico-lateral Junction

This compartment is composed of the aPKC complex which is required to establish polarity in many different cell types. This complex is localized in follicle cells right above the adherens junctions (*Horne-Badovinac and Bilder,* 2005) and, besides aPKC, it is composed of Bazooka (Baz, homolog of PAR-3) and dmPAR-6 (homolog of Par6), cytosolic scaffolds with PDZ domains and other binding domains for protein-protein interactions (Figure 4). Mutations that affect these genes cause pluristratification and epithelium discontinuity (*Abdelilah-Seyfried et al.,* 2003; *Tanentzapf et al.,* 2000), loss of monolayer organization, polarity and correct cell shape (*Wodarz et al.,* 2000).

The subapical region (SAR), located right below the apical domain, is marked by Crumbs (Crb), a transmembrane protein required for the establishment of this domain, together with its cytoplasmic-binding partners, such as aPKC (*Knust and Bossinger,* 2002; *Tepass et al.,* 1990). Interestingly aPKC during *Drosophila* embryogenesis is required for the phosphorylation of Crb. This phosphorylation may be necessary for Crb to adopt a correct conformation and/or to interact with proteins required for Crb stabilization at the apical domain (*Sotillos et al.,* 2004). More in general, it has been shown that aPKC kinase activity is essential and instructive for proper localization of apical and baso-lateral proteins for establishing and/or maintaining cell polarity (*Sotillos et al.,* 2004).

Adherens Junction

The lateral compartment is characterized by the adherens junction (AJ; Zonula adherens in vertebrate's epithelia), a belt composed of protein complexes and actin filaments that encircle the cell just below its apical face (Figure 4). AJs are one of the crucial components for the establishment and maintenance of both the polarized shape of individual epithelial cells and the integrity of cell sheets. These functions can be attributed to the ability of DE-Cadherin (encoded by the gene *shotgun*) to set up during early stages of oogenesis the initial polarity of the follicular epithelium (*Dobens and Raftery,* 2000; *Godt and Tepass,* 1998). Moreover DE-Cadherin is able to interact with

the cytoskeleton on the one hand and with neighboring cells via homophilic interactions on the other (*Knust,* 2000). The cytoplasmic tail of the Ca^{++}-dependent homophilic adhesion protein DE-Cadherin is in fact linked to the actin filaments via β-Catenin (Armadillo) (*Yap et al,* 1997; *Tepass,* 1997; *Tepass,* 1999) and α-Catenin (*Peifer et al.,* 1993). DE-Cadherin turnover, which results in its asymmetrical distribution, is necessary to ensure follicle cells movements and rearrangements during oogenesis (*Schober and Perrimon,* 2005).

Baso-lateral Junction (BLJ)

The baso-lateral domain in *Drosophila* epithelial cells is represented by the Septate Junction (SJ), functional barrier that enables transepithelial circulation. The Scrib complex localizes at this domain, that includes the tumor suppressor genes *scribble* (*scrib*), *lethal giant larvae* (*lgl*) and *discs large* (*dlg*) (Figure 4). Genetic studies have revealed that these three tumor suppressor genes cooperatively regulate cell polarity, junction formation and cell growth in epithelial cells (*Bilder and Perrimon,* 2000; *Yamanaka and Ohno,* 2008). During oogenesis, SJ builds up from stage 6 when follicle cells stop proliferating, although the complete development takes place at stage 10 (*Horne-Badovinac and Bilder,* 2005). Discs Large (Dlg) is involved in maintaining the structure of the follicular epithelium, by inhibiting cell growth and maintaining cell adhesion and cell polarity. Lethal giant larvae (Lgl), a WD40 domain-containing protein, is implicated in cellular asymmetry formation in a number of cell types (*Vasioukhin,* 2006; *Wirtz-Peitzand and Knoblich,* 2006). It is not clear through which interactions Lgl is brought to membranes. However, in *scrib* or *dlg* mutant embryos, Lgl plasma membrane association is also lost (*Bilder et al.,* 2000). This finding suggests that a critical role of Scrib and Dlg is to recruit Lgl to the membrane (*Tepass,* 2001). Loss of *lgl* in *Drosophila* results in loss of apico-basal polarity in epithelial cells and in the neoplastic transformation of the imaginal discs which lose their epithelial monolayer structure (*Agrawal et al.,* 1995; *Bilder et al.,* 2000; *Ohshiro et al.,* 2000; *Peng et al.,* 2000). Upon cell-cell contact-induced cell polarization, Lgl is phosphorylated by aPKC

resulting in a dissociation of Lgl from Par6/aPKC followed by an accumulation of Lgl along the baso-lateral membrane, where it contributes to the formation of the baso-lateral membrane domain (*Tanentzapf and Tepass*, 2003; *Hutterer et al.*, 2004) and to correct positioning of epithelial junctions (*Borg*, 2004).

Basal Junction

The follicle cell's basal membrane is facing the basal lamina or basement membrane (BM) (Figure 4). The BM is a highly specialized form of extracellular matrix (ECM) found on the basal side of every polarized epithelium, which is made up primarily of protein networks containing collagen and other glycoproteins, laminin and Collagen IV (*Fessler and Fessler*, 1989; *Quondamatteo*, 2002*).*

The attachment of the epithelium to its BM substrate is largely mediated by integrins, heterodimers of α and β subunits that bind components of ECM along the basal surfaces (*Brown*, 2000). It has been shown that integrin-mediated signaling during *Drosophila* oogenesis is required for proper alignment of the mitotic spindle and thus for the maintenance of the follicular epithelium monolayer, through an interaction between the acto-myosin cytoskeleton and integrin activity (*Fernández-Miñán et al.*, 2007; *Fernández-Miñán et al.*, 2008).

1.3 Embryogenesis

Drosophila embryo develops immediately after egg laying (AEL), and it is characterized by a superficial meroblastic segmentation.

The mature oocyte is quiescent at the metaphase of the first division of meiosis until fertilization. After that, male and female pro-nuclei perform a syncronous division followed by fusion, that generates the zygote. The first 12 rounds of cell division lead to the syncytial blastoderm formation; at 9^{th} division, nuclei migrate toward periphery originating the *syncytitial blastoderm* (*Mazumdar and Mazumdar*, 2002). At the same time, a small number of nuclei reach the posterior pole and are enclosed by cell

membranes to become the first formed cells of the embryo; they will give rise to the germ line.

At the end of syncitial phase, cellularitazion takes place (*Muller and Bossinger*, 2003). The cellularization of the nuclei marks the beginning of the blastodermal stage with the segregation of the somatic and germinal cell lines (the latter derived by the polar cells), 6.3h AEL (*Glover*, 1991). This is a key step because while the early stages are governed by the maternal genome, from this moment onward the development is driven by the zygotic genome.

During the successive phases of gastrulation, major migratorial events (medioventral furrow and cefalic furrow) occur, generating mesodermal structures and the head region. During this stage, mesoderm is subdivided into splancnopleura, responsible for visceral muscles, and somatopleura, from which all the other mesodermal structures originate (muscles, circulatorial system, fat bodies and somatic components of the gonads).

The nervous system is constituted by a series of elements distributed longitudinally to the embryo body. Successively to the formation of the germinative "stria", there is the invagination of the polar cells and other structures, and the formation of the tracheas.

The last morphological event is the "*head involution*". The mascellar, mandibular and labial segments of the larval head and the external cells of the imaginal discs, invaginate inside the embryo, and this process is followed by an external cuticular deposition and by the differentiation of internal organs.

1.4 Larval and pupal development

After 23h AEL the L1 larva emerges; the three larval instars are spaced out by molts and followed by metamorphosis. Molts and metamorphosis are governed by ecdysone peaks, a steroid hormone produced by the ring gland. The larva is characterized by two cellular types: larval cells, that are polyploid, and imaginal cells that are diploid. Imaginal cells segregate precociously from the surrounding larval cells, forming small cell groups at 9-10h AEL and are organized in two fundamental groups,

imaginal discs and abdominal histoblasts. Imaginal discs begin an intense proliferative activity from the second larval instar until pupariation, while abdominal histoblasts proliferate later, during the pupal stage. At this moment the majority of larval cells are eliminated and substituted by imaginal cells that originate the integument and the adult appendages. Imaginal discs originate the structures of the head, thorax external appendages, genitalia and adult muscles. The histoblats originate the abdomen structures at the exception of the 8^{th} segment that derivates from the genital imaginal disc.

During metamorphosis three important steps occur:

1. elongation
2. eversion of the imaginal structures
3. enlargement and fusion of the imaginal structures, with the formation of a continuous epithelium (*Fristrom and Fristrom,* 1993).

1.5 Imaginal tissues

Adult insects, differently from larvae, show several external appendages. To allow for the concurrent organization of the radically different larval and adult body plans, the primordial of the adult structures are segregated from the larval tissues during embryogenesis (Figure 5) (*Cohen,* 1993). Once established, these primordia follow a developmental program distinct from the larval one. As previously mentioned, epidermal structures of the adult head, thorax appendages and genitalia derive from imaginal discs, sac-like clusters of primordial cells.

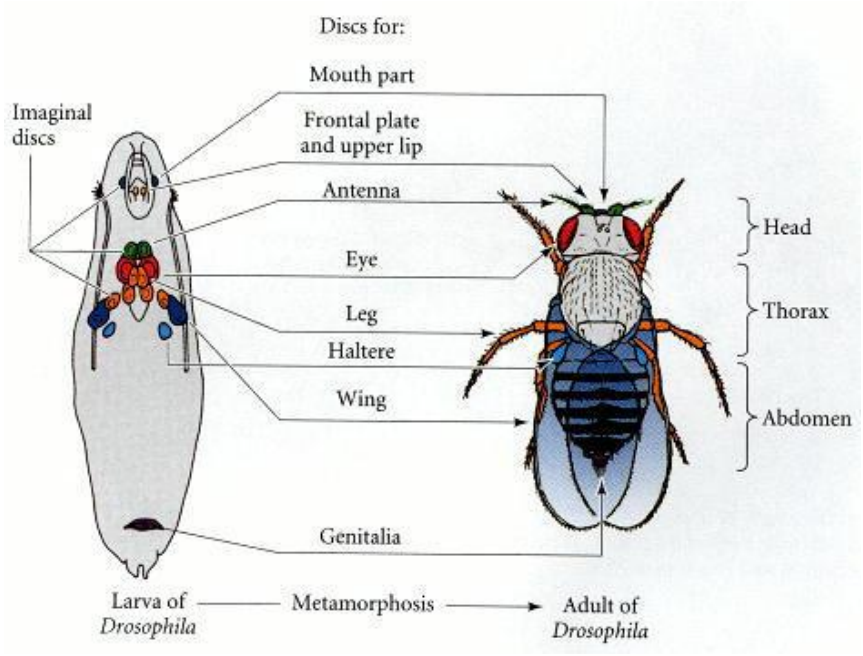

Figure 5: **Location and developmental fates of the imaginal discs in *Drosophila melanogaster* L3 larva** (*Fristrom and Fristrom,* 1993).

Imaginal discs at the end of larval development are composed of a pseudostratified columnar epithelial sheath made of undifferentiated, proliferating cells, that represent the actual imaginal disc, and by a squamous epithelium that forms the peripodial membrane. The first will originate the integument and the appendages, the second will originate the epithelial veil that welds the structures derived from imaginal discs. Different imaginal discs have their particular size and shape, and are named after the part of the body they form: wing disc, leg disc, eye-antenna disc and genital disc.

1.6 Wing imaginal disc structure, specification and development

Imaginal wing discs represents an excellent model for studying tissue growth and proliferation control. This tissue encounters a dramatic increase in cell number in a relatively short length of time with an average cycle time of 8.5 hours (*Garcia-Bellido and Merriam,* 1971).

Proliferation in the imaginal wing disc is random but uniform across the tissue. It also uniformly ceases when correct disc size is attained. Control of organ final size appears to be an intrinsic mechanism. Rather than cell number, overall tissue dimension seems

to be regulated (*Johnston and Gallant*, 2002). Indeed, changes in cell size yield to compensatory modifications of cell number and *viceversa*.

The wing imaginal disc is an excellent model for the elucidation of organogenesis and proliferation mechanisms; at the end of L3 it is subdivided in a series of folds. The centrifugal regions of the imaginal disc originate the thorax structures, the notum and the pleura (Figure 6). The middle region originates the hinge region while the central region is the presumptive territory that makes the wing lamina. Imaginal tissues are virtually two-dimensional structures, but they originate adult appendages with three axes (AP, DV, PD); this is due to a mechanism of eversion during methamorposis, in which the most central regions of the disc originate the distal structures (wing from distal to proximal), while the external regions originate the most proximal structures of the appendage. During the embryogenesis the action of the segment-polarity genes generates parasegmental restriction boundaries and positional information for the specification of the imaginal discs primordia (*Cohen*, 1990). The patterned expression of the selector gene *engrailed* is present in the anterior region of the parasegmental compartment and in the posterior region of the wing imaginal disc, suggesting a derivation from two different parasegments (*DiNardo et al.*, 1985).

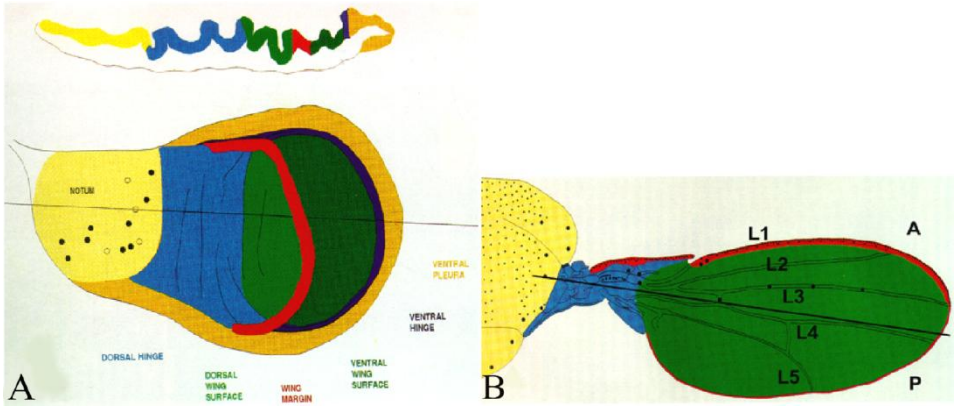

Figure 6: **Schematic representation of the wing imaginal disc at L3 instar (A) and of the adult wing (B).** Different colors in A indicate the presumptive territories of the structures visualized in B (*Bate and Martinez-Arias*, 1991).

Imaginal discs primordia are constituted by 20 founder cells, identified by the expression of specific markers. The direct source for the genesis of positional signals for the founder cells is Wingless. Without this signal, no imaginal structures arise. Escargot (Esg) is a marker of all the primordial imaginal cells and it is indispensable for the diploid maintainment. Several indications exist that wing imaginal disc originates ventrally and represents a branch of the second leg imaginal disc (*Cohen*, 1997). The activation of differential selector genes separates the two structures early making them become independent, and the imaginal disc grows dorsally, while legs are ventral appendages.

The A/P boundary is inherited from the embryo and is a consequence of the homeobox gene *engrailed* (*en*) which belongs to the segment polarity genes class (*Morata and Lawrence*, 1975) (Figure 7). e*n* determines differentiation of anterior and posterior cells acting as a selector gene. Its activity is confined to the posterior compartment where it activates *hedgehog* (*hh*), which encodes a secreted protein (*Blair and Ralston*, 1997). The effect of the Hh protein in the posterior compartment cells is inhibited by En, but the protein diffuses across the A/P border and, in the anterior cells close to the border, it induces the activity of the *decapentaplegic* (*dpp)* gene, which triggers complexes signaling cascades responsible for patterning the appendages (*Affolter and Basler*, 2007).

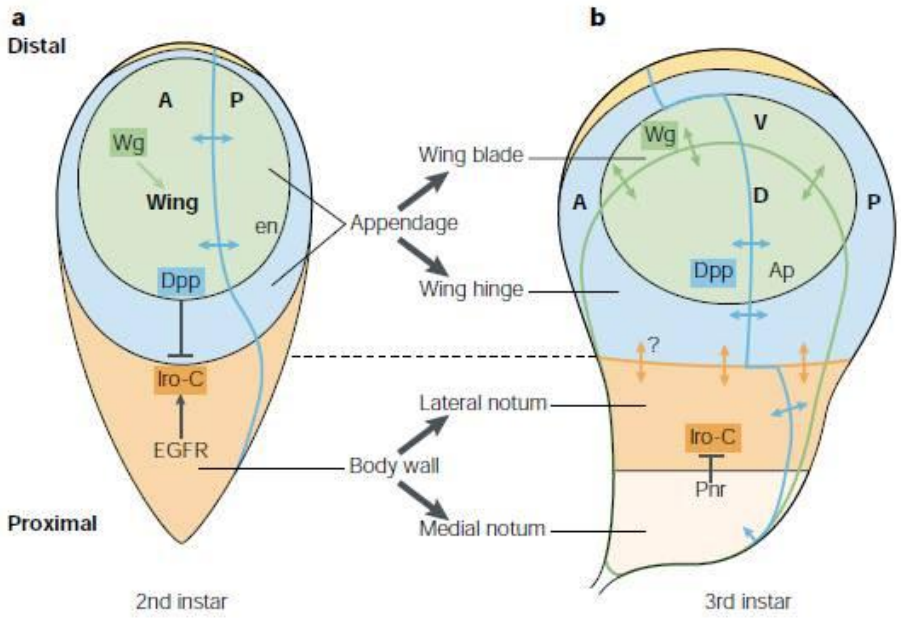

Figure 7: **A second instar and a third instar wing imaginal discs.** Wing imaginal disc growth and patterning occurs during larval development and depends on two orthogonal systems. The first is inherited from the embryo and subdivides the disc into anterior (A) and posterior (P) compartments, defined by cell lineage restrictions. It is effected by the expression of Engrailed (en) and Invected in the P compartment (panel a). Signalling from the P cells to the A cells by means of the secreted molecule Hedgehog (Hh) causes A cells near the compartment border to express dpp (a, b), which diffuses into both compartments, acts as a morphogen, and induces activation of different target genes in distinct domains of both A and P compartments. The second system subdivides the disc along the proximal/distal axis early in development, when the disc has just a few hundred cells. This is accomplished by three signalling pathways actions: Wg, EGFR and Dpp (a). In the early third instar, Dpp signalling subdivides the notum territory into lateral and medial domains (b) by activating pnr that represses Iro-C and provides identity to the medial notum. The lateral notum is defined by the continuing expression of Iro-C (*Gómez-Skarmeta et al.*, 2003).

This process is the basis of a complex regulative pathway, that leads to the activation and the repression of a large number of genes. The final result is the definition of the anterior-posterior axis and the definition of positional information that leads to the creation of the anterior-posterior boundary and the specification of the vein and intervein regions. Anterior and posterior compartment thus represent independent developmental units and the A/P border is for that reason defined a restriction border that cells never cross during development.

A second, fundamental compartment division appears at the beginning of the second larval instar which defines the dorsal and ventral compartments (Figure 7).

The D/V border depends on the action of the selector gene *apterous* (*ap*), expressed only in the dorsal compartment (*Diaz-Benjumea and Cohen,* 1993). Ap activates *fringe* (*fng*). Fng is a secreted factor that modulates the ability of two ligands, Delta and Serrate, to activate their receptor Notch. In particular, it induces the activation of Serrate and inhibits the expression of Delta ligand (*Panin et al.,* 1997). In turn, activated Notch induces *vestigial* and *wingless* activity at the D/V border (*Neumann and Cohen,* 1996). Wg acts as a morphogen and establishes the D/V restriction boundary.

While much is known about the development of the patterning mechanisms that specify the A/P and D/V axes, very little is known about the determination of the P/D. The formation of the three structures of this axis (notum, hinge and wing blade) is due to the sequential activation-repression of a multitude of selector genes, in response to the formation of the A/P and D/V axes (*engrailed*-A/P axis and *apterous*-D/V axis) and to the generation of morphogen activity at the boundary of the two axes (Dpp at the A/P border and Wg at the D/V border). The correct wing patterning requires the activity of Wg morphogen. Wg expression begins in a ventral-anterior wedge of the early second instar wing disc and is extremely dynamic throughout the larval stages (*Couso,* 1993). At this stage, after the formation of A/P and D/V axes, another subdivision occurs in the formation of the proximal-distal axis that subdivides the wing disc in the Notum, Hinge and Blade regions (*Klein,* 2001). The activity of Wingless promotes the repression of *teashirt* homeobox gene that drives the body wall formation, and *vg* expression (*Wu and Cohen,* 2002).

EGFR signaling is most active in the proximal part of the discs and defines the presumptive notum by activating notum-specific genes, while Dpp signaling at early stages represses the same homeodomain gene expression in the distal territory, confining its expression to the proximal part of the disc (*Cavodeassi et al.,* 2002).

1.7 Eye-antenna imaginal disc structure, specification and development

The progressive development of identical units within a monolayer epithelium makes the *Drosophila* eye disc an excellent system in which to address the regulatory mechanisms of pattern formation. Positive autoregulatory loops play an important role in driving the progression of differentiation, and a temporal delay can be introduced into such loops by requiring the production of a second signal dependent on the first. The range over which signals are distributed is also an important factor in controlling the sequence of differentiation. Several aspects of this differentiation process have now been described at a level at which mathematical modeling could be applied to test and extend our understanding of the mechanisms involved.

The transformation leading from an unpatterned epithelial monolayer within the larval eye imaginal disc to the highly ordered adult eye has been extensively studied during the three decades since it was first introduced as an experimental system (Ready *et al.*, 1976; reviewed in *Roignant and Treisman*, 2009).

The eye-antenna discs originate from different embryonic segments (antennal, maxillar, mandibular, intercalary and labial) plus the nonsegmented acron. By the end of embryogenesis, the discs invaginate from the dorsal pouch of the embryo as two small flat epithelial sacs of approximately 70 cells each. During the three larval instars the disc grows mostly by cell proliferation. The organ primordium will be specified in only one of two layers of the disc (the main epithelium) whereas the other layer, called peripodal epithelium, becomes a squamous epithelium (Figure 8). The peripodal epithelium will participate in the eversion and fusion of the discs during metamorphosis. The eye-antennal disc cells retain considerable developmental plasticity until late stages of development.

The eye disc is specified in the embryonic and early larval stages through the action of a network of transcription factors known as the retinal determination genes (*Silver and Rebay*, 2005). Recent analyses of the expression and function of genes involved in the development of the different organs of the eye-antennal discs are coalescing into a model of progressive restriction of “eye-forming competence” and gradual subdivision

of the discs primordium into distinct organ domains. This subdivision is led by the interplay between several transcription factors and signaling molecules.

First instar disc expresses uniformly the Pax6 paralogues *eyeless* (*ey*) and *twin of eyeless* (*toy*), which act as "eye selector genes" (reviewed in *Gehring,* 2002). *ey* is required for identity and eye development, at least in part, by preventing apoptosis (*Czerny et al.,* 1999), and each of the two Pax6 proteins can induce eye development when ectopically expressed elsewhere in the fly body, even in the absence of the other. Toy acts upstream of *ey* by inducing *ey's* transcription, so their expression patterns are very similar. The expression of these genes is maintained in the eye primordium cells until these commence to differentiate.

During the second larval instar, a series of gene expression changes result in the first molecular definition of the eye field. First, the expression of *ey*/*toy* retracts to the posterior while the homeodomain encoding gene *cut* is turned on in the anterior region. The *ey/toy* and *cut* complementary domains mark out the territories of the future eye and antenna, respectively. The activation of the homeodomain-encoding gene *Distalles* (*Dll*) within the *cut* domain leads to the coexpression of *homothorax* (*hth*) and Dll which together specify the antennal fate (Figure 8) (*Casares and Mann,* 1998). At the time of the antenna-eye partition, the expression of the nuclear factor encoded *Eye absent (Eya)* gene starts at the posterior region (*Kenyon et al.,* 2003). Eya is the first of a group of nuclear factors, as Sine oculis and Dachsous, expressed within the presumptive eye field, collectively known as "early retinal genes". Of interest, although these genes are expressed elsewhere in the fly embryo, they are all first coexpressed in the eye disc during second instar. Because all of these genes are required for the initiation of retinal differentiation, it has been proposed that it is this coexpression that locks-in the eye competence in the *ey*-expressing cells (*Kumar and Moses,* 2001).

The peripodal layer also undergoes significant changes in transcription factor gene expression although their regulation and functional meaning, if any, are still unknown.

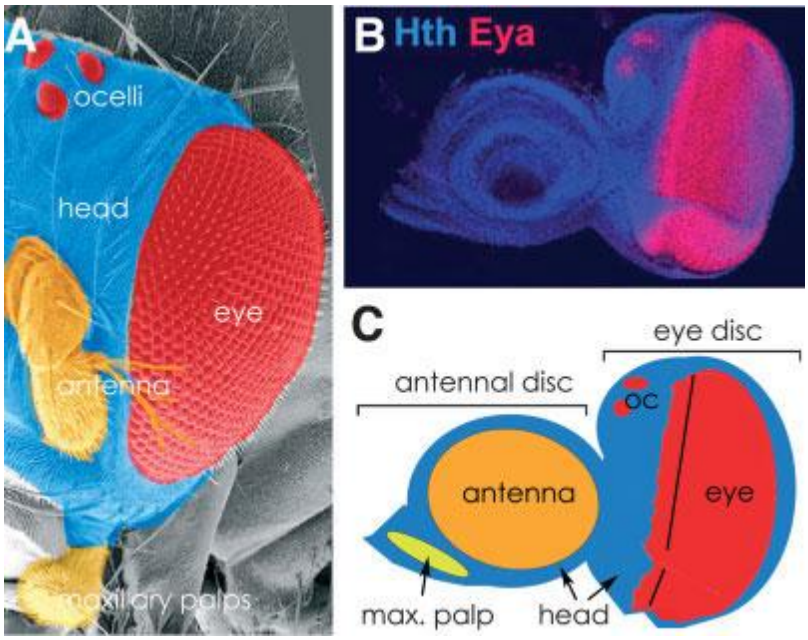

Figure 8: **The adult head of *Drosophila melanogaster* develops from a pair of composite discs called the eye-antennal discs.** A) A scanning photomicrograph of an adult head. B) A third instar eye-antennal disc labeled with antibodies against Homothorax (Hth, blue) and Eyes absent (Eya, red) proteins. C) The boundaries of the primordial of the antenna (orange) are clearly defined by the expression of *Distalles* (*Dll*) gene at this stage. In yellow is the region of the disc fate mapped to become maxillar palp. The discrete organs of the adult head are marked out in the same color code as the corresponding organ forming primordial in the eye-antennal imaginal disc (*Roignant and Treisman*, 2009).

Pattern formation and ommatidial differentiation begin in the third larval instar with the appearance of a groove called the morphogenetic furrow (MF) at the posterior margin of the eye disc (*Ready et al.*, 1976). This indentation in the epithelium, which results from an apical constriction and apico-basal contraction of the cells, sweeps progressively across the eye disc from posterior to anterior over a 2-day period. Cells anterior to the MF are undifferentiated and proliferate asynchronously, whereas cells posterior to the MF are organized into columns of regularly spaced clusters within which photoreceptor differentiation occurs in a defined sequence (*Tomlinson and Ready*, 1987; *Wolff and Ready*, 1991). An average of 30 columns, each initiated every 90-120 minutes, will form the entire retinal field. Unlike other imaginal discs, which are patterned by organizers formed at stable boundaries between cellular territories, the eye disc has a progressive pattern of differentiation controlled by signals that are constantly changing their spatial positions.

One critical signal driving the initiation and progression of the MF is the secreted protein Hedgehog (Hh) (*Heberlein et al.,* 1995; *Heberlein et al.,* 1993b; *Ma et al.,* 1993). Hh is expressed at the posterior margin of the eye disc prior to MF initiation, and induces differentiation of anterior cells; as they differentiate into photoreceptors, these cells also begin to express Hh and can therefore act on cells anterior to them (*Heberlein and Moses,* 1995). One target of Hh signaling is Dpp, which functions redundantly with Hh in MF progression (*Burke and Basler,* 1996; *Curtiss and Mlodzik,* 2000). Another Hh target is the basic Helix-Loop-Helix (bHLH) transcription factor Atonal (Ato), which is required for the specification of R8 cells, the first photoreceptors to differentiate in each cluster. Ato is initially expressed in a broad stripe just anterior to the MF, and its expression is gradually refined to single R8 cells within the MF in a process requiring lateral inhibition mediated by the Notch receptor (*Baker and Zitron,* 1995; *Jarman et al.,* 1995).

R8 orchestrates subsequent ommatidial development by recruiting surrounding uncommitted cells to differentiate into other photoreceptors, cone cells and pigment cells. Secretion of the EGFR ligand Spitz (Spi) from R8 and subsequently recruited cells promotes the sequential differentiation of photoreceptors R2/R5, R3/R4, R1/R6, R7, the cone cells and the primary pigment cells, as well as the survival of secondary and tertiary pigment cells (*Freeman,* 1996; *Miller and Cagan,* 1998). The Notch ligand Delta (Dl) acts as a critical secondary signal for several of the later differentiating cell types (*Flores et al.,* 2000; *Nagaraj and Banerjee,* 2007). The founder role of R8 cells makes their specification and spacing critical for the organization of the adult eye. Both Hh and Spi are also transported along the photoreceptor axons and act on photoreceptor target cells in the brain (*Huang and Kunes,* 1996), coordinating the development of the two tissues.

1.8 Biological role and function of the steroid hormone ecdysone in *Drosophila melanogaster*

The transformation from larval to adult is one of the miracles of insect biology. This process is characterized by diverse developmental phenomena, including cellular proliferation, tissue remodeling, cell migration and programmed cell death. Cells undergo one or more of these processes in response to hormone secretion. In particular, in *Drosophila* most of developmental processes are governed primarily by ecdysone and juvenile hormone (JH). It is likely that the balance between these two hormones affects the nature of developmental transitions and, in particular, juvenile hormone has a classic 'status quo' action in preventing the program-switching action of ecdysone during larval molts and in maintaining the developmental arrest of imaginal primordia during the intermolt periods (*Riddiford,* 2010).

The molting process is initiated in the brain, where neurosecretory cells release prothoracicotropic hormone (PTTH) in response to neural, hormonal or environmental signals (Figure 9). PTTH itself is synthesized as a pre-prohormone and released as a shorter, glycosilated, homodimeric molecule. Once released into the hemolymph, this neuropeptide stimulates the prothoracic glands to produce ecdysone.

The PTTH transductory cascade has been well studied in *M. sexta* where the interaction of PTTH with a yet uncharacterized receptor at the cell membrane surface of prothoracic gland cells causes an influx of extracellular calcium followed by an increase in cAMP. This finding suggests that cAMP synthesis requires Ca^{++}-calmodulin dependent adenylyl cyclase activity. This is followed by the activation of the Protein Kinase A (PKA) in the prothoracic gland and a number of rapid protein phosphorylation dependent on PKA, MAPKs.

Recent results obtained in Gilbert lab suggest that PTTH also activates a MAPK pathway resulting in a rapid increase of ERK phosphorylation, indicating that ecdysteroidogenesis in the prothoracic gland requires the presence of a small basal population of phosphorylated (active) ERK molecules (*Gilbert,* 2004).

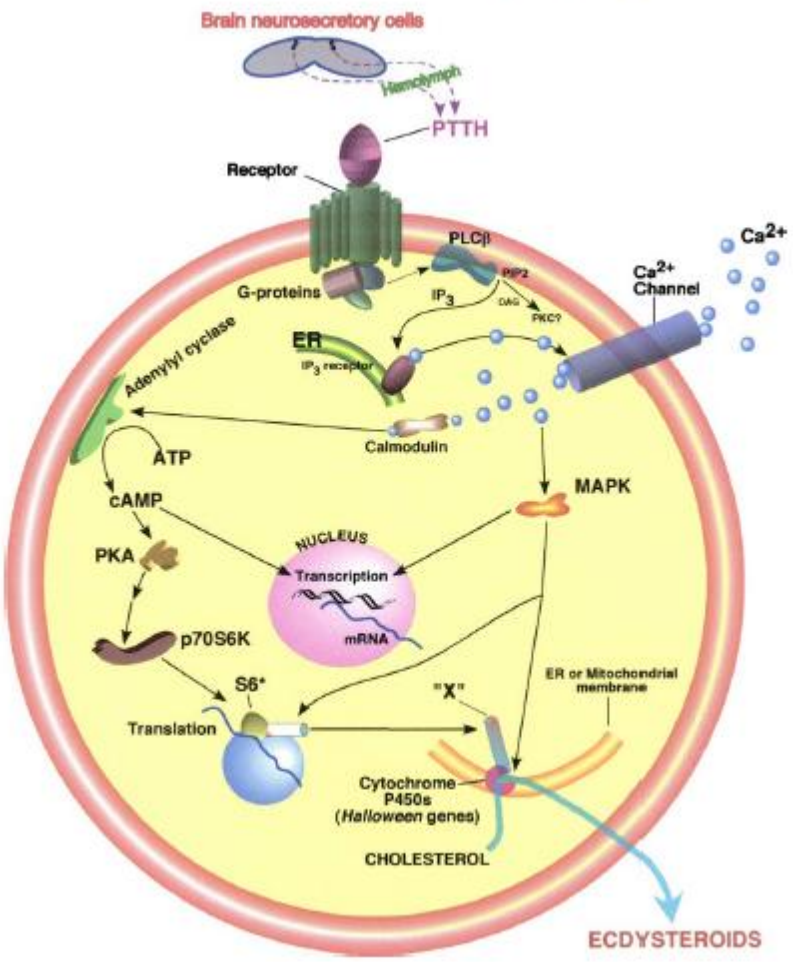

Figure 9: **Transductory cascade of PTTH interaction with a prothoracic gland cell** (*Gilbert,* 2004).

Despite the biochemical and pharmacological characterization of several steroidogenic enzymes in various insect species, the biosynthetic pathway leading to the formation of ecdysone from cholesterol remains undefined.

Recent studies have demonstrated that a family of genes encoding cytochrome P450 enzymes, named *Halloween*, is involved in ecdysone biosynthesis. These genes have likely been highly conserved since the presence of these genes has been confirmed in other insect species (*Niwa et al.,* 2004; *Warren et al.,* 2004; *Warren et al.,* 2006).

spook (CYP307A1), *phantom* (CYP306A1), *disembodied* (CYP302A1), *shadow* (CYP315A1) and *shade* (CYP314A1) belong to *Halloween* family and encode

hydroxylases that are believed to act sequentially in the biosynthesis of ecdysone (Figure 10).

Kozlova and Thummel (2000) identified the *defective in the avoidance of repellents (dare)* gene that encodes a close homolog of the vertebrate adrenoxin reductase (AR). AR transfers electrons from NADPH to adrenoxin protein, which in turn, donates them to the mitochondrial steroidogenic cytochrome P450 hydroxylases. AR is required for the synthesis of all vertebrate steroid hormones, implying that the *Drosophila* homolog may play a similar central role in steroidogenesis.

Over the last years, many other genes were identified and characterized, like *without children (woc), molting defective (mld)* and *ecdysoneless (ecd) (Neubueser et al.,* 2005; *Gaziova et al.,* 2004). Since these genes do not encode enzyme products, it has been proposed that they could have a role in regulating ecdysone biosynthesis and in the transfer of the biosynthetic intermediate between cellular organelles.

During larval stages, ecdysone is produced and released in the prothoracic glands, that are specialized structures of the ring gland that is considered the most important endocrine larval tissue. In the adult this tissue does not persist and the hormone is produced in the fat body and in the ovary.

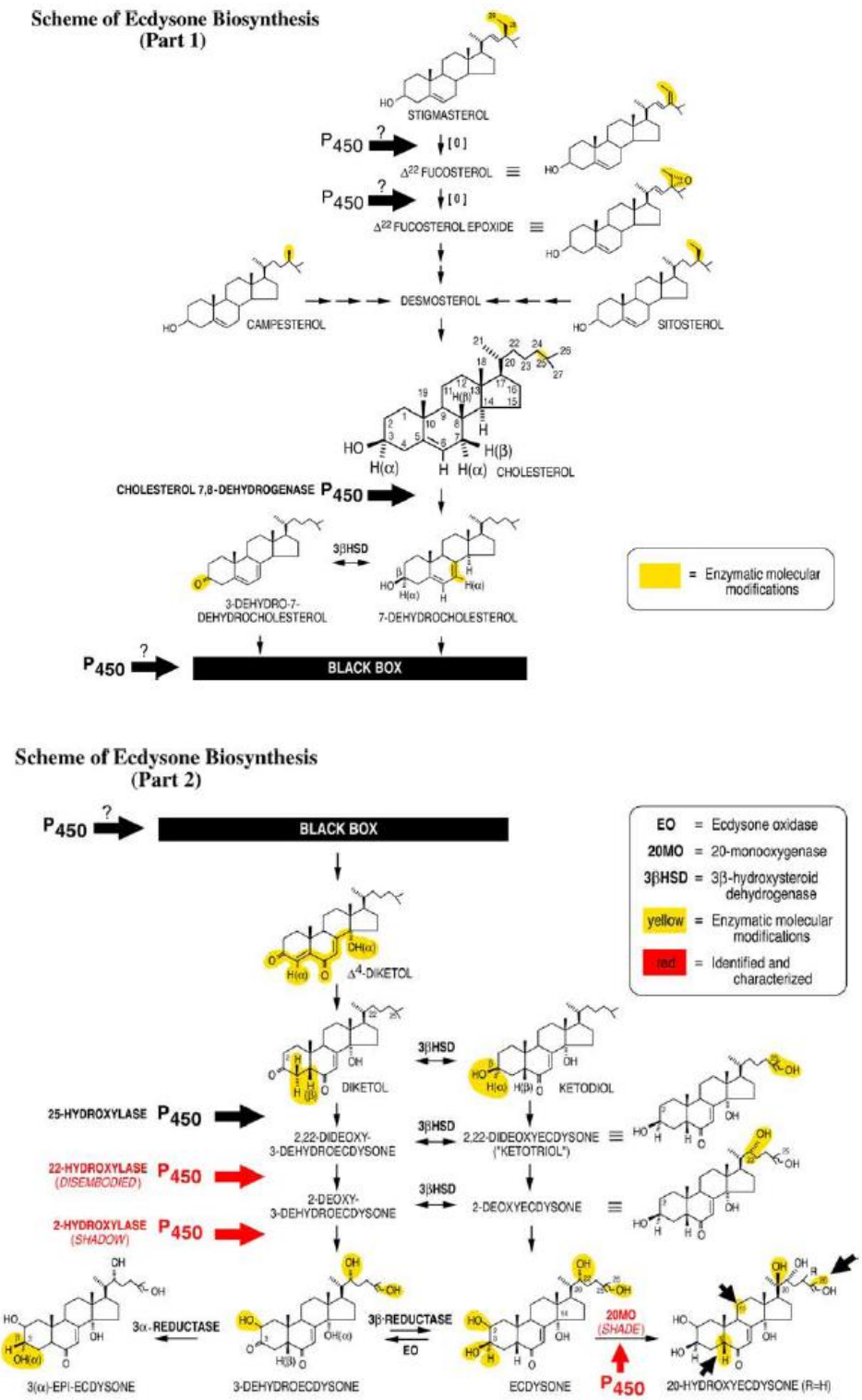

Figure 10: **Scheme of ecdysone biosynthesis from cholesterol.** Question marks denote possible involvement of P450 enzymes. Note specifically where the *Halloween* gene products act (red). 3-Dehydroecdysone is synthesized in the prothoracic glands of many insects and converted to ecdysone in the hemolymph (left column of part 2). For *Drosophila*, ecdysone is synthesized in the prothoracic cells of the ring gland (right column of part 2) (*Gilbert*, 2004).

Once released into the hemolymph, ecdysone is modified in peripheral tissues to become the active molting hormone 20-hydroxyecdysone (20E).

Each molt is initiated by one or more pulses of 20E. For a larval molt, the first pulse produces a small rise in the 20E concentration in the larval hemolymph and elicits a change in cellular commitment. A second, large pulse of 20E initiates the differentiation events associated with molting. The hydroxyecdysone produced by these pulses commits and stimulates the epidermal cells to synthesize enzymes that digest and recycle the components of the cuticle.

Juvenile hormone is secreted by the corpora allata, one of the two parts of the prothoracic gland. The secretory cells of the corpora allata are active during larval molts but inactive during the metamorphic molt. As long as JH is present, the 20-hydroxyecdysone-stimulated molts result in a new larval instar. In the last larval instar, however, the medial nerve from the brain to the corpora allata inhibits the gland from producing JH, and there is a simultaneous increase in the body's ability to degrade existing JH (*Safranek and Williams,* 1989). Both these mechanisms cause JH levels to drop below a critical threshold value. This triggers the release of PTTH from the brain. The resulting hydroxyecdysone, in the absence of high levels of JH, commits cells to pupal development. Larva-specific mRNAs are not replaced, and new mRNAs are synthesized whose protein products inhibit the transcription of the larval mRNAs.

After the second ecdysone pulse, new pupa-specific gene products are synthesized and the subsequent molt shifts the organism from larva to pupa. It appears, then, that the first ecdysone pulse during the last larval instar triggers the processes that inactivate the larva-specific genes and prepare the pupa-specific genes to be transcribed. The second ecdysone pulse transcribes the pupa-specific genes and initiates the molt (*Nijhout,* 1994). At the imaginal molt, when ecdysone acts in the absence of juvenile hormone, the imaginal discs differentiate, and the molt gives rise to the adult. Larval tissues such as the gut, salivary glands, and larval-specific muscles undergo programmed cell death and subsequent histolysis. The imaginal discs undergo physical restructuring and

differentiation to form rudimentary adult appendages such as wings, legs, eyes and antennae.

Ecdysone regulates a wide range of developmental and physiological responses in *Drosophila*, including reproduction, oogenesis, embryogenesis, post-embryonic development other than metamorphosis. Ecdysone also triggers neuronal remodeling in the central nervous system (*Schubiger et al.*, 1998).

Moreover, *Colombani et al.,* (2005) have demonstrated that ecdysone controls larval growth rate and final adult size and this function is mediated by an antagonistic interaction with insulin signaling.

Hence, ecdysone tightly coordinates the array of physiological changes that characterize each stage of the life cycle. Interestingly, while all tissues are exposed to the hormone, different tissue types have unique responses to the signal. This is ensured by the different spatial and temporal expression profile and unique biochemical properties of its nuclear receptors and by the ability of these receptors to interact with many cofactors.

1.9 Ecdysone-triggered programmed cell death during *Drosophila* development

Programmed cell death (PCD) plays a central role in animal development eliminating unwanted tissue, controlling cell numbers and removing cells that are dangerous for the organisms. Vast number of cells die during embryogenesis and imaginal discs differentiation, and entire structures are destroyed during pupal metamorphosis. Extensive cell death also occurs in the adult female during oogenesis as part of normal development and in response to poor environmental conditions.

A critical balance between death activators and death inhibitors determines the decision to live or to die. The steroid hormone ecdysone is one of the signals that could affect this balance regulating the patterns of PCD in a precise temporal and spatial pattern (*Yin and Thummel,* 2005).

Final effectors of PCD are caspases, a highly specialized class of cysteine proteases, whose activation is tightly controlled and occurs through proteolytic processing (*Danial*

and Korsmeyer, 2004). There are three initiator and four effector caspases in *Drosophila*. Caspases are negatively regulated by inhibitor of apoptosis proteins (IAPs) a highly conserved class of proteins that directly bind and inhibit caspases (*Steller,* 2008).

Ecdysone acts as a critical temporal signal in the insect and the most dramatic response to the hormone occurs during metamorphosis, when two sequential pulses of ecdysone direct the transformation of a crawling larva into a highly mobile and sexually reproductive adult fly. Two divergent developmental programs are activated by ecdysone during this process, a) the massive destruction of obsolete larval tissues by programmed cell death and b) the simultaneous growth and differentiation of adult tissues from small clusters of progenitor cells (*Riddiford,* 1993). In contrast to the balance between cell death activators and death repressors that determines the precise patterns of cellular apoptosis, destruction of the larval tissues during metamorphosis results from a major transcriptional switch in which multiple pro-apoptotic genes are coordinately induced by ecdysone. The hormone induces the death activator genes *reaper (rpr)* and *head involution defective (hid)*, the caspase gene *dronc*, the *Apaf-1* mammal ortholog *dark* and the CD36 *croquemort (crq)* (*Jiang et al.,* 2000; *Lee et al.,* 2003).

Interestingly, a similar regulatory pathway appears to be operative during latest stages of metamorphosis, when selected groups of neurons in the central nervous system undergo programmed cell death in response to the decreasing titer of ecdysone (*Robinow et al.,* 1993).

Also during *Drosophila* oogenesis PCD occurs at distinct stages and is triggered by both developmental and environmental stimuli (*McCall,* 2004). In particular, there is a key checkpoint at stage 8/9 controlled by ecdysone (*Terashima and Bownes,* 2005) and it is believed that this hormone is also involved in the germarium checkpoint (*McCall,* 2004).

It has been demonstrated that ovaries from nutrient-deprived flies are significantly reduced in size compared to ovaries from flies that have been conditioned on food

supplemented with yeast. Based on TUNEL assay, starved flies show an increase in apoptosis in the germarium and cell death is thought to serve as a mechanism to maintain the proper number of follicle cells that are needed to surround a germline cyst during oogenesis. Caspase-3 and Dcp-1 activity can be detected in the region 2 of the germarium implying that nutrient sensing pathways regulate the checkpoint in region 2 of the germarium through activation of caspases (*Peterson et al.*, 2003; *Hou et al.*, 2008). Increased levels of 20E are seen following nutrient deprivation and ectopic 20E can induce egg chamber degeneration at this stage suggesting that germarium checkpoint is controlled by ecdysone (*McCall*, 2004; *Pritchett et al.*, 2009).

In addition to the germarium, mid stage egg chambers from nutrient-deprived flies undergo cell death, characterized by nurse cell nuclear condensation and fragmentation, and engulfment by follicle cells. At this checkpoint, the egg chambers undergo a developmental selection, becoming committed to produce a mature egg or to undergo apoptosis.

Terashima and Bownes (2005) have demonstrated that this survival decision is regulated by the hormones 20E and JH. Also during mid-oogenesis increased levels of 20E are seen following nutrient deprivation suggesting that 20E induces PCD. Paradoxically, at this stage signaling of 20E is required for survival. These findings could be reconciled by a model in which a threshold level of 20E may determine the outcome in mid-oogenesis. Known 20E target genes *E74*, *E75* and *Br-C* show dynamic expression changes at this stage, with some Br-C isoforms increasing and others decreasing expression in response to nutrient deprivation. Interestingly, these genes also regulate each other and can be pro- or anti-apoptotic.

1.10 Ecdysone activity is mediated by an heterodimer of two nuclear receptor proteins

The ecdysone signal is transduced to target genes in the genome via the ecdysone receptor complex. This complex is made up of a heterodimer of the Ultraspiracle protein (USP) (*Shea et al.*, 1990; *Oro et al.*, 1990; *Henrich et al.*, 1994)

and the Ecdysone Receptor (EcR) proteins (*Koelle et al.,* 1991; *Koelle,* 1992; *Talbot et al.,* 1993; *Thomas et al.,* 1993; *Yao et al.,* 1992; *Yao et al.,* 1993). The EcR/USP complex binds ecdysone and affects transcription of ecdysone target genes. This molecular interaction is the means by which ecdysone regulates the genes responsible for the plethora of physiological changes that are characteristic of the developmental progression through the life cycle. These early genes encode transcription factors that coordinate the induction of large sets of secondary-response late genes, leading to the appropriate stage and tissue-specific biological responses.

1.10.1 EcR/USP heterodimer binds DNA to a consensus sequence EcRE

The DNA binding specificity plays a critical role in defining the repertoire of target genes that respond to the hormone.

Transcriptional regulation by the EcR/USP complex is mediated through binding to specific sequences, the so-called ecdysone response elements (EcREs), in the vicinity of ecdysone responsive target genes. Although several genes are known that are directly regulated by ecdysone, high-resolution mapping of the corresponding EcREs has been achieved only for a small set of tissue- and stage-specific genes from *Drosophila.*

The EcRE consensus finding suggests strongly that ecdysone receptors are members of the steroid receptor superfamily and that ecdysone acts by mechanisms homologous to those for the other steroids.

Similar to the hormone response elements (HREs) of vertebrate steroid hormones, most of the characterized EcREs are composed as imperfect palindromes GAGGTCA with two hexameric half-sites spaced by one A/T nucleotide. However, high affinity binding of the EcR/USP complex is also detected on direct repeats. This is the first report of a palindromic sequence being identified as the highest affinity DNA binding site for a heterodimeric nuclear hormone receptor complex.

The first characterized EcRE was mapped to the promoter of the *Drosophila* heat shock gene *hsp27,* a gene which is activated by both heat shock and ecdysone and which is expressed in pre-pupae and in ovarian nurse cells (*Riddihough and Pelham,* 1986). The

hsp27 EcRE is located in a 23 bp region upstream of the start codon (*Riddihough and Pelham*, 1987). It is the most efficient response element of genomic origin identified to date.

1.10.2 Ultrapiracle (USP)

USP is a transcription factor that plays a uniquely important role in differentiation, development and homeostasis through its ability to serve as a heterodimeric partner to many other nuclear receptors. It is homologous to the vertebrate Retinoid-X receptor (RXR), which demonstrates the ancient lineage of the nuclear receptor superfamily. Like USP, the RXR functions in numerous hormone driven developmental pathways as a partner with other hormone receptors.

In *Drosophila* there is one transcript of *usp*, which is expressed throughout larval life and metamorphosis (*Andres et al.*, 1993; *Henrich et al.*, 1994). *usp* mRNA encodes a single 507 amino acid product that is characterized by the presence of two zinc finger domains. Toward the N-terminal end there is a transactivation domain. The hormone binding domain is located toward the C-terminal end (*Henrich*, 1990).

1.10.3 Ecdysone Receptor (EcR)

The *EcR* gene was identified in a screen of the *Drosophila* genome for members of the steroid receptors superfamily (*Koelle et al.*, 1991) and later it has been shown that it is more closely related to the vertebrate Farnesoid X-receptor (*Mangelsdorf*, 1995).

Three protein isoforms are encoded by *EcR* locus, designated EcR-A, EcR-B1 and EcR-B2. The A and B isoforms are encoded by overlapping transcription units that have different promoters and can be separately controlled. The N-terminal amino acids of EcR-A are encoded by three exons specific to that isoform, while both the DNA binding and ligand binding domains of EcR-A are encoded by exons shared with the other two isoforms. The B1 and B2 isoforms are encoded by mRNAs that derive from the *EcR-B* primary transcript by alternative splicing (*Talbot et al.*, 1993) (Figure 11).

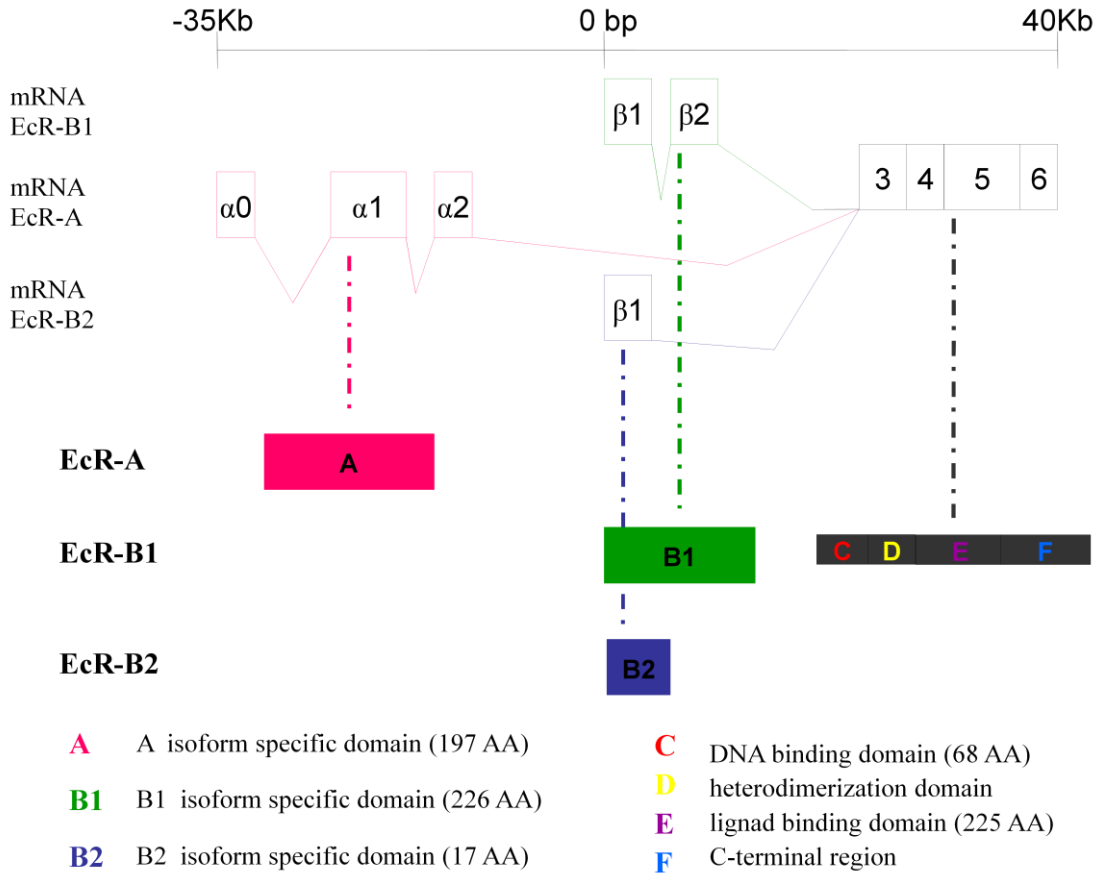

Figure 11: **Schematic view of *EcR* locus and of the products encoding different EcR isoforms** (Modified from *Talbot et al.*, 1993).

EcR isoforms are defined by the presence of a specific N-terminal region and by the presence of common structural elements, that are conserved domains characteristic of steroid receptor superfamily members: a highly conserved DNA-binding domain (DBD) and a ligand-binding domain (LBD) that are joined by a flexible hinge region. The DBD or C region is a 66-68 amino acid domain and comprises two C4 zinc fingers. The first zinc finger provides DNA-binding specificity through a stretch of five amino acids known as the P-box143. The second zinc finger harbors a relatively weak dimerization interface that allows DBD to dimerize only in the presence of a target DNA molecule.

The other conserved domain, LBD or E region, is a 225 amino acid domain located at C-terminal to the DBD, and constitutes the principal dimerization interface of the protein. The LBD allows different receptors to dimerize, thereby vastly expanding the repertoire of potential DNA target sequences and regulatory functions. The LBD

comprises 11-13 α-helices that generally form a hydrophobic pocket for the binding of small lipophilic molecules.

These two domains are separated by a ~70 amino acid hinge called "D region", whose function could be required in heterodimerization (*Mouillet et al.*, 2001; *Cherbas et al.*, 2003; *Hu et al.*, 2003).

Moreover, EcR is characterized by the presence at C-terminal of a 223 amino acid unusual domain called "F region" which function remains still unclear. *Cherbas* et al. (2003) demonstrated that EcRs lacking this region are indistinguishable in ligand binding, affinity for USP, affinity for DNA and transcriptional activation.

The isoform-specific N-terminal domains, called A/B region, are not significantly similar to each other or to other known protein sequences. This region is of 197, 226 and 17 amino acids in length respectively for EcR-A, EcR-B1 and EcR-B2 (Figure 10) and it has been demonstrated that it is responsible for the response specificity to the ecdysone stimulus (*Talbot et al.*, 1993).

Nuclear receptors activate the transcription of target genes through a specific region called activation function AF. EcR contains two activation surfaces: a strongly conserved activation function (AF2) in its ligand binding domain that is often ligand-dependent, and a second activation function (AF1) located at the N-terminal that can act in a ligand-independent fashion. Detailed structural and molecular studies have shown that, upon hormone binding, the LBD switches into an active state by rotating helix 12 into a configuration in which it can recruit transcriptional co-activators through its AF2 domain.

The expression patterns of the EcR isoforms show an intricate spatial and temporal pattern that in many cases can be correlated with specific cellular responses to the hormone (*Robinow et al.*, 1993; *Talbot et al.*, 1993; *Truman et al.*, 1994).

From the observed expression patterns, it has been inferred that EcR-A is primarily responsible for adult differentiation, and that EcR-B1 directs metamorphosis of larval tissues (*Talbot et al.*, 1993; *Truman et al.*, 1994). This hypothesis is supported by the phenotypes of *EcR* mutants: loss of EcR-B1 leads to developmental arrest at the onset

of metamorphosis, with an uncoupling of developmental events. Larval structures fail to undergo the first phases of metamorphosis, such as retraction of the gastric cecae, larval neuronal pruning, and formation and tanning of the puparium, whereas adult tissues begin metamorphosis, e.g. elongation of imaginal discs and expansion of the optic lobes of the brain (*Bender et al.,* 1997; *Schubiger et al.,* 1998, *Schubiger et al.,* 2005). Mutants that lack both *EcR-B1* and *EcR-B2* die primarily at the first and second molts, with some escaping to the third instar where they show a similar, but more pronounced, phenotype as the *EcR-B1* mutants (*Schubiger et al.,* 1998).

Moreover EcR-A mutants have been isolated and show arrest during early to mid pupal development, indicating a requirement for EcR-A subsequent to formation of the basic pupal body plan (*Davis et al.,* 2005). The developmental arrest in the EcR-A mutants occurs later than in EcR-B mutants and might reflect a specific role for EcR-A in adult differentiation.

2-Aim of research

Like in metazoan, hormonal signaling plays key regulatory roles in *Drosophila* development and principally involves the steroid hormone ecdysone (*Riddiford et al.,* 2000). Few hormones have puzzled and fascinated entomologists as ecdysone did. This is obviously due to this hormone's pleiotropic functions, ranging from orchestrating metamorphosis in concert with the juvenile hormone to regulating female fertility by stimulating vitellogenin synthesis in the fat body and its uptake by the growing oocyte.

Ecdysone tightly coordinates the array of physiological changes that characterize each stage of the life cycle of insects and this activity is mediated by its nuclear receptor that regulates ecdysone-response genes. Interestingly, while all tissues are exposed to the hormone, different tissue types have unique responses to the signal.

During my PhD research program I've analyzed the role of ecdysone signaling during *Drosophila melanogaster* development. The aim of my studies is to gain insight into the molecular mechanisms through which the hormone fulfills its pleiotropic functions in two different developmental stages: the oogenesis and the imaginal wing disc morphogenesis.

To address this issue, I analyzed the effect of blocking ecdysone signaling in follicle cells during oogenesis and/or in wing and eye imaginal disc development using reverse genetic approaches.

I focused my studies on investigating the role of ecdysone in follicular epithelium morphogenesis through silencing of the hormone nuclear receptor gene, *EcR* taking advantage of dominant negative forms of this receptor and using RNA interference approach.

In addition, during the period that I spent in Prof. Jindra's lab, I explored in imaginal disc morphogenesis the function of *ecd*, a gene involved in ecdysone signaling. In particular, I analyzed the effect of an *ecd* loss-of-function mutation, ecd^{l23}, in eye imaginal discs and the effect of *ecd* silencing through RNA interference transgene expression in wing disc development.

3-Materials and Methods

3.1 Fly food

The *Drosophila melanogaster* strains used were grown on a corn meal based food supplemented with glucose, yeast, agar and water. The food is prepared by melting 10 gr and 50 gr of glucose in 1600 ml water. Then 150 gr of corn meal are added and food is cooked for 15 minutes mixing well. Afterward 50 gr of yeast are added and food is cooked for 10 minutes more, again on medium and mixing well. While food is cooking, 4 gr of Nipagine, an antimicotic, are dissolved in 16 ml of EtOH 98% and added. The food is left to dry for at least 2 hours.

3.2 Fly strains

The following stocks are used:

- y^1, w^{67c23} as a wild-type stock;
- 7: *P{ry*$^{+t7.2}$*=hsFLP}1, y*^{1}*, w*^{1118}*; +/+; Dr*^{Mio}*/TM3, ry***, Sb*^{1} (*Golic*, 1991, Bloomington). In the text the transgene will be referred as *hs-Flp*;
- 4775: *w*^{1118}*; P{w*$^{+mc}$*=UAS-GFP.nls}14; +/+* (*Robertson et al.*, 2003, Bloomington). In the text the transgene will be referred as *UAS-GFP*;
- 4779: *y*^{1}*, w***, P{w*$^{+mc}$ *=GAL4-act5c(FRT.CD2).P}D; +/+; +/+* (*Pignoni and Zipursky*, 1997, Bloomington). In the text the transgene will be referred as *act5c>CD2>Gal4;*
- 5138 : *w***; +/+; TM6B/P{w*$^{+mc}$*=tubP-GAL4}LL7* (*Lee and Luo*, 1999, Bloomington). In the text the transgene will be referred as *tub-Gal4*;
- 7018: *w**; *noc*^{Sco}/CyO; P{*w*$^{+mC}$*=tub*P-GAL80^{ts}}7 (*Davis et al.*, 2003, Bloomington). Here the transgene will be referred as *tub-Gal80*^{ts}*;*
- 7019: *w**; P{*w*$^{+mC}$*=tub*P-GAL80^{ts}}20; TM2/TM6B, *Tb*^{1} (*Davis et al.*, 2003, Bloomington). In the text the transgene will be referred as *tub-Gal80*^{ts}*;*
- 9328: *w*^{1118}*; +/+; P{w*$^{+mc}$*=UAS-EcR.AdsRNA}91/TM3, P{w*$^{+mc}$*=ActGFP}JMR2, Ser*^{1} (*Roignant et al.*, 2003, Bloomington). In the text the transgene will be referred as *UAS-IR-EcR-A*;

- 9329: *w^{1118}; +/+; P{w^{+mc}=UAS-EcR.B1.dsRNA}168 (Roignant et al*, 2003, Bloomington). In the text the transgene will be referred as *UAS-IR-EcR-B1*;
- 9449: *w^{*}; P{w^{+mc}=UAS-EcR.B2.W650A}TP5; +/+* (*Cherbas et al.*, 2003, Bloomington). In the text the transgene will be referred as *UAS-EcR-DNW650A*;
- 9450: *w^{*}; +/+; P{w^{+mc}=UAS-EcR.B2.F645A}TP1* (*Cherbas et al.*, 2003, Bloomington). In the text the transgene will be referred as *UAS-EcR-DNF645A*;
- *w^{*}; IF/CyO; TM6B/MKRS*, generated in our lab;
- *w^{*}; Cy2-Gal4; +/+* (*Queenan et al.*, 1997), kindly provided by T. Schüpbach, Princeton University;
- *w^{*}; en-Gal4, UAS-GFPnls/GBc; +/+*, kindly provided by D.Grifoni;
- *hs-Flp; act5c>y^{+}>Gal4, UAS-GFPnls* (*Gaziova et al.*, 2004), generated in M. Jindra's lab;
- *ey-Flp; act>y^{+}>Gal4, UAS-GFPnls/CyO; FRT2A,tub-Gal80/TM6B* (*Gaziova et al.*, 2004), generated in M. Jindra's lab;
- *w^{*}; +/+; FRT2A, ecd ^{l23}/TM6B* (*Gaziova et al.*, 2004), generated in M. Jindra's lab;
- *w^{*}; +/+; FRT2A* (*Gaziova et al.*, 2004), generated in M. Jindra's lab;
- *w^{*}; +/+; UAS-ecdRNAi/TM6B* generated in M. Jindra's lab.

3.3 Clonal Analysis

Clonal overexpression of *UAS-EcR-DNF645A* transgene was obtained using the Flp/Gal4 technique by crossing the appropriate fly strains. Females of the genotype *y^{1}, w, P{w^{+mc}=Gal4-Act5C(FRT.CD2).P}D*; *SM5/P{w^{+mc}=UAS-GFP.nls}14* were crossed to males *P{$ry^{+t7.2}$=hsFLP}1, w^{1118}; P{w^{+mc}=UAS-EcR.B2.F645A}TP1* at 25°C. Freshly eclosed females *P{$ry^{+t7.2}$=hsFLP}1, w^{1118}/y^{1}, w, P{w^{+mc}=Gal4-Act5C(FRT.CD2).P}D; P{w^{+mc}=UAS-GFP.nls}14/+; P{w^{+mc}=UAS-EcR.B2.F645A}TP1/+* were collected and heat shocked three times for 1 hour at 37°C. After each heat shock these females were transferred to fresh vials with *yw^{67c23}* males and incubated at 25°C. Before dissection, the flies were transferred to fresh, yeasted food daily at 29°C for two days.

Clonal overexpression of two copies of *UAS-IR-EcR-B1* transgene was obtained using the Flp/Gal4 technique by crossing the appropriate fly strains. Females of the genotype y^1, *w, P{w*$^{+mc}$*=Gal4-Act5C(FRT.CD2).P}D; P{w*$^{+mc}$*=UAS-EcR.B1.dsRNA}168/TM3, ry Sb*^{1} were crossed to males of the genotype *P{ry*$^+$*, hsFLP}, y*^{1}*, w*^{1118}*/Y; P{w*$^{+mc}$*=UAS-EcR.B1.dsRNA}168/TM3, ry, Sb*^{1} at 25°C. Freshly eclosed females of the genotype *P{ry*$^+$*, hsFLP}, y*^{1}*, w*^{1118}*/y*^{1}*, w, P{w*$^{+mc}$*=Gal4-Act5C(FRT.CD2).P}D; P{w*$^{+mc}$*=UAS-EcR.B1.dsRNA}168/P{w*$^{+mc}$*=UAS-EcR.B1.dsRNA}168* were collected and heat shocked four times for 1 hour at 37°C. After each heat shock these females were transferred to fresh vials with *yw*^{67c23} males and incubated at 25°C. Before dissection, the flies were transferred to fresh, yeasted food daily at 29°C for seven days.

ecd ^{l23} clonal analysis was carried out using Flp/FRT system (*Lee and Luo,* 1999). Females of the genotype *ey-Flp; act>y*$^+$*>Gal4, UAS-GFPnls/CyO; FRT2A,tub-Gal80/TM6B* were crossed respectively to males of the genotype *w***; FRT2A, ecd*^{l23}*/TM6B and w***; FRT2A* at 25°C. L3 larvae with genotype *ey-Flp; act>y*$^+$*>Gal4, UAS-GFPnls/+; FRT2A, ecd*^{l23} */+* and *ey-Flp; act>y*$^+$*>Gal4, UAS-GFPnls/+; FRT2A/+* were dissected and imaginal eye discs were extracted.

Clones overexpressing the *UAS-ecdRNAi* transgene were obtained crossing females of the genotype *hs-Flp; act5c>y*$^+$*>Gal4, UAS-GFPnls* to males *w***; UAS-ecdRNAi/TM6B* at 25°C. After two heat shock (48 hours and 72 hours after AEL), L3 larvae were dissected and imaginal eye and wing discs were extracted.

3.4 Gal4 Driven Expression in Follicle Cells

Females *P{w*$^{+mc}$*=tubP-GAL80*^{ts}*}7/+;P{w*$^{+mc}$*=UAS-EcR.B2.F645A}TP1/P{w*$^{+mC}$*=tubP-GAL4}LL7,* females *w; P{w*$^{+mc}$*=tubP-GAL80*^{ts}*}7/+; P{w*$^{+mc}$*=UAS-EcR.B1.dsRNA}168/P{w*$^{+mC}$*=tubP-GAL4}LL7* and females *w; P{w*$^{+mc}$*=tubP-GAL80*^{ts}*}7/+; P{w*$^{+mC}$*=UAS-EcR.AdsRNA}91/P{w*$^{+mc}$*=tubP-GAL4}LL7* were obtained by crossing the parental strains. The crosses were performed at 18°C and before

dissection, female progeny was transferred with *yw*^{67c23} males to yeasted vials at 31°C for six days.

Females *w; Cy2-Gal4/+; P{w*$^{+mC}$*=tubP-GAL80*^{ts}*}7/ P{w*$^{+mC}$*=UAS-EcR.B2.F645A}TP1* and *w; Cy2-Gal4/+; P{w*$^{+mC}$*=tubP-GAL80*^{ts}*}7/ P{w*$^{+mC}$*=UAS-EcR.B1.dsRNA}168* were obtained by crossing the parental strains. The crosses were performed at 18°C and female progeny was transferred with *yw*^{67c23} males to yeasted vials at 18°C for 24 hours and then was transferred to yeasted vials at 31°C for 48 hours before dissection.

Females *w***;en-Gal4, UAS-GFPnls/+; UAS-ecdRNAi* were obtained by crossing the parental strains at 25°C. L3 larvae were dissected and imaginal eye and wing discs were extracted.

3.5 Immunofluorescence Microscopy

Ovaries were dissected at room temperature in phosphate buffer saline (1xPBS) pH 7.5, fixed in 4% paraformaldehyde in 1xPBS pH7.5 freshly prepared for 20 minutes at room temperature. After three washes 5 minutes each in 1xPBT (1xPBS pH7.5+ 0.1% Triton X-100), egg chambers were dissected with needles and permeabilized without rotation with 1xPBS pH7.5+ 1% Triton X-100 overnight at 4°C. Next day egg chambers were washed three times 10 minutes each in 1xPBT and 10 minutes in 1xPBT+3%BSA solution. After that the egg chambers were incubated for 4 hours at room temperature on a rotating wheel with primary antibodies diluted in 1xPBT+3%BSA. After three washes 15 minutes each in 1xPBT, egg chambers were incubated at room temperature on a rotating wheel with secondary antibodies diluted in 1xPBT+3%BSA. After several washes in 1xPBT, egg chamber were mounted on miscroscopy slides in Fluoromount G (Electron Microscopy Sciences), an anti-quenching slide mounting medium. Subsequently samples were analyzed with conventional epifluorescence on a Nikon Eclipse 90i microscope and with TCS SL Leica confocal system.

For DAPI nuclear staining after incubation with secondary antibodies the ovaries were washed two times in 1xPBT and then incubated for 10 minutes with DAPI (4'-6-diamidino-2-phenylindole, Sigma) at 1μg/ml in 1xPBS and, after several washes with 1xPBT, the egg chambers were mounted in Fluoromount G**.**

For Propidium Iodide and To-Pro-3 nuclear counterstaining the ovaries were washed three times in 1xPBT and treated with RNase A (400 μg/ml in PBS, Sigma) for 2 hr. After three 10 minutes washes in 1xPBT, the ovaries were labeled for 15 minutes with Propidium Iodide (5 μg/ml in 1xPBT, Molecular Probes) or for 30 min with To-Pro-3 (1 μg/ml in 1xPBT, Molecular Probes). Afterwards, the egg chambers were washed three times in 1xPBT and mounted in Fluoromount G for Propidium Iodide or DABCO (Sigma Chemicals) for To-Pro-3.

FITC-Phalloidin and TRITC-Phalloidin staining were carried out, after incubation with secondary antibodies, by washing ovaries three times with 1xPBS and then by incubating for 20 minutes at room temperature the egg chambers with FITC-Phalloidin (40 μg/ml in 1xPBS, Sigma) or TRITC-Phalloidin (40 μg/ml in 1xPBS, Sigma) and after several washes with 1xPBT, the egg chambers were mounted as indicated above**.**

Larvae were dissected in 1xPBS at room temperature and fixed for 20 minutes in 4% formaldehyde. After three washes in 1xPBS, tissues were permeabilized for 1 hour in 1xPBS+0.3% Triton X-100 without rotation and incubated with 1xPBS+0.3% Triton X-100+2%BSA to increase antibody specificity reducing background. Tissues were then incubated with primary antibodies in 1xPBS+0,3% Triton X-100+2%BSA solution overnight at 4°C without rotation. The day after, tissues were accurately washed three times in 1xPBT+0,3% Triton X-100 (10 minutes) and subsequently incubated with 1xPBT+0,3% Triton X-100+2%BSA for 15 minutes. Next, tissues were incubated with secondary antibodies for 2 hours at room temperature on a rotating wheel. After several washes in 1xPBT+0,3% Triton X-100, wing and eye imaginal discs were mounted on microscopy slides with Fluoromount G. Subsequently, samples were analyzed as described above.

3.6 Tunel Analysis

Ovaries were dissected at room temperature in phosphate buffer saline (1xPBS) pH 7.5, fixed in a solution freshly prepared of 100 μl Devitellinizing buffer (100mM K-phosphate pH6.8, 450mM KCl, 150mM NaCl, 20mM $MgCl_2.6H_2O$, formaldehyde 37% in H_2O) and 600 μl eptan for 30 minutes at room temperature on a rotating wheel. After three washes 10 minutes each in 1xPBS, egg chambers were dissected with needles and permeabilized for 30 minutes with a solution of 1xPBS pH7.5+0.1% Triton X-100+0.1% Na-Citrate at room temperature on a rotating wheel. After two washes 10 minutes each with 1xPBS, egg chambers were incubated in 250 μl of TUNEL slution (5X Reaction Buffer, 25mM $CaCl_2$, 1mM d-UTP-digoxigenin, 25U/μl TdT) for 90 minutes at 37°C in dark condition. Afterward, egg chambers were accurately washed several times with 1xPBS and then for 15 minutes in 1xPBT+3%BSA. Next, egg chambers were incubated with FITC-conjugated-digoxigenin antibody for 1 hour at room temperature on a rotating wheel. After incubation, ovaries were washed many times with 1xPBT, mounted with Fluoromount G and then analyzed with conventional epifluorescence microscope.

3.7 Antibodies

The following primary antibodies were used in this study:

- monoclonal mouse anti-Armadillo (N27A1, DSHB, *Riggleman et al.,* 1990) detects the N-terminal region of Armadillo protein (58 aa, bp 2011-2175) and was used at 1:10 dilution;
- monoclonal mouse anti-CD2 (MCA154G, SEROTEC, *Whiteland et al.,* 1995) recognizes the rat CD2 cell surface antigen, a 50-54 kDa glycoprotein expressed by thymocytes and mature T cells and was used at 1:250 dilution;
- polyclonal rabbit anti-Cleaved Caspase-3 (9661, Cell Signaling Technology, *Fernandes-Alnemri et al.,* 1994) detects endogenous levels of a large fragment (17/19 kDa) of activated caspase-3 resulting from cleavage adjacent to Asp175 and was used at 1:50 dilution;

- monoclonal mouse anti-DE-Cadherin (DCAD2, DSHB, *Oda et al.,* 1994) is directed against a 41 aminoacids region in the N-terminal domain and was used at 1:25 dilution;
- monoclonal mouse anti-Diap1 protein, kindly provided by B. Hay, was used at 1:1000 dilution;
- sheep anti-Digoxigenin-fluorescein (1207741, Roche) is directed against the whole Digoxigenin protein and conjugated with 5(6)-carboxy-fluorescein-N-hydroxy-succinimide ester (FLUOS) and was used at 1:100 dilution;
- monoclonal mouse anti-Discs large, DLG (4F3, DSHB, *Parnas et al.,* 2001) recognizes the second PDZ domain of Dlg protein and was used at 1:50 dilution;
- polyclonal rabbit anti-ecdisoneless (*Gaziova et al.,* 2004) recognized a specific domain of the *Drosophila* ecdysoneless protein (aa 270-429) and was used at 1:500 dilution;
- monoclonal mouse anti-EcR-B1 (AD4.4, DSHB, *Talbot et al.,* 1993) specifically recognizes the B1 isoform (aa 68-222) of EcR and was used at 1:10 dilution;
- monoclonal mouse anti-Phospho-SAPK/JNK (G9, Cell Signaling Technology, *Whitmarsh and Davis*, 1998) is against residues surrounding Thr183/Tyr185 of human SAPK/JNK and was used at 1:100 dilution;
- polyclonal rabbit anti-pSMad (PS1, *Persson et al.,* 1998) was raised against a synthetic peptide corresponding to the phosphorylated C-terminus of human Smad1 whose amino acid sequences at C-terminal tails (SSVS) are identical to the *Drosophila* counterpart, Mad and was used at 1:500 dilution;
- monoclonal mouse anti-dMyc, kindly provided from P. Gallant (*Gallant et al.,* 1996) is directed against the *Drosophila* whole protein and was used at 1:5 dilution;
- polyclonal rabbit anti-phospho-histone-H3 (06-570, Upstate Biotechnology, *Mahadevan et al.,* 1991) recognizes and is specific for the N-terminal (aa 7-20) of the human phosphorylated histone H3 and was used at 1:200 dilution;

- polyclonal rabbit anti-ξPKC (C-20, sc-216, Santa Cruz Biotechnology, *Takai et al.,* 1979) is against the C-terminal peptide of ξPKC and was used at 1:200 dilution;
- polyclonal rabbit anti-Scribble, kindly provided by C.Q. Doe (*Albertson and Doe,* 2003), recognizes the C-terminal 431 aminoacids region of Scribble protein and was used at 1:200 dilution;
- monoclonal mouse anti-Wingless, Wg (4D4, DSHB, *Brook and Cohen,* 1996), recognizes a region of *Drosophila* Wingless protein (aa 3-468) and was used at 1:50 dilution.

Secondary antibodies:

- rabbit antibodies were detected with Cy3-conjugated sheep anti-rabbit used 1:3000 (Sigma), Cy3-conjugated goat anti-rabbit used 1:2000 (Jackson), Cy5-conjugated goat anti-rabbit used 1:500 (Jackson) and BODIPY-conjugated goat anti-rabbit used 1:2000 (Sigma);
- mouse antibodies were detected with Cy3-conjugated goat anti-mouse used 1:800 (Jackson), Cy5-conjugated goat anti-mouse used 1:500 (Jackson), FITC-conjugated goat anti-mouse used 1:250 (Molecular Probes) and TEXAS RED goat anti-mouse used 1:400 (Sigma).

4-Results

4.1 Ecdysone and oogenesis

The steroid hormone ecdysone regulates larval development and metamorphosis in *Drosophila melanogaster* through a complex genetic hierarchy that begins with a small set of early response genes (*Thummel,* 1996).

The major and best-studied source of ecdysone in insect larvae is the prothoracic gland, which in *Drosophila* consists of the lateral lobes of the ring gland (*Dai and Gilbert,* 1991). After this, part of the ring gland degenerates during metamorphosis, fat bodies and adult ovaries contribute to the whole body steroid titer (*Garen et al.,* 1977; *Bownes,* 1989; *Warren et al.,* 1996). The main role of ecdysone in the ovary of adult females is to regulate vitellogenesis (*Hagedorn,* 1985; *Bownes et al.,* 1996).

Although ecdysone response has been characterized successfully in larval development and metamorphosis, the precise role of this hormone in *Drosophila* oogenesis has not been extensively studied.

Several findings have demonstrated that ecdysone signaling is required for normal oogenesis and in particular, *Buszczak et al.,* (1999) provided evidence that components at several levels of the ecdysone response pathway, such as steroidogenic enzymes, ecdysone receptors and ecdysone response genes, are each functionally required in the ovary. The authors reported that transcription of the early ecdysone response genes *E75* and *E74* is up-regulated during stage 8 in both the nurse cells and somatic follicle cells. Germline clones of *E75* mutant cells result in degeneration of egg chambers after stage 8.

Broad-Complex expression in the somatic follicle cells regulates the establishment of dorso-ventral polarity of the eggshell in late oogenesis (*Deng and Bownes,* 1997) and leads to prolonged endoreplication and to additional amplification of selected genes (*Tzolovsky et al.,* 1999). In addition, Br-C expression in the follicle cells controls the cell fate of the egg chamber, determining if it will progress to develop into an egg or induce apoptosis (*Terashima and Bownes,* 2004). Hence the ovarian ecdysone titer controls the apoptosis/development decision of individual egg chambers by regulation of the patterns of Br-C isoform expression.

Furthermore, the finding and characterization of different mutations of *ecdysoneless*, that is a gene required for ecdysteroids biosynthesis, supports that ecdysone is required for egg chamber progression past stage 8. Germline clones completely lacking *ecd* function arrest at pre-vitellogenic stages thus showing that *ecd* is autonomously required for oocyte maturation (*Gaziova et al.*, 2004).

The ecdysone receptor EcR, which is crucial for regulation of expression of the early response genes, has also been shown to be fundamental in the germline, as mutant germline clones arrest development during mid-oogenesis (*Carney and Bender*, 2000; *Buszczak et al.*, 1999). Mutants trans-heterozygous for EcR^{A483T} and an *EcR* null mutation are viable when raised at low temperature but do not survive to adulthood at elevated temperature, suggesting that *EcR* function is lost or reduced at high temperature. At restrictive temperature, *EcR* mutant females show severely reduction of fecundity and defects in oogenesis, including an excess of mature stage 14 egg chambers, loss of vitellogenic egg chambers, and presence of abnormal egg chambers. In addition to the defects mentioned above, ovaries from *EcR* females contain many defective or degenerating egg chambers. These defects include small nurse cell nuclei, breakdown of nurse cell nuclei in early vitellogenic egg chambers, and breakdown or loss of both follicle cell and nurse cell nuclei in some egg chambers.

It has been demonstrated that tissue-specific modulation of EcR activity by the Ras signaling pathway refines temporal ecdysone signals that regulate follicle cell differentiation and cadherin-mediated epithelial cell shape changes. Using a dominant negative form of EcR in combination with two drivers active in the follicle cells, *Hackney et al.,* (2007) the authors showed that expression of EcR-DN resulted in thin eggshell, small egg and dorsal appendage phenotypes. Moreover, it has been reported that EcR is involved on eggshell production by controlling chorion gene transcription and amplification (*Hackney et al.,* 2007).

During my PhD, I have been also involved in a project focused on the regulatory elements controlling the expression of the eggshell gene *VM32E* and we have shown that this gene is positively regulated by the B1 isoform of EcR (*Bernardi et al.,* 2009).

Thus ecdysone, the ecdysone receptor and ecdysone response genes are clearly crucial for a number of developmental decisions in normal oogenesis.

4.2 Ubiquitous expression of EcR-DN in follicular epithelium causes degeneration of egg chambers

The *EcR* locus is located on the right arm of the second chromosome at 42A, close to the centromere and proximal to available FRT insertion sites (*Koelle et al.*, 1991; *Koelle*, 1992), hampering Flp-mediated mosaic analysis. Given this technical limitation, to study *EcR* function during oogenesis I took advantage of two dominant negative forms of EcR, EcR-DNF645A and EcR-DNW650A, expressed through the UAS/Gal4 system (*Brand and Perrimon*, 1993).

The dominant negative forms used cannot mediate transcriptional activation and disrupt EcR signaling by competing with wild-type EcR binding to ligand, USP and DNA (*Cherbas et al.*, 2003). These mutants are characterized by the presence of a single mutation in the helix 12 in the ligand binding domain (LBD) (Figure 12, see upper panel). In particular, the receptor EcR-DNF645A presents the substitution of a conserved phenylalanine with an alanine in position 645, while EcR-DNW650A presents the substitution of the tryptophane in position 650. The F645A mutation is in the co-activator binding groove in the AF2 domain and results in a receptor that binds ligand but cannot mediate activation. The W650A mutation prevents hormone binding, and consequently, also results in a lack of ligand-dependent activation.

Moreover, these receptors lack the unusual F region (223 aa) located at C-terminal. *In vitro* assays demonstrated that EcR lacking this region is indistinguishable in ligand binding, affinity for USP and DNA and transcriptional activation (Figure 12, see lower panel).

WT	KNRK**L**PK **F** **LEEI** **W** DVHAIPPSVQSHLQITQEENER
ΔC655	KNRK**L**PK **F** **LEEI** **W** DVHAI
F645A	KNRK**L**PK **A** **LEEI** **W** DVHAI
W650A	KNRK**L**PK **F** **LEEI** **A** DVHAI

	Binding to DNA	**Binding to ligand**	**Dimerization with USP**	**Activation of transcription**
Δ655A	wild type	wild type	wild type	100%
F645A	wild type	wild type	wild type	1%
W650A	wild type	undetectable	wild type	0%

Figure 12: **Properties of dominant-negative mutant forms of EcR used**. In the upper panel are shown sequences for the region around helix 12 of the ligand binding domain (LBD). Bold type indicates strongly conserved residues, while mutated residues are green and underlined. In the lower panel are shown *in vitro* functional assays describing dominant negative receptors abilities to bind the partner USP, bind DNA and activate transcription of early response genes (Modified from *Cherbas et al*., 2003).

EcR-DNF645A and EcR-DNW650A both act as competitive inhibitors of wild type EcR in cell culture assays; therefore they are dominant negative mutants that interfere with ecdysone-induced gene activation (*Cherbas et al.,* 2003). *In vivo* these mutants have been already employed to block EcR signaling to gain insight into its involvement in larval neuronal remodeling, endoreplication and chorion gene amplification (*Cherbas et al.*, 2003; *Brown et al.*, 2006; *Hackney et al.*, 2007; *Sun et al.*, 2008).

To determine the effects of blocking *EcR* signaling through dominant negative overexpression in all somatic cells during oogenesis, I expressed EcR-DNF645A or EcR-DNW650A using the ubiquitous and strong *tub-Gal4* driver (*O'Donnell et al.,* 1994).

To circumvent the lethality during development, I utilized the *tub-Gal80^{ts}* transgene encoding a temperature-sensitive form of the Gal4 inhibitor Gal80 (Gal80^{ts}), which blocks Gal4 activity at the permissive low temperature (18°C), while it fails to inhibit Gal4 at the higher restrictive temperature (31°C) (*McGuire et al.*, 2003) (Figure 13).

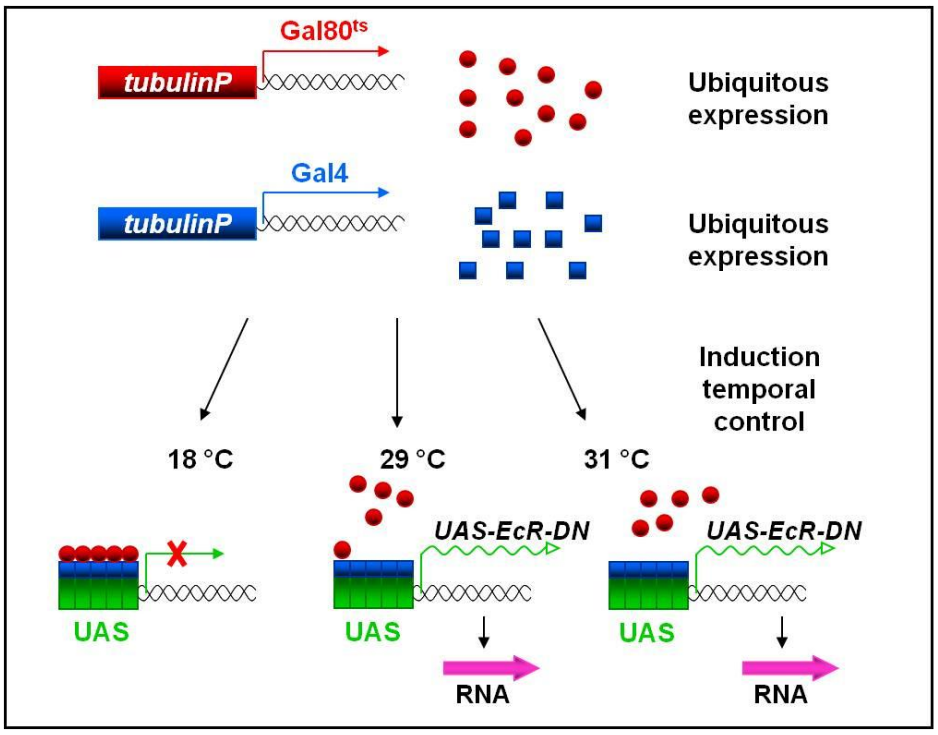

Figure 13: **Schematic representation of the UAS/Gal4 and Gal80^{ts} system used to ubiquitously knock down *EcR* in the follicular epithelium.** At the permissive low temperature (18°C) the temperature-sensitive Gal80^{ts} form blocks Gal4 activity. At higher temperature (29°C) Gal80^{ts} is still active while at 31°C Gal80^{ts} fails to inhibit Gal4 which can lead transcription of UAS-linked transgenes (Modified from *Roman*, 2004).

To this purpose, adult flies of the correct genotype were crossed at 18°C. F1 female progeny *tub-Gal80^{ts}/+; tub-Gal4/UAS-EcR-DN* were kept at 31°C for 6 days to induce Gal4 activity and thus EcR-DN expression. After that, flies were dissected and ovaries extracted.

I analyzed egg chambers from females expressing the transgene encoding EcR-DNW650A and from females expressing EcR-DNF645A and in both cases I found degeneration of egg chambers since early stages of oogenesis, degeneration that is not found in wild type ovarioles (Figure 14).

In particular, by a deep analysis of the egg chambers (Figure 14A), I found that 97% of the ovarioles expressing EcR-DNF645A (n=215) and 93% (n=107) of the stage 10B are completely degenerated, as the DAPI staining shows (Figure 14C). Figure 14B shows a wild type ovariole from control females treated in the same experimental condition where degeneration did not occur.

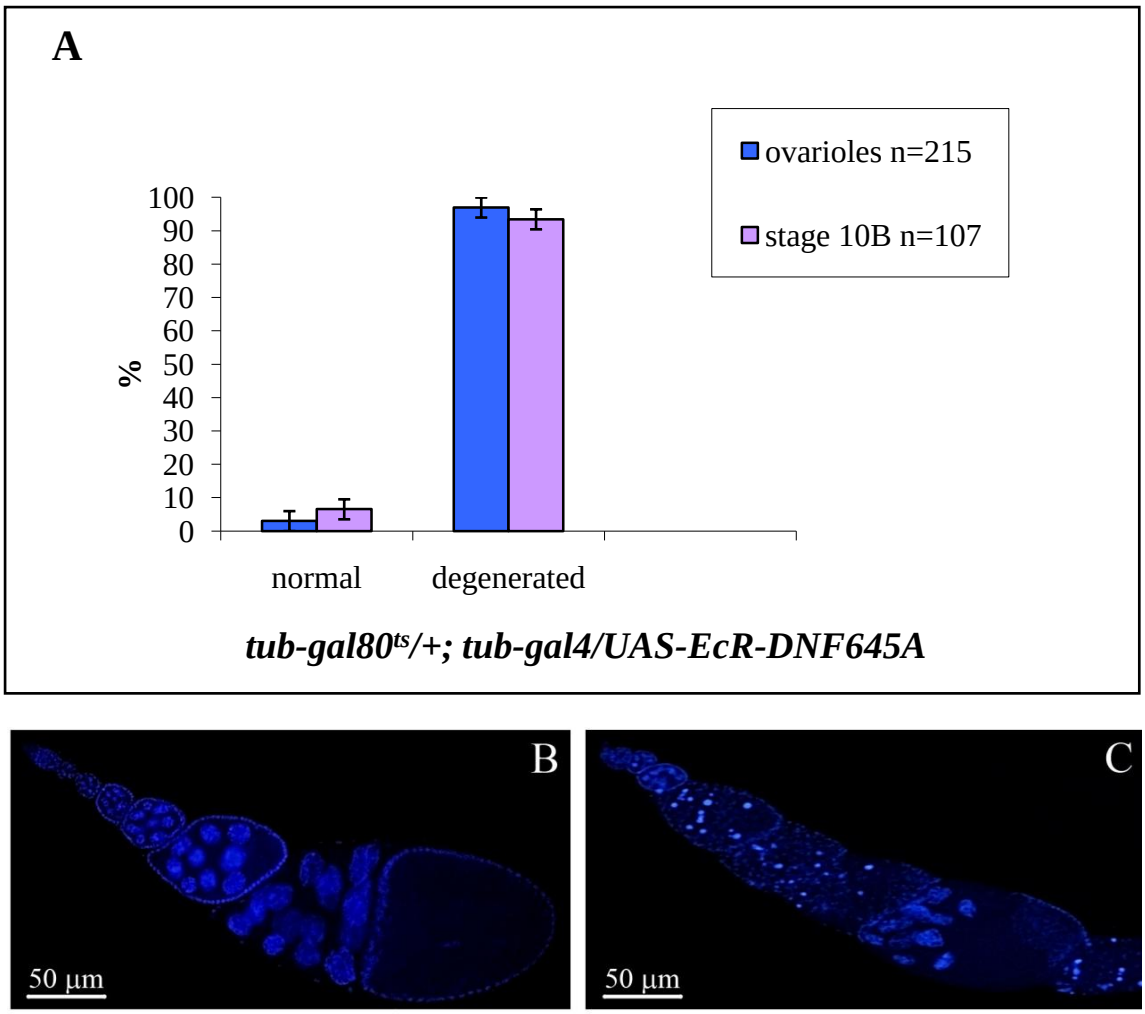

Figure 14: **Ubiquitous expression of EcR-DNF645A blocks egg chamber development.** A) Histograms plotting the number of normal and degenerated ovarioles (blue) and stage 10B (pink) from females *tub-Gal80^{ts}/+;tub-Gal4/UAS-EcR-DNF645A*. I counted the % of ovarioles (n=215) and stage 10B egg chambers (n=107) showing degeneration. (B-C) Fluorescence images of ovarioles from control females (B) and from females overexpressing the *UAS-EcRDNF645A* transgene (C) treated in the same experimental conditions. As DAPI staining (blue) shows, the control ovariole contains normal egg chambers at different stages (B). Conversely, in the ovarioles overexpressing the mutant receptor degeneration occurs at different stages (C). Scale bars in this figure represent 50 µm.

By analyzing the effects of the expression of EcR-DNW650A I observed a lower percentage of ovarioles degenerated (data not shown). This spread could be due to the difference between the two dominant negative forms. Hence difference between the biological effects of the two mutant receptors are probably due to the fact that one can bind steroid and the other cannot (*Brown et al.*, 2006).

In light of this consideration, in order to understand ecdysone involvement in follicular epithelium morphogenesis, I continued my analysis exploring only the effects of EcR-DNF645A overexpression.

4.3 Expression of EcR-DNF645A during mid-oogenesis alters follicle cells distribution

In order to address the functional role of *EcR* in follicular epithelium morphogenesis, I carried out tissue- and stage-specific overexpression of *UAS-EcR-DNF645A* using the *Cy2-Gal4* enhancer trap line. This driver promotes UAS-linked gene expression mainly in the follicle cells covering the oocyte from stage 7 onward (*Queenan et al.,* 1997) (Figure 15A). Again, the *tub-Gal80^{ts}* system was employed in combination with this driver to avoid any lethal effects associated with the mutant receptor expression during development. Adult females *Cy2-Gal4/+; tub-Gal80^{ts}/UAS-EcR-DNF645A* were kept at 18°C for two days and then shifted at 31°C for 1 day to induce Gal4 activity. After that, females were dissected and ovary extracted.

By analyzing these ovaries, I observed that the majority of stage 10B egg chambers exhibited many defects (Figure 15). In particular, 23% of stage 10B egg chambers expressing EcR-DNF645A (n=217) seemed to be normal, while 17% of stage 10B were completely degenerated (Figure 15B). In addition, I detected 3% of stage 10B that presented an altered distribution of the main body follicle cells on the surface of the egg chamber as well illustrated by DAPI staining (Figure 15B and C).

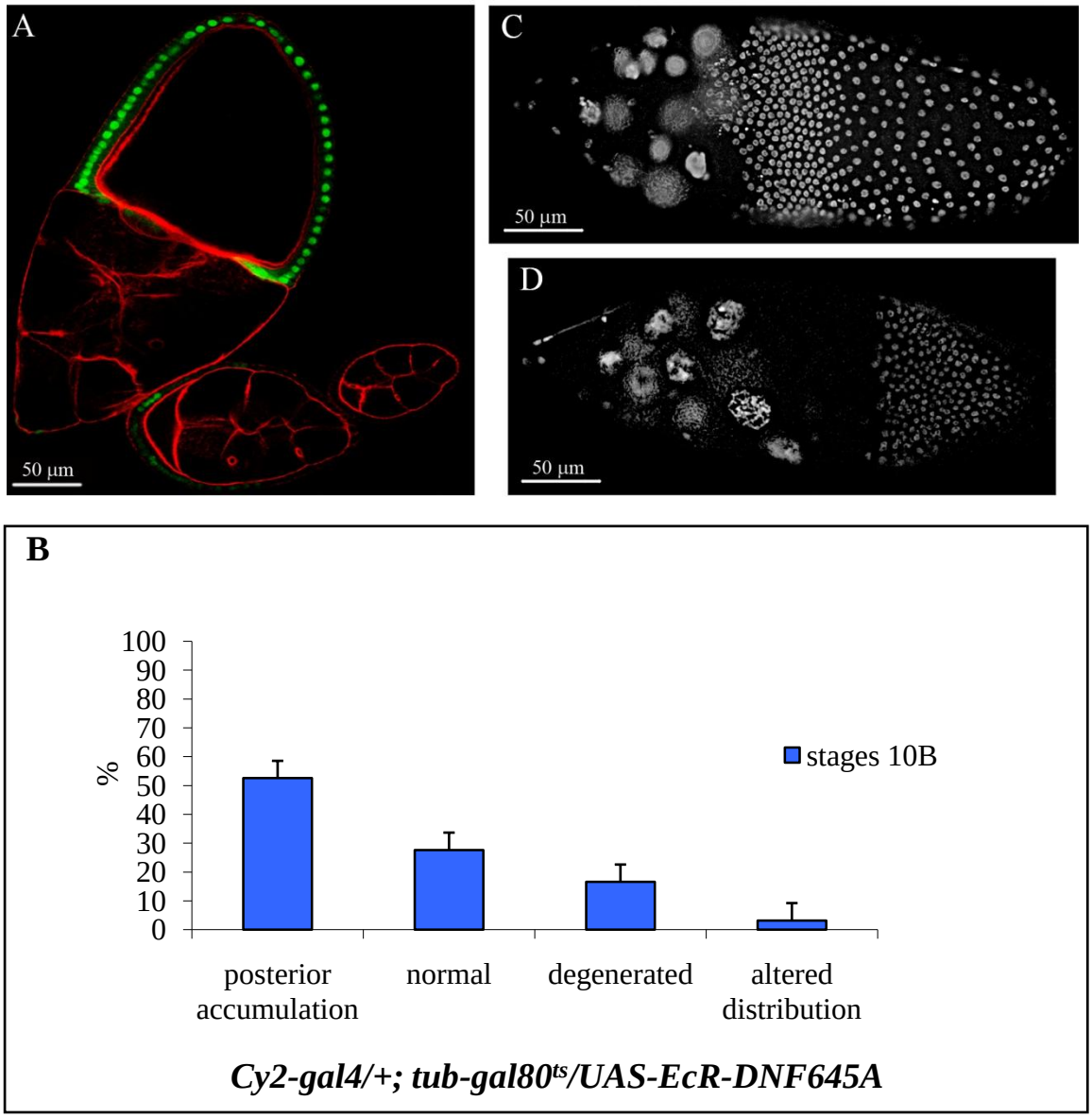

Figure 15: **Expression of EcR-DNF645A during mid-oogenesis induces several alteration in follicle cells.** (A) Fluorescence cross-section of egg chambers from females expressing UAS-GFP reporter (green) stained with TRITC-Phalloidin (red). (B) Histograms plotting the different phenotype observed in stage 10B egg chambers from females *Cy2-Gal4/+;Tub-Gal80^{ts}/UAS-EcR-DNF645A* (C-D). I counted the % of egg chambers showing the different phenotype (n=217). (C-D) Fluorescence images of egg chambers from females overexpressing the *UAS-EcR-DNF645A* transgene under the control of the *Cy2-Gal4* promoter. DAPI staining (white) shows the altered distribution of main body follicle cells on the surface of the egg chamber (C) and the accumulation of follicle cells at the posterior end of the egg chamber (D). Anterior is left in all the panels. Scale bars in this figure represent 50 µm.

Interestingly, in the majority of the stage 10B examined (52,5%) follicle cells accumulated at the posterior of the egg chamber leading uncovered the anterior part of the swelling oocyte (Figure 15B and D).

TRITC-phalloidin staining shows that in stage 10B egg chambers exhibiting high degree of degeneration caused by expression of EcR-DNF645A in main body follicle cells, positively marked by GFP signal (Figure 16A), actin cytoskeleton structure is completely altered (Figure 16B and C).

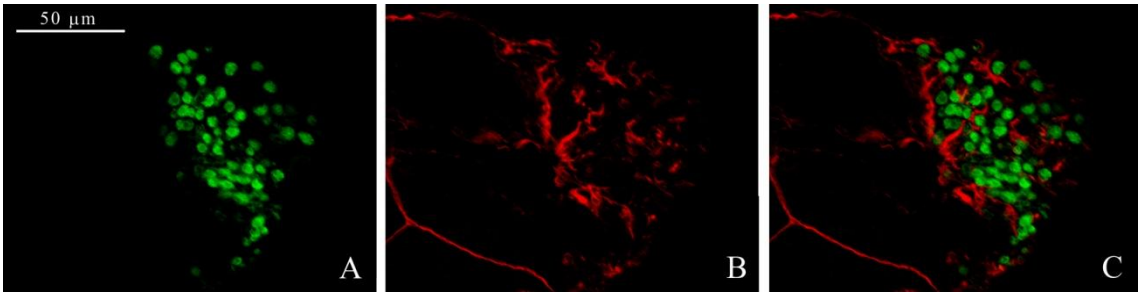

Figure 16: **Expression of EcR-DNF645A during mid-oogenesis alters actin cytoskeleton.** (A-C) Confocal image of egg chamber from females *Cy2-Gal4/+; tub-Gal80^{ts}/UAS-EcR-DNF645A* stained with TRITC-Phalloidin (B; red). Egg chamber expressing *UAS-EcR-DNF645A* (A) that exhibits degeneration, shows strong alteration of actin cytoskeleton (B). (C) is merge of the two signals. Anterior is left in all the panels. Scale bar in this figure represents 50 µm.

It has been previously described that at this stage of oogenesis, follicle cells complete their migration and their differentiation in different subpopulations (*Horne-Badovinac and Bilder*, 2005). In particular, the most anterior follicle cells exhibit high levels of the posphorylated form of the transcription factor Mad, that is a target of the Dpp signaling pathway (Figure 17A-D).

In order to check whether in the follicle cells expressing the EcR mutant receptor the phosphorilation of Mad protein occurs, I performed a standard immunostaining analysis by incubating the egg chambers with an antibody specific for pMad (PS1, *Persson et al.,* 1998) (Figure 17). From my analysis, it results evident that in the egg chambers where follicle cells accumulated in the posterior region (Figure 17E and F), the

phoshorilated form of Mad is not detected in the most anterior follicle cells (Figure 17G). This result indicates that probably these cells cannot acquire the proper fate.

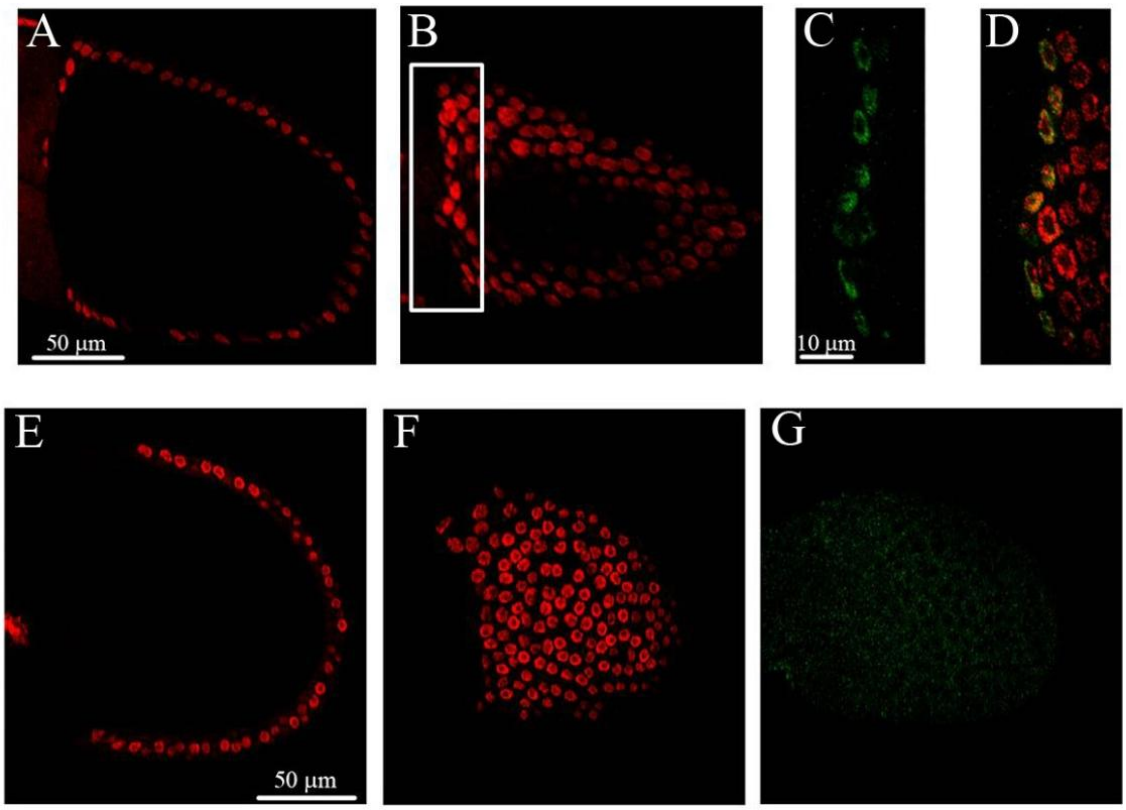

Figure 17: **Expression of EcR-DNF645A during mid-oogenesis induces several alteration in follicle cells.** Confocal images of control stage 10B egg chambers (A-D) and stage 10B expressing the *UAS-EcRDNF645A* transgene (E-G). (A-G) Immunolabeling with anti-pMad (C and G; green) and propidium iodide (A,B and E,F; red) shows that at this stage of oogenesis in the most anterior follicle cells Mad protein is phoshorilated (see magnification in D), while in follicle cells expressing EcR mutant receptor pMad signal is not detected (G) indicating that these cells might not acquire the proper fate. Anterior is left in all the panels. Scale bars in this figure represent 10 µm and 50 µm.

4.4 EcR-DNF645A overexpression in follicle cell clones causes follicle cell size reduction and affects migration of main body follicle cells

Tissue- and stage-specific overexpression of EcR-DNF645A showed that EcR signaling is involved in maintaining follicular epithelium integrity at mid-oogenesis and in cell survival.

Next to deeply explore *EcR* function, I overexpressed the receptor EcR-DNF645A in follicle cells through clonal analysis. Using the Flp-out/Gal4 technique (*Pignoni and*

Zipursky, 1997), I randomly co-expressed the *UAS-EcR-DNF645A* and the *UAS-GFP* transgenes under the *actin* promoter in clonal patches of cells by using the Flp-out cassette *act5C>CD2>Gal4* and a *heat-shock-Flp-recombinase* (*hs-Flp*). The locations of clones were mapped by the presence of GFP. To induce clones, adult females were heat-shocked twice at 37°C for 1 hour and incubated for 2 days at 29°C before having their ovaries dissected.

Figure 18A-F shows the analysis of a stage 10B egg chamber stained with DE-Cadherin antibody (Figure 18A and D) containing one clone of follicle cells overexpressing EcR-DNF645A (Figure 18, boxed area). These follicle cells, marked by the presence of the GFP marker (Figure 18B and magnification in E), exhibit reduced (nuclear) size, as assessed by To-Pro-3 staining of DNA (Figure 18C and magnification in F).

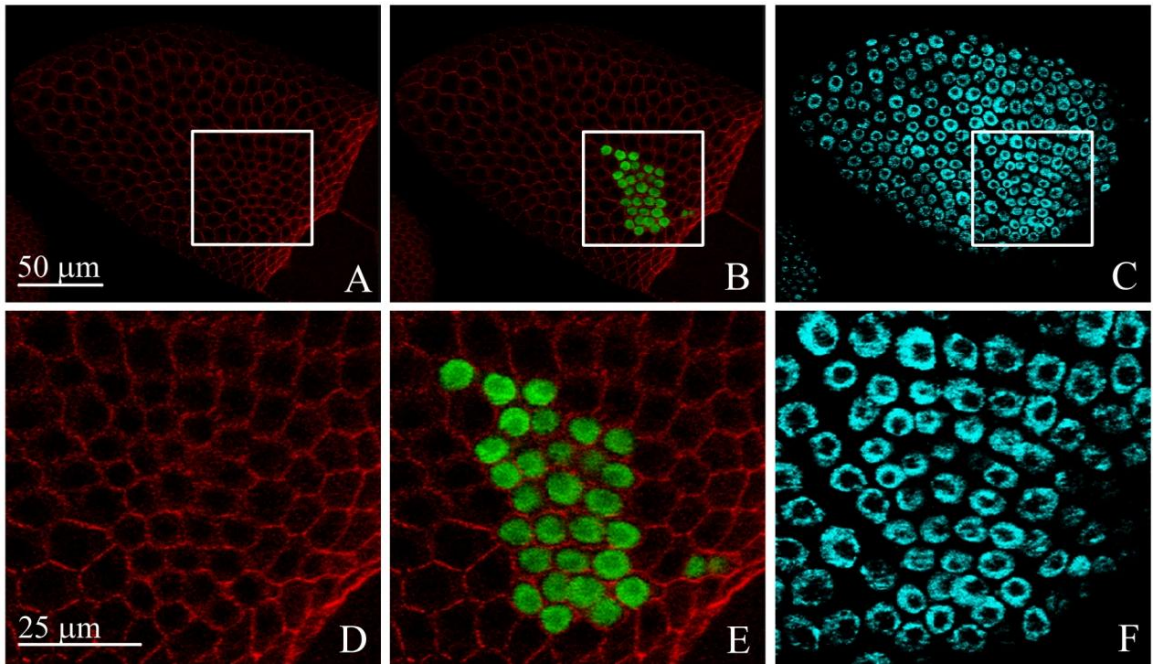

Figure 18: **EcR-DNF645A overexpression in follicle cell clones causes follicle cell size reduction.** Confocal image of stage 10B egg chamber stained with DE-Cad antibody (A,D; red) and To-Pro-3 (C,F; cyan). (D-F) are magnification of the boxed areas in (A-C). In this egg chamber is visible a clone of follicle cells overexpressing EcR-DNF645A, positively marked by GFP (B and E), whose size results strongly reduced (see magnification in D-F) if compared to wild type neighboring follicle cells that do not express the mutant receptor. Anterior is right in all panels. Scale bar in this figure is 50 µm (A-C) and 25 µm (D-F).

The reduced cell size could be due to perturbation of the three endoreplication cell cycles (*Lilly and Spradling*, 1996) through which the follicle cells become polyploid and increase their size by the end of stage 10B (*Calvi et al.*, 1998). I noted that in mutant clones the intensity of To-Pro-3 staining is similar to the wild type neighboring cells (Figure 18C and F). Because the overall size of the mutant nucleus is smaller, the total DNA content within the mutant cell is proportionally reduced. This might suggest that EcR-DNF645A overexpression affects endoreplication of follicle cells.

Interestingly, extensive analyses of these egg chambers (Figure 19) stained with DE-Cadherin antibody (Figure 19A and D) reveal clones of follicle cells overexpressing EcR-DNF645A and positively marked by GFP (Figure 19B and E), incorrectly located in the anterior part of the egg chamber (Figure 19C and F).

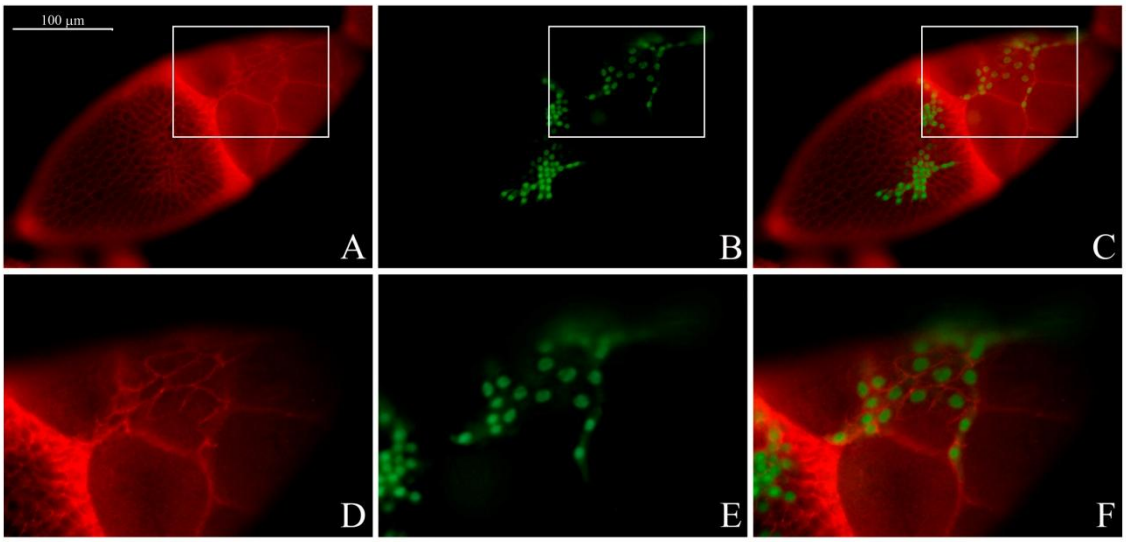

Figure 19: **EcR-DNF645A overexpression in follicle cell clones affects follicle cells migration.** Fluorescence images of stage 10B egg chamber stained with anti-DE-Cadherin antibody (A,D; red) from females overexpressing *UAS-EcR-DNF645A* in clonal patches of follicle cells marked by the presence of the GFP marker (B,E; green). Panels (D-F) are higher magnification views of the boxed areas in (A-C). In this figure is visible a follicle cell clone located at the anterior of the egg chamber. At this stage of oogenesis main body follicle cells should surround the oocyte (C and F). Anterior is right in all panels. Scale bar in this figure is 100 µm.

These results indicate that blocking *EcR* signaling through overexpression of a dominant negative form of this receptor causes indeed altered cell distribution on the surface of the egg chamber. These data, in agreement with the results previously shown overexpressing the mutant receptor using *Cy2-Gal4*, raise the possibility that EcR could be involved in the regulation of the mechanism that leads to proper migration of follicle cells during oogenesis.

4.5 Ubiquitous *EcR-B1* silencing in the follicular epithelium strongly affects egg chamber development

In order to deeply investigate the role of EcR in egg chamber development, I analyzed the effect of specific knocking down of the different EcR isoforms in somatic follicle cells. The three EcR isoforms show different spatial and temporal expression profiles triggering specific cellular responses to ecdysone stimuli during different developmental stages. *Carney and Bender,* (2000) have previously shown that EcR-A and EcR-B1 proteins are present in both germline and somatic cells of the ovary throughout oogenesis.

To analyze EcR-B1 function, I used an RNA interference approach coupled with the UAS/Gal4 system (*Brand and Perrimon,* 1993) to obtain *EcR-B1* knockdown in follicle cells (*Kennerdell and Carthew,* 2000). I took advantage of the *UAS-IR-EcR-B1* transgene containing inverted repeat (IR) sequences designed to target the 5'-*EcR-B1*-specific exon β2 (*Roignant et al.,* 2003) (Figure 20).

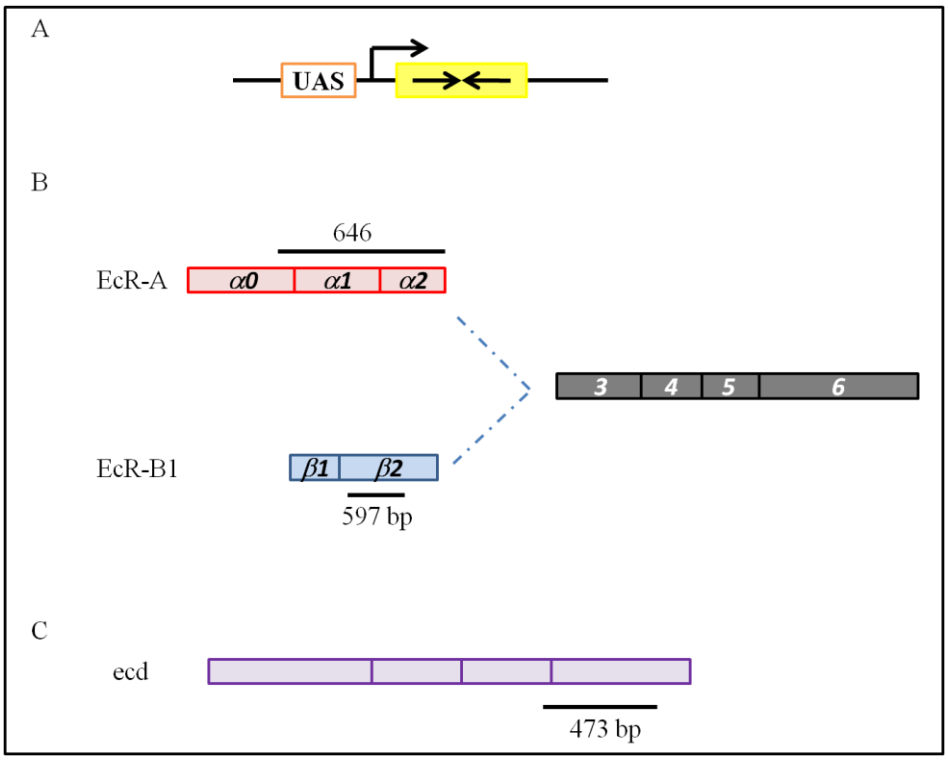

Figure 20: **Structure of the RNAi constructs used.** A portion of the coding sequence of the gene of interest is dimerized in a head-to-head orientation and placed in the pUAST expression vector under the control of UAS transcription elements (A). Map of *EcR* gene depicts the arrangement of the exons (B). Exons common to all isoforms are numbered 3-6. Specific exons of the EcR isoforms are designated by greek letters (α and β). All the *UAS-IR-EcR* are generated in Antoniewski's lab (*Roignant et al.*, 2003). The length of sequences cloned in the *UAS-IR-EcR-A* construct is 646 bp corresponding to exons specifics α0, α1 and α2, while the *UAS-IR-EcR-B1* cloned sequence is 597 bp long corresponding to exon specific β2 (see solid black bars). The *UAS-ecdRNAi* transgene used was generated in M. Uhlirova's lab and contains a sequence of 473 bp of C-terminal domain of ecd transcript (C, see solid black bars).

The transgene was expressed using the ubiquitous *tub-Gal4* driver coupled with *tub-Gal80^{ts}* transgene. Also in this case, to induce Gal4 activity and thus *EcR-B1* knockdown, adult females of the correct genotype were kept at 31°C for 6 days and then dissected and ovary analyzed.

By analyzing ovaries, I detected an excess of mature stage 14 egg chambers. In addition, I found that ubiquitous knockdown of EcR-B1 causes a strong decrease in the number of vitellogenic stages (7-13) and breakdown of egg chambers (Figure 21A-F) that is not detected in wild type ovarioles (Figure 21G).

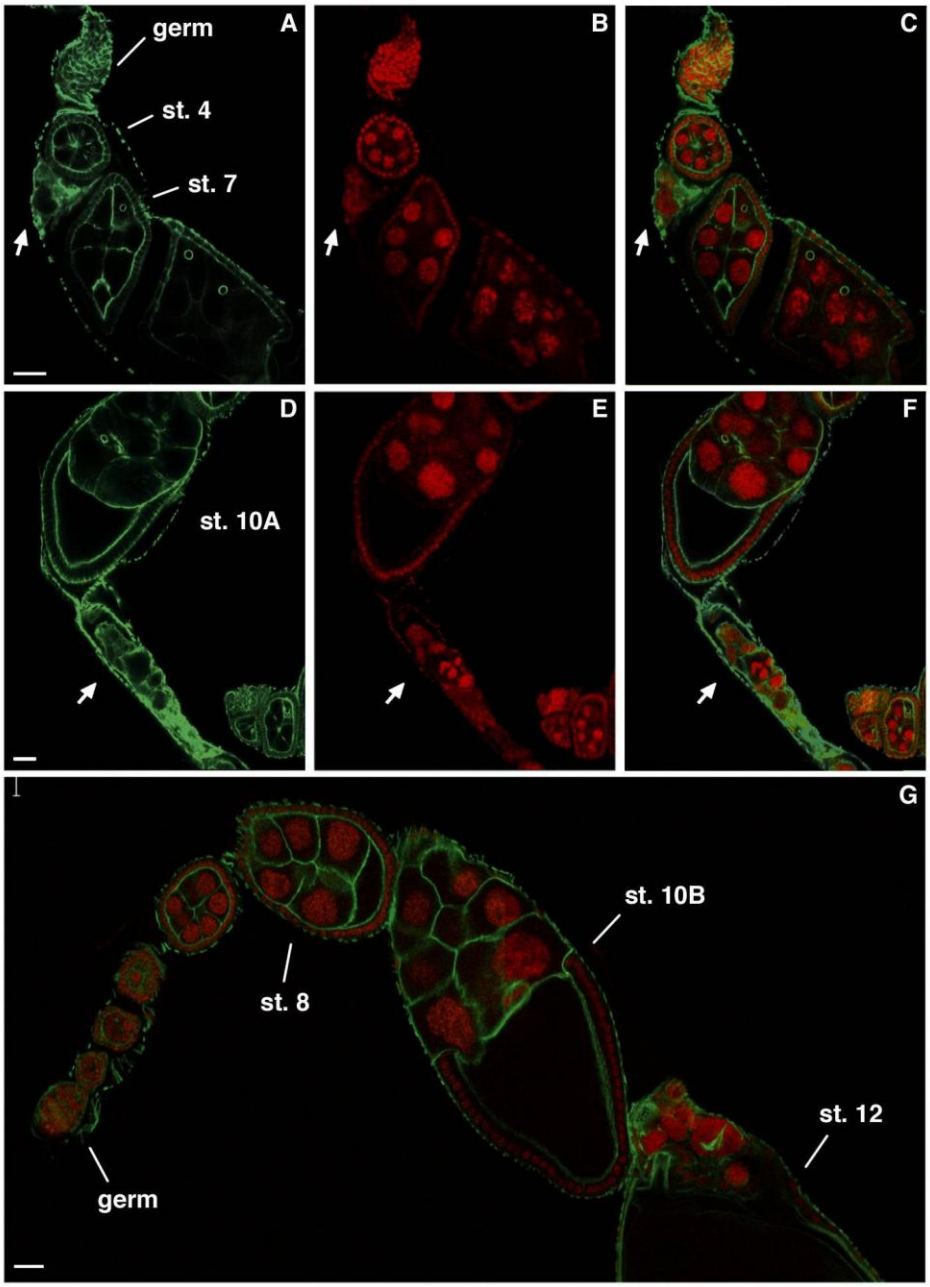

Figure 21: ***EcR-B1* ubiquitous silencing in the follicular epithelium induces egg chamber degeneration.** Confocal cross-sections of ovarioles from females overexpressing the *UAS-IR-EcR-B1* transgene under the control of the *tub-Gal4* promoter (A-F) and from wild type females (G). FITC-Phalloidin (A,D; green), propidium iodide staining (B,E; red) and their merged signals (C,F) show the presence of degenerated egg chambers inside ovarioles (see white arrows). In comparison, in the wild type ovariole (G) FITC-phalloidin and propidium iodide merged signals illustrate the absence of degenerating egg chambers. Anterior is up in all the panels. Abbreviation: germ: germarium; st: stage. Scale bar in this figure represents 20 μm (*Romani et al.*, 2009).

More deeply, in 54% of mutant ovarioles (n=177) I observed remnant egg chamber material as shown by FITC-phalloidin (Figure 21A and D) and propidium iodide stainings (Figure 21B and E). These results show that EcR-B1 plays a key role in egg chamber integrity.

These data have been published on Genetics (*Romani et al.*, 2009).

4.6 During mid-oogenesis EcR-B1 is required to maintain follicle cell polarity

To further analyze *EcR-B1* involvement in follicular epithelium morphogenesis, I carried out tissue- and stage-specific RNAi mediated knockdown of *EcR-B1* gene function taking advantage of the *UAS-IR-EcR-B1* transgene described and used above. Again, the *tub-Gal80^{ts}* system was employed in combination with *Cy2-Gal4* driver to prevent the lethality of *EcR-B1* knockdown during development. As shown in Figure 22B, propidium iodide staining of follicle cell nuclei reveals the loss of monolayer integrity of the follicular epithelium during mid-oogenesis in *Cy2-Gal4/+;tub-Gal80^{ts}/UAS-IR-EcR-B1* egg chambers. The follicle cells accumulated in multiple layers and their nuclei had an altered shape and a high degree of DNA staining (dashed line in Figure 22B, dotted areas in Figure 22D, G and J). Piling up of follicle cells is variable (see arrows in Figure 22B) reflecting spotted and patchy *Cy2-Gal4* driver expression pattern (Figure 22A).

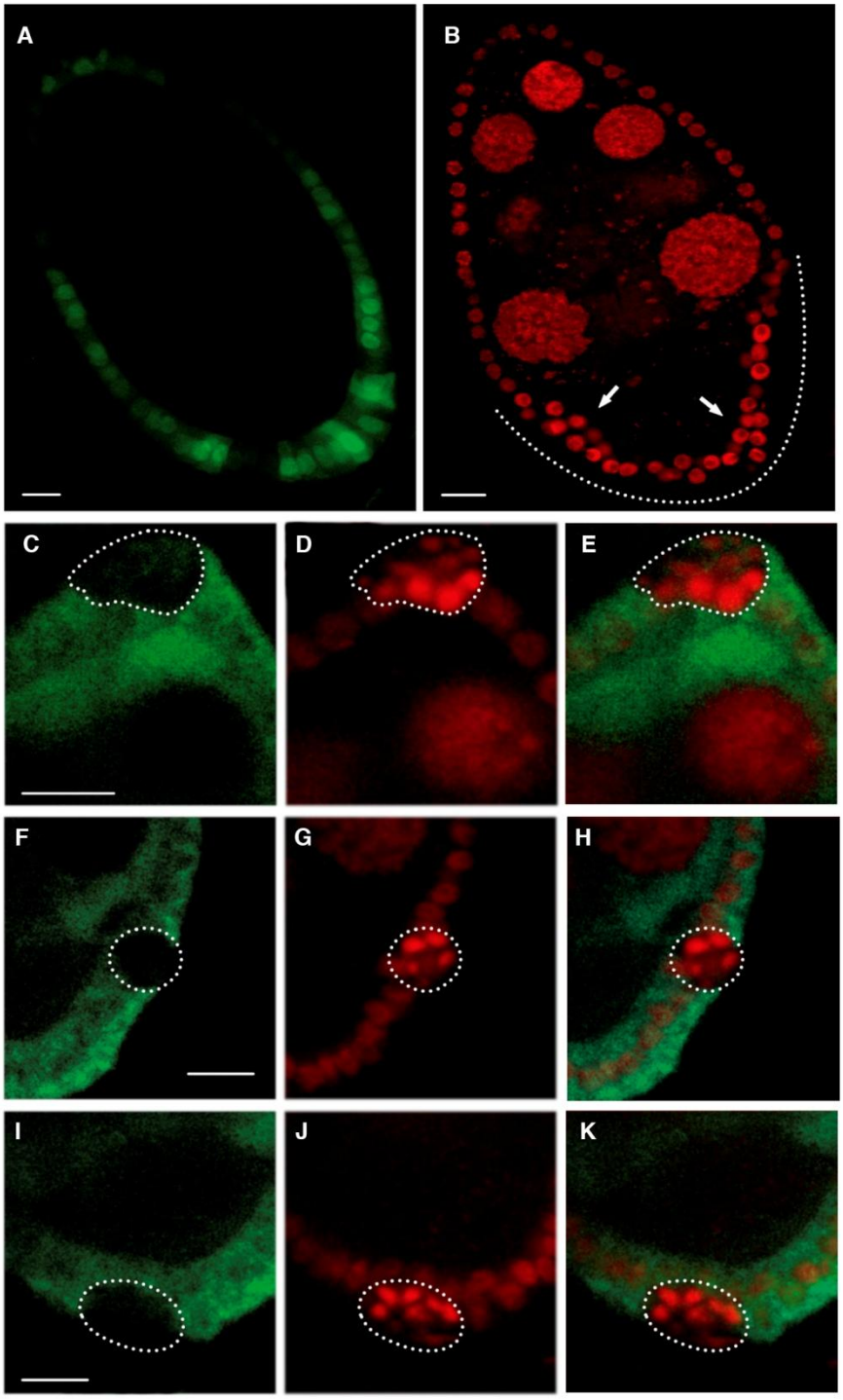

Figure 22: **Silencing of *EcR-B1* in follicle cells at mid-oogenesis disrupts follicular epithelium integrity.** Confocal cross-sections of stage 8 egg chambers from females expressing the *UAS*-GFP reporter (A; green) or the *UAS-IR-EcR-B1* transgene (B-K) under the control of the *Cy2-Gal4* driver. Propidium iodide staining allows the detection of multilayered follicle cells (dashed lines in B and dotted areas in D,G and J). EcR-B1 protein (C,F and I; green) is undetectable in multilayered follicle cells localized in anterior (E), lateral (H) and posterior (K) areas of the follicular epithelium. Scale bars in this figure represent 10 μm (*Romani et al.*, 2009).

In order to assess if expression of the targeted interfering RNA was effective at reducing EcR-B1 protein levels, egg chambers from *Cy2-Gal4/+;tub-Gal80^{ts}/UAS-IR-EcR-B1* females were immunostained with anti-EcR-B1 antibody (AD4.4, DSHB; *Talbot et al.*, 1993) (Figure 22).

Delamination of follicle cells always occurs in areas of strongly reduced EcR-B1 expression. As shown in Figure 22C-K, follicle cells that show the multilayered phenotype localized at anterior (Figure 22D), lateral (Figure 22G), and posterior (Figure 22J) domains of the follicular epithelium exhibit quite undetectable EcR-B1 levels (Figure 22C and E,F and H,I and K, respectively) indicating that delamination is associated with effective knockdown of EcR-B1 levels.

I next investigated whether the multilayered epithelium was a result of late stage overproliferation by immunodetection of the phospho-histone H3 (PH3) mitotic marker (06-570, Upstate Biotechnology; *Mahadevan et al.*, 1991). In wild type follicle cells, at stage 6 of oogenesis, Notch-Delta signaling induces the transition from mitotic cell cycle to endocycle so that after this stage the PH3 mitotic marker is not detected (*Deng et al.*, 2001). I observed that after stage 6 the PH3 marker is never detected in *Cy2-Gal4/+;tub-Gal80^{ts}/UAS-IR-EcR-B1* egg chambers, indicating that the multilayered epithelium does not arise from loss of proliferation control (data not shown).

Delamination of cells in multiple layers is a typical terminal phenotype for polarity defects in epithelial cells. Adherens junctions (AJs), considered the primary epithelial polarity landmark, are required for both epithelial sheet formation and maintenance (reviewed in *Bilder*, 2004). After stage 6, the follicle cells undergo complex morphogenetic processes associated with changes in adherens junction levels (*Spradling*, 1993; *Wu et al.*, 2008). The *Drosophila* β-catenin encoded by the *armadillo (arm)* locus is enriched at the adherens-type junctions. Arm protein is abundantly expressed in follicle cell epithelium and is enriched at the apico-lateral plasma membrane surface juxtaposed to the germline (*Peifer et al.*, 1993).

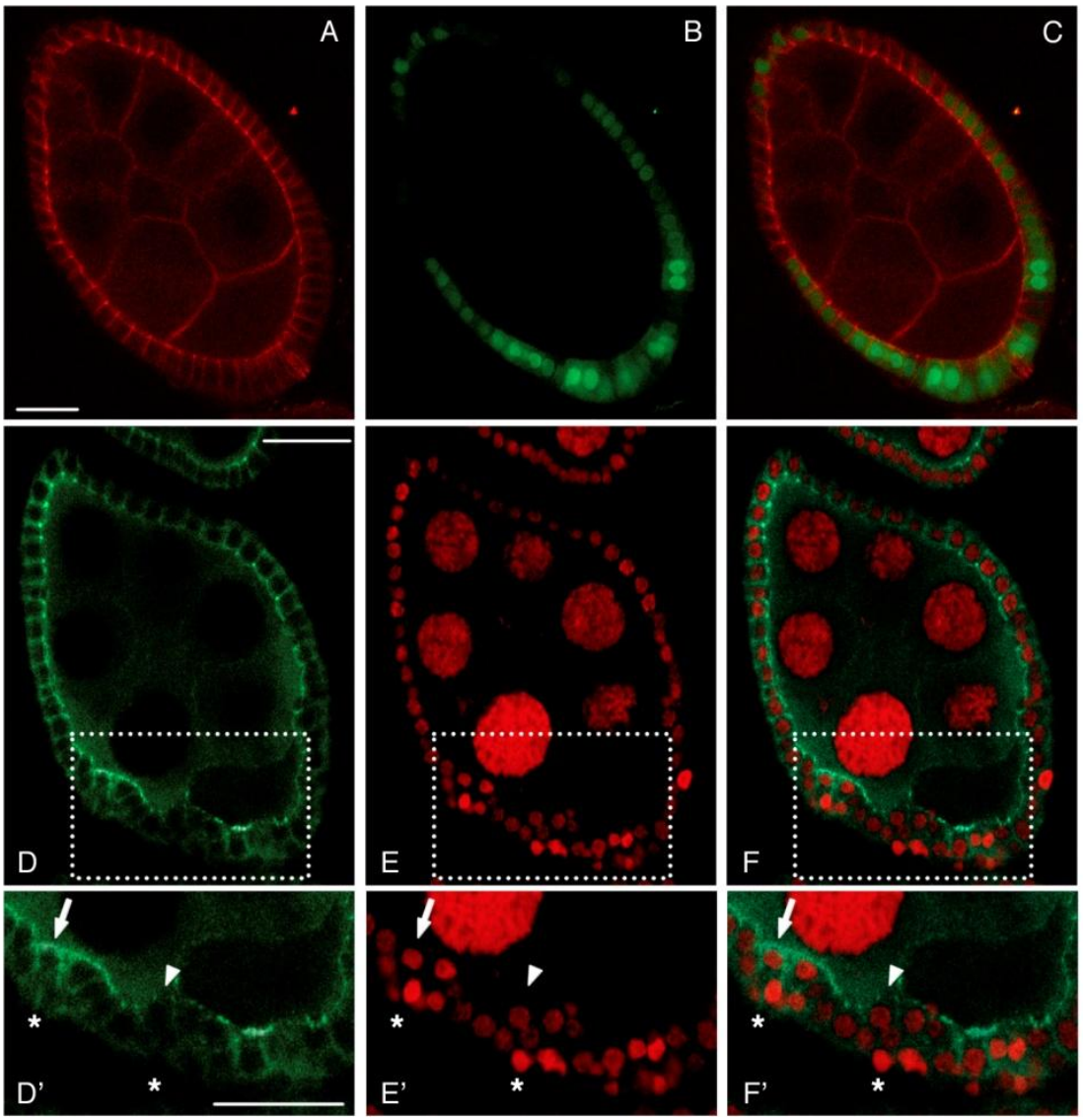

Figure 23: **Knockdown of EcR-B1 isoform in follicle cells at mid-oogenesis affects AJs core components.** Confocal cross-sections of a stage 8 egg chamber from females expressing the *UAS-GFP* reporter (B; green) under the control of the *Cy2-Gal4* driver. The *Gal4*-induced GFP expression is uneven due to the *Cy2-Gal4* driver activity. Arm protein (A; red) is abundantly expressed in the follicular epithelium and is enriched at the apical and lateral surfaces of the plasma membranes that are juxtaposed to the germline cells. Merged image of GFP and Arm signals is shown in panel C. Confocal cross-sections of stage 8 egg chambers from females overexpressing the *UAS-IR-EcR-B1* transgene under the control of the *Cy2-Gal4* driver (D-F'). (D'-F') are higher magnification views of the boxed regions in (D-F), respectively. Knockdown of *EcR-B1* causes multilayering of follicle cells, as assessed by propidium iodide staining (E,E'; red) and altered localization of Arm protein (D,D'; green). F, F' are merged images of Arm (D,D') and propidium iodide (E,E') stainings. Follicle cells facing the germ line show either strong (see arrows in D',F') or quite absent (see arrowheads in D',F') Arm staining. In the misplaced follicle cells, Arm staining is undetectable (see asterisks in D',F'). Anterior is up in all the panels. Scale bars in this figure represent 20 μm (*Romani et al.*, 2009).

To determine if *EcR-B1* knockdown defects in follicular epithelium integrity were associated with altered AJ structure, I examined the localization of the Arm protein in egg chambers from females overexpressing the *EcR-B1* RNAi transgene under the control of the *Cy2-Gal4* driver (Figure 23D-F'). Compared with Arm staining (N27A1, DSHB; *Riggleman et al.*, 1990) of control egg chambers (Figure 23A-C), we observed two significant changes in Arm accumulation: (1) in cells that remain in contact with the germline, Arm accumulation is either strong (see arrow in Figure 23D' and F') or barely detectable (see arrowhead in Figure 23D' and F') and (2) in follicle cells that delaminate from the follicular epithelium, apical Arm staining is quite absent (see asterisks in Figure 23D' and F').

I next analyzed the localization of AJs core proteins in order to investigate if *EcR-B1* knockdown in follicle cells affects their distribution. AJs are complexes composed of cadherin transmembrane proteins linked to cytoplasmic β-catenin, α-catenin and actin (*Tepass et al.*, 2001; *Müller and Bossinger*, 2003). To investigate AJs structure in egg chambers from *Cy2-Gal4/+;tub-Gal80^{ts}/UAS-IR-EcR-B1* females, I checked the localization of DE-Cad and the F-actin cytoskeleton. DE-Cad levels are strongly reduced (Figure 24A-C') in multilayered follicle cells (see arrows in Figure 24A' and C') and similar to Arm localization, the F-actin cytoskeleton is not detectable in delaminating follicle cells (Figure 24D-F'; see bracket in D'-F').

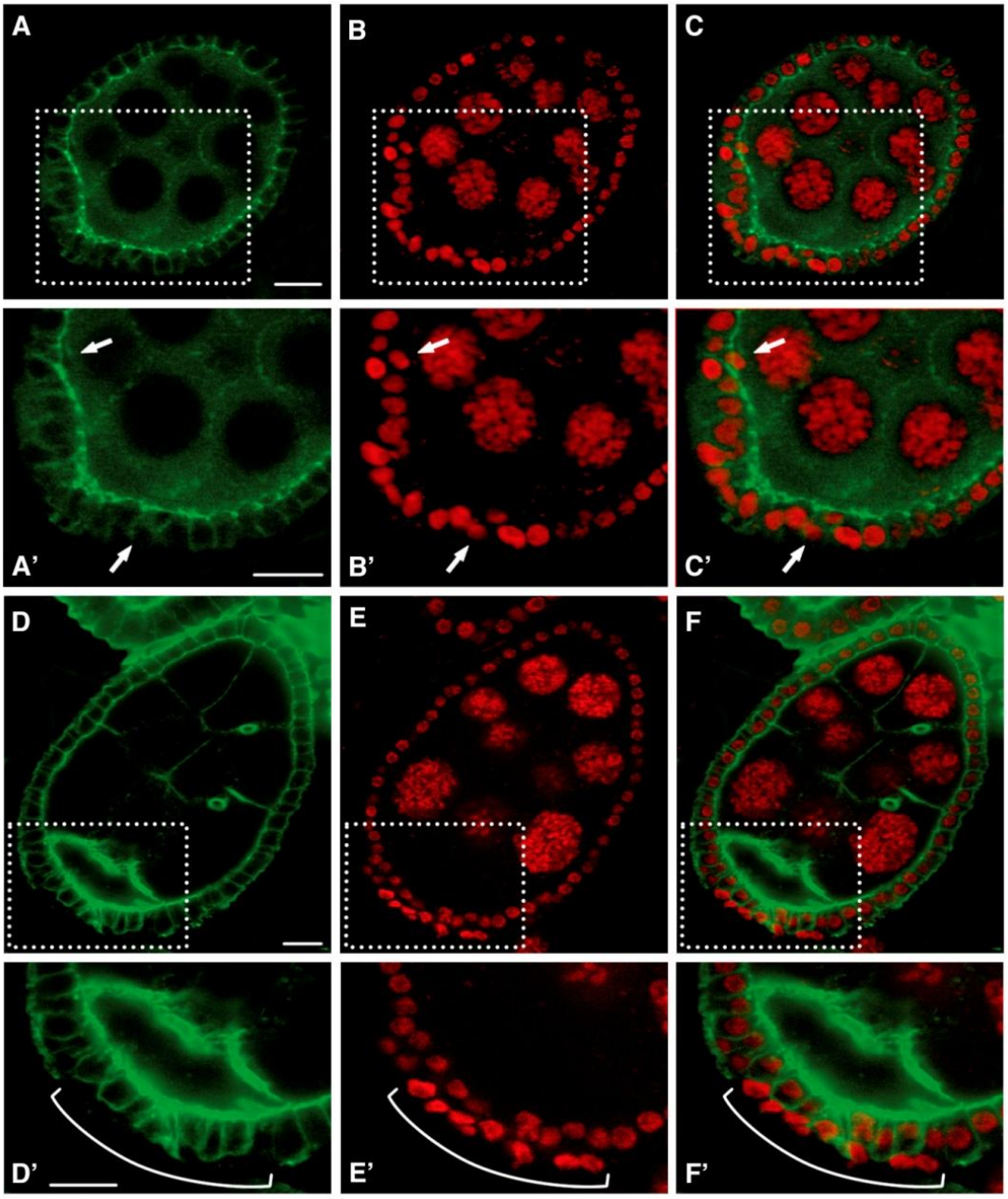

Figure 24: **Silencing of *EcR-B1* in follicle cells at mid-oogenesis disrupts apico-basal polarity.** Confocal cross-sections of stage 7 (A-C') and stage 8 (D-F') egg chambers from females overexpressing the *UAS-IR-EcR-B1* transgene under the control of the *Cy2-Gal4* driver. (A'-F') are higher magnification views of the boxed region in (A-F), respectively. Knockdown of EcR-B1 causes multilayering of follicle cells, as assessed by propidium iodide staining (B,B', E,E'; red). These misplaced follicle cells exhibit loss of apical polarity, as assessed by alteration of DE-Cad distribution (A,A'; green) and loss of F-actin cytoskeleton (D,D'; green). C,C',F and F' are merged images of propidium iodide (B,B' and E,E'), DE-Cad (A,A') and FITC-phalloidin (D,D') stainings. DE-Cad staining is lowered in multilayered follicle cells (arrows in A'). F-actin staining is not detectable in delaminating follicle cells (bracket in D'-F'). Anterior is up in all the panels. Scale bars in this figure represent 10 μm (*Romani et al.*, 2009).

I next analyzed the effect of *EcR-B1* silencing on the baso-lateral junction (BLJ) that interconnects follicle cells and that contains proteins conserved in vertebrate epithelia. In particular, I focused on two proteins, Dlg and Scrib, which are localized to lateral domains of the cell membrane, just basal to the AJs to form a barrier known as septate junction, analogous to the tight junction of mammalian cells (*Knust,* 2002).

Immunodetection of the Dlg protein (4F3, DSHB; *Parnas et al.*, 2001) in egg chambers expressing the *UAS-IR-EcR-B1* transgene shows an aberrant circumferential localization of this protein in delaminating follicle cells (Figure 25A-C', see asterisks in A'-C').

Multi-layered follicle cells also show aberrant distribution of the Scrib protein (the antibody was kindly provided by C.Q. Doe, *Albertson and Doe,* 2003) that is present in both apical and lateral domains (Figure 25D-F', see asterisk in D'-F'). In addition, *UAS-IR-EcR-B1* follicle cells whose nuclei show high levels of DNA staining also exhibit aberrant basal localization of the Scrib protein (see arrowheads in Figure 25D'-F').

I then investigated the localization of aPKC, a functionally conserved component of an apical protein complex that includes Par6 and Baz (*Müller and Bossinger,* 2003) and regulates apico-basal polarity in both epithelial and non-epithelial cell types. In wild type follicle cells, aPKC localizes to the apical membrane, however knockdown of the EcR-B1 isoform causes a reduction of aPKC levels in follicle cells facing the germline, and undetectable levels in delaminating follicle cells (C-20, sc-216, Santa Cruz Biotechnology; *Cox et al.,* 2001, see bracket in Figure 25G'-I'), consistent with defective polarity in cells with reduced EcR-B1 activity (Figure 25G-I', see arrowheads G'-I'). In summary these data show that reduced EcR-B1 level is associated with the loss of apico-basal polarity in follicle cells. Because delamination of follicle cells can arise from activation of an apoptotic cell death program, I used the TUNEL technique to detect DNA fragmentation resulting from programmed cell death (*Gavrieli et al.,* 1992) in *Cy2-Gal4/+;tub-Gal80^{ts}/UAS-IR-EcR-B1* females. No TUNEL staining was detectable in multilayered follicle cells of egg chambers in which EcR-B1 levels were reduced after stage 7 (data not shown).

These data have been published on *Genetics* (*Romani et al.*, 2009).

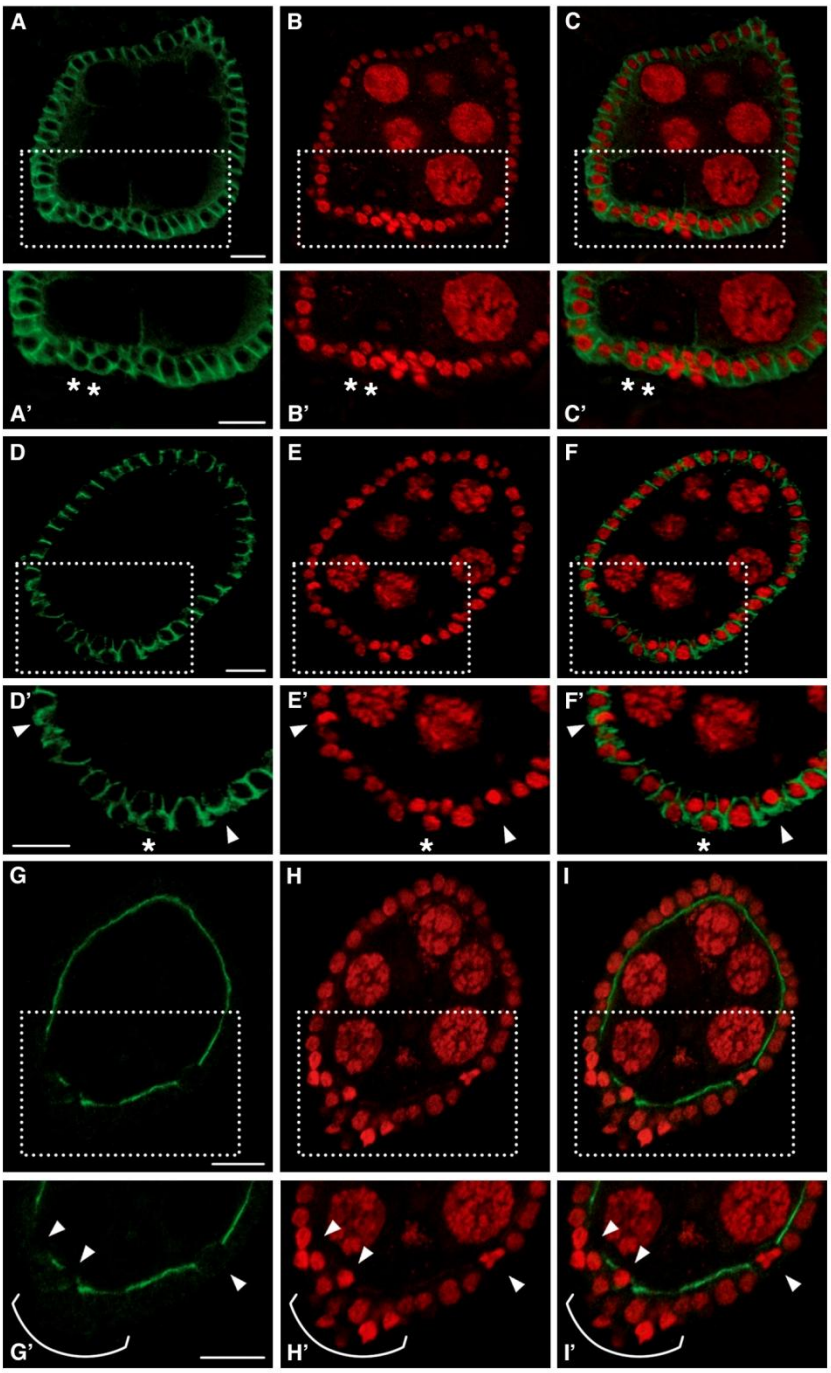

Figure 25: **Knockdown of EcR-B1 isoform in follicle cells affects apical and baso-lateral polarity.** Confocal cross-section of stage 7 egg chambers from females in which the *Cy2-Gal4* driver controls the *UAS-IR-EcR-B1* expression (A-I'). Boxed areas in A-I are enlarged in A'-I', respectively. Propidium iodide staining shows the piling up of follicle cells whose nuclei are strongly stained and show altered shape (B,B',E,E',H,H'; red). Dlg immunodetection (A,A'; green) in multilayered follicle cells (asterisks in A'-C') shows a circumferential localization of this protein (C'; merged propidium iodide and Dlg signals). The Scrib signal (D,D'; green) is detected at higher levels and it is mislocalized. Follicle cells with strong nuclei staining show a basal Scrib localization (see arrowheads in D',E' and in their merge F'). Asterisk in D'-F' point to a delaminating follicle cell that exhibits apico-lateral distribution of the Scrib signal. Apical PKC localization (G,G'; green) in multilayered follicle cells (H,H'; red) is absent (I,I'; merged propidium iodide and aPKC signals) (see bracket in G'-I'). Also some follicle cells facing the germline lack apical aPKC staining (see arrowheads in G'-I'). Anterior is up in all the panels. Scale bars in this figure represent 10 μm (*Romani et al.*, 2009).

4.7 EcR-B1 depletion in clones of follicle cells affects follicular epithelium integrity and follicle cell survival

Cy2-Gal4-induced knockdown of EcR-B1 isoform determined its role in maintaining proper follicle cell polarity and follicular epithelium integrity at mid-oogenesis.

I next performed a clonal analysis of EcR-B1 receptor in order to knock down its function also at earlier stages of oogenesis. Using the Flp-out/Gal4 technique (*Pignoni and Zipursky,* 1997), I randomly expressed the *UAS-IR-EcR-B1* transgene under the actin promoter in clonal patches of cells by using the Flp-out cassette driver *act5C>CD2>Gal4* and a *heat-shock-Flp-recombinase* (*hs-Flp*). Clones were produced prior to stage 6 and the locations of knockdown clones were mapped by the absence of the membrane-targeted CD2 marker. Extensive analyses of these egg chambers revealed that *EcR-B1* silencing in follicle cell clones at early stages also results in multilayering and loss of proper columnar monolayer organization, similar to knockdown at later stages (data not shown). In addition, in follicle cell clones expressing the *UAS-IR-EcR-B1*, marked by the absence of the CD2 marker (Figure 26A and A'), many pycnotic nuclei were detected (Figure 26B,B' and C,C').

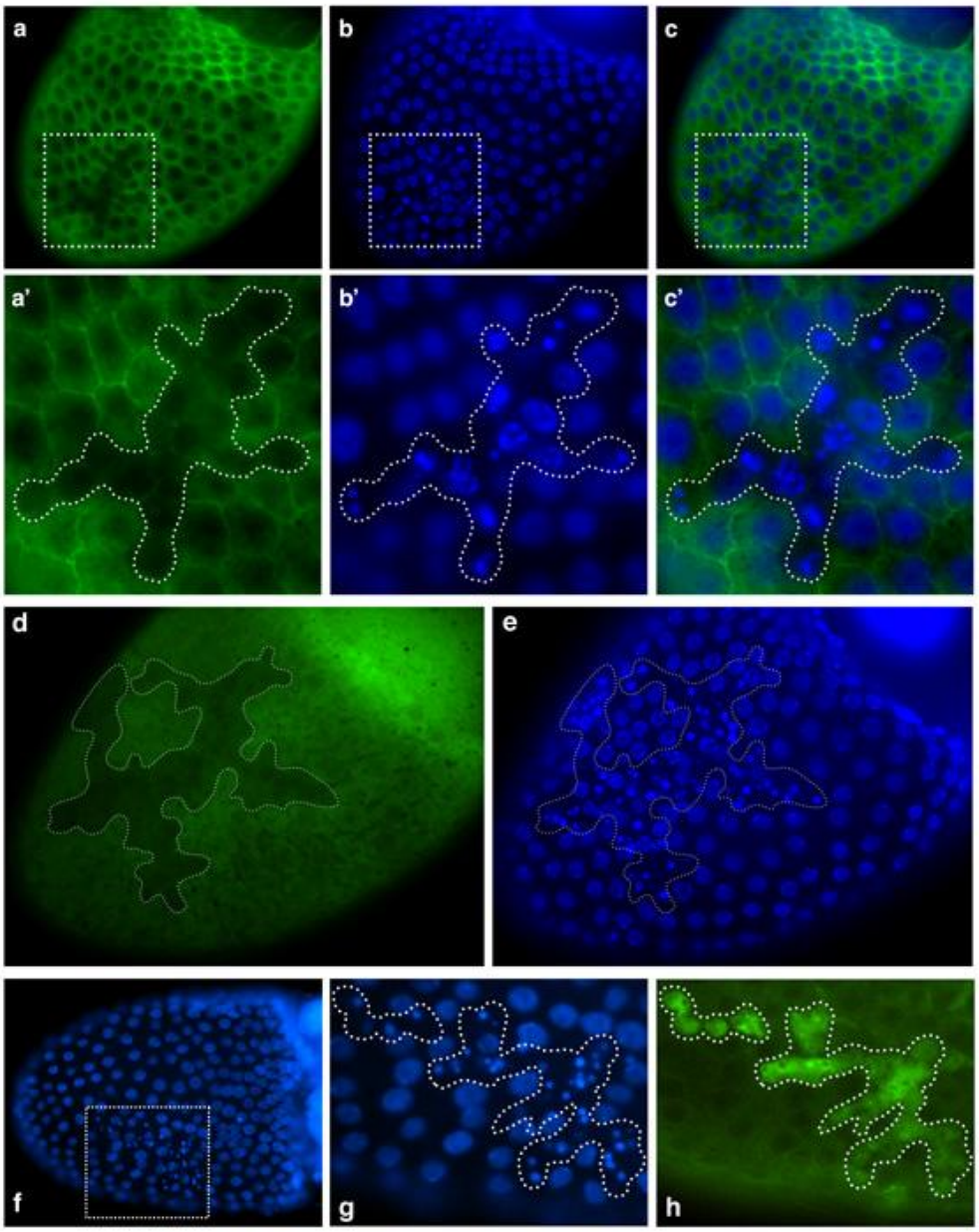

Figure 26: **Clonal knockdown of *EcR-B1* results in multilayering and apoptotic death of follicle cells.** Fluorescence images (A-C') of a stage 10B egg chamber from females overexpressing the *UAS-IR-EcR-B1* silencing transgene in clonal patches of follicle cells marked by the absence of the CD2 marker (A,A'; green). Pycnotic nuclei are detected by DAPI staining (B,B'; blue) in follicle cell clones overexpressing the RNAi transgene (C,C'; merged CD2 and DAPI signals). Panels A'-C' are higher magnification views of the boxed areas in A-C. Fluorescence images (D-E) of a stage 10B egg chamber from females of the same genotype. Anti-EcR-B1 staining (D, green) shows decreased Ecr-B1 protein level in a large area of the follicular epithelium (dotted area in D) containing many pycnotic nuclei (DAPI staining, E; blue). Fluorescence images (F-H) of a stage 10B egg chamber from females of the same genotype. Pycnotic nuclei (dotted area in G), detected by DAPI staining (F,G; blue), exhibit TUNEL positivity (dotted area in H; green). Panels G and H are higher magnification views of the boxed area in F. Posterior is towards the left in all the panels (*Romani et al.,* 2009).

Immunostaining of these egg chambers with anti-EcR-B1 antibody confirmed that clonal expression of the RNA interfering transgene is effective in reducing EcR-B1 levels (Figure 26D). Follicle cell pycnotic nuclei (Figure 26E) were always detectable in follicular epithelium areas showing a strong decrease in EcR-B1 levels (see dotted areas in Figure 26D and E).

Strongly reduced size of follicle cell nuclei could arise from an extension of the proper proliferative program beyond stage 6 and consequent reduced endocycling of follicle cells. By using the PH3 antibody previously described, I did not find any PH3-positive cells after stage 6 (data not shown). TUNEL positivity was detected in *UAS-IR-EcR-B1* follicle cell clones (Figure 26H) that exhibited as well a condensed state of chromatin as judged by DAPI staining (Figure 26F and G). These data indicate that cells with reduced EcR-B1 levels undergo apoptosis.

I next analyzed these egg chambers with active caspase-3 antibody (9664, *Fernandes-Alnemri et al.*, 1994). Caspase activity (Figure 27B and B') was detected in follicle cell clones overexpressing the *EcR-B1* interfering transgene (Figure 27C,C' and D,D'). Interestingly, caspase-3 immunoreactivity is detected in these follicle cell clones exhibiting highly condensed nuclei (Figure 27A,A' and D,D').

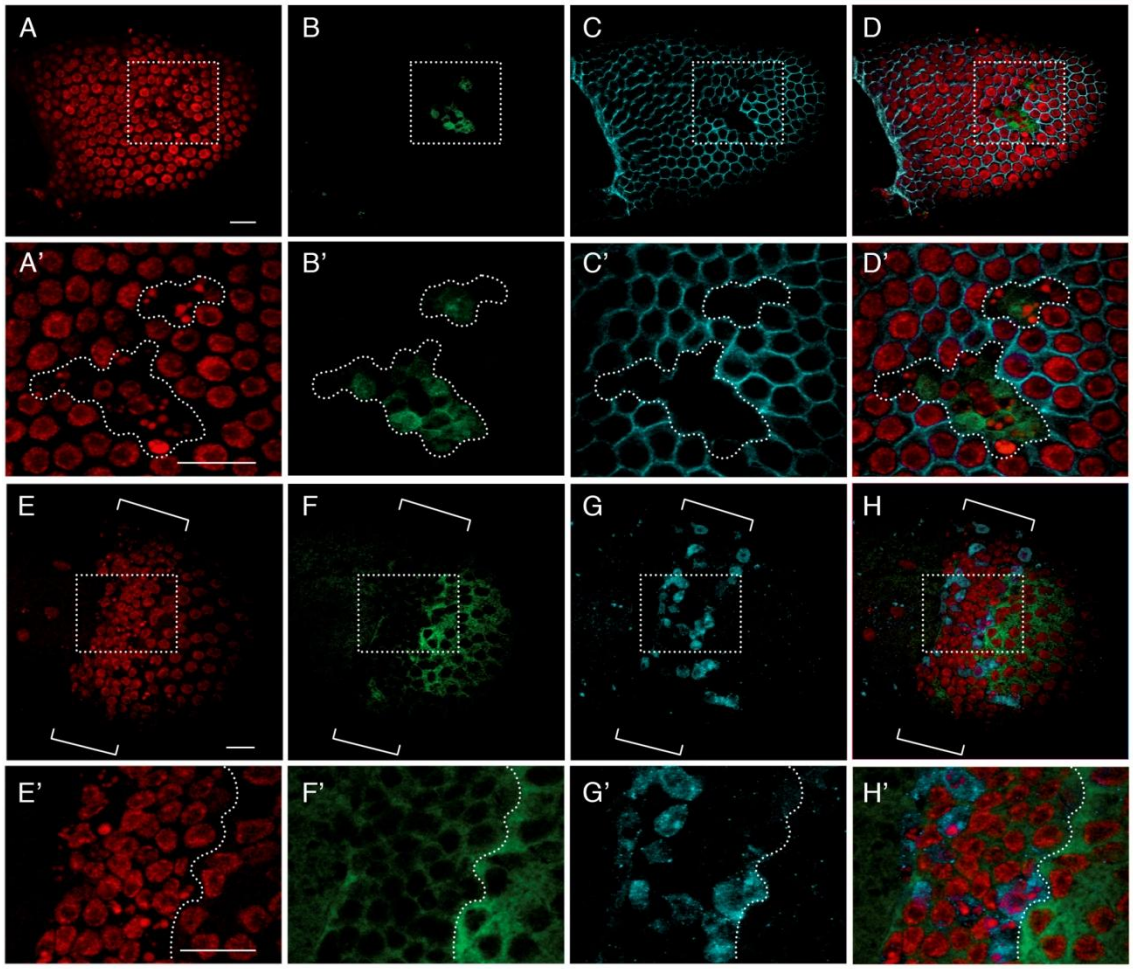

Figure 27: **Silencing of *EcR-B1* in clones of follicle cells causes caspase-3 activation and Diap1 downregulation.** Confocal images of stage 10B mosaic egg chambers expressing the *UAS-IR-EcR-B1* transgene (A-H'). Double immunolabeling with anti-active caspase-3 (B,B'; green) and anti-CD2 (C,C'; cyan) coupled with propidium iodide staining (A,A'; red) shows that in clones expressing the *EcR-B1* interfering transgene, follicle cells with highly condensed nuclei and active caspase-3 are recognizable (D,D'; merge of all signals). Egg chamber from females of the same genotype immunostained with anti-Diap1 (F,F'; green), anti-cleaved caspase-3 (G,G'; cyan) and stained with propidium iodide (E,E'; red). (H,H') are merged images of all signals. The brackets in (E-H) point to a wide area of strongly decreased Diap1 staining in follicular epithelium (F). In this area, follicle cells showing highly condensed nuclei (E) and active caspase-3 (G) are detectable. Higher magnification views of the boxed areas in (E-H) are shown in panels (E'-H') where a dotted line marks the border between very low levels (on the left) and high levels (on the right) of Diap1 staining. Anterior is left in all the panels. Scale bars in this figure represent 20 μm (*Romani et al.,* 2009).

I then examined the expression of the *Drosophila* inhibitor of apoptosis protein 1 (Diap1) a potent caspase inhibitor that is essential to prevent inappropriate caspase activation and ubiquitous apoptosis (*Goyal et al.,* 2000; *Wang et al.,* 1999; *Xu et al.,* 2005). This anti-apoptotic protein is ubiquitously expressed at stage 9 and 10 of

oogenesis in follicle cells (*Geisbrecht and Montell*, 2004). Diap1 is involved in PCD that occurs at the mid-oogenesis checkpoint and that leads to egg chambers degeneration in response to poor environmental condition. It has been reported that degenerating egg chambers exhibit strongly lowered levels of Diap1 cytoplasmic staining in nurse cells while high levels of caspase-3 activity is detectable throughout the egg chambers (*Baum et al.*, 2007).

To determine if this relationship also exists in follicle cells lacking *EcR-B1* function, I performed an immunostaining on *EcR-B1* RNAi egg chambers with both Diap1 (kindly provided by B. Hay) and caspase-3 antibody (Figure 27E-H and E'-H').

Coimmunostaining of egg chambers clonally expressing the *UAS-IR-EcR-B1* transgene showed a dramatic downregulation of Diap1 (Figure 27F and F') that is concomitant with high levels of caspase-3 activity (Figure 27G and G') in follicle cells exhibiting highly condensed nuclei (Figure 27E,E' and H,H'). These results indicate that knocking down the EcR-B1 isoform at early stages of oogenesis alters proper follicular epithelium monolayer structure and leads to premature apoptotic death of follicle cell.

These data have been published on *Genetics* (*Romani et al.*, 2009).

4.8 Ubiquitous silencing of *EcR-A* causes the formation of altered dorsal appendages

To investigate *EcR-A* gene function in follicular epithelium morphogenesis, I used reverse genetic approach by overexpressing RNA interference transgene specific to knock down *EcR-A* gene function. The transgene used for this analysis was *UAS-IR-EcR-A* containing inverted repeat sequences designed to target the three 5'-*EcR-A*-specific exons *α0*, *α1* and *α2* (*Roignant et al.*, 2003) (Figure 20).

To study the effects of *EcR-A* silencing, also in that case, the transgene was expressed using the ubiquitous and strong *tub-Gal4* driver coupled with *tub-Gal80^{ts}* transgene expression. Again, to induce Gal4 activity and thus *EcR-A* knock down, adult females of the correct genotype were kept at 31°C for 6 days and then dissected and ovary analyzed.

I found that specific knock down of *EcR-A* does not alter follicular epithelium integrity indicating that EcR-A and EcR-B1 have distinct functions also during oogenesis.
Interestingly, I observed that *EcR-A* silencing causes the production of eggs with short and flattened dorsal appendages as showed in Figure 28B,C and D, compared with a wild type egg whose dorsal appendages are normally formed (Figure 28A).

Figure 28: **Ubiquitous knockdown of *EcR-A* in the follicular epithelium alters dorsal appendage formation.** Fluorescence images of stage 14 egg chambers from control females (A) and from females overexpressing the *UAS-IR-EcR-A* transgene under the control of the *tub-Gal4* promoter (B-D) treated in the same experimental condition. As acquisition in light field (B and magnification in C) and propidium iodide staining (D) show, *EcR-A* silencing causes the production of stage 14 egg chambers with short and flattened dorsal appendages compared with a wild type stage 14 where dorsal appendages are normally formed (A).

The eggshell appendages are formed starting from columnar follicle cells during late oogenesis. Each dorsal appendage arises from a cluster of epithelial follicle cells originally situated anteriorly and on either side of the dorsal midline of the oocyte. Midway through egg chamber development, the cells in each primordium reorganize from a flat epithelial sheet to produce a tube, which serves as a mold for secreted chorion destined to become an appendage (reviewed by *Spradling,* 1993; *Waring,* 2000). The dorsal appendage follicle cells are specified by a combination of spatial information provided by both the anterior/posterior and dorsal/ventral axes. Previous

genetic analyses demonstrated that two major signal transduction pathways control this process: the EGFR and Dpp pathways. Moreover, the Z1 isoform of Broad Complex (Br-CZ1) plays a key role in this process integrating EGFR and Dpp signaling (*Deng and Bownes*, 1997; *Tzolovsky et al.*, 1999). Because Br-C is an early ecdysone response gene, this result suggests that ecdysone involvement in this control is mediated by EcR-A isoform acting on Br-CZ1.

4.9 The *ecdysoneless* gene in *Drosophila melanogaster*

The ecdysoneless gene (*ecd*) was initially identified as a temperature-sensitive mutant ecd^{1} with deficiency of the steroid hormone ecdysone (*Garen et al.*, 1977) and several additional larval lethal mutants (*Sliter et al.*, 1989; *Henrich et al.*, 1993). The actual gene responsible for the phenotype was not discovered until 27 years later, when *ecd* was identified with gene CG5714 by *Gaziova et al.*, (2004). It is localized on the left arm of the third chromosome, in the cytological region 62D2-62D4 and covers a region of 2158 bp. *Gaziova et al.*, (2004) demonstrated that the gene encodes a 684 amino acid-long protein that migrates with an apparent molecular weight of 77,9 kDa.

Drosophila Ecd has an overall 43% amino acid identity to homologs in *Anopheles gambiae*, 31% in *Homo sapiens* and *Mus musculus*, 30% in *Danio rerio*, 26% in *Arabidopsis thaliana* and 21% in *Schizosaccharomyces pombe* (Figure 29).

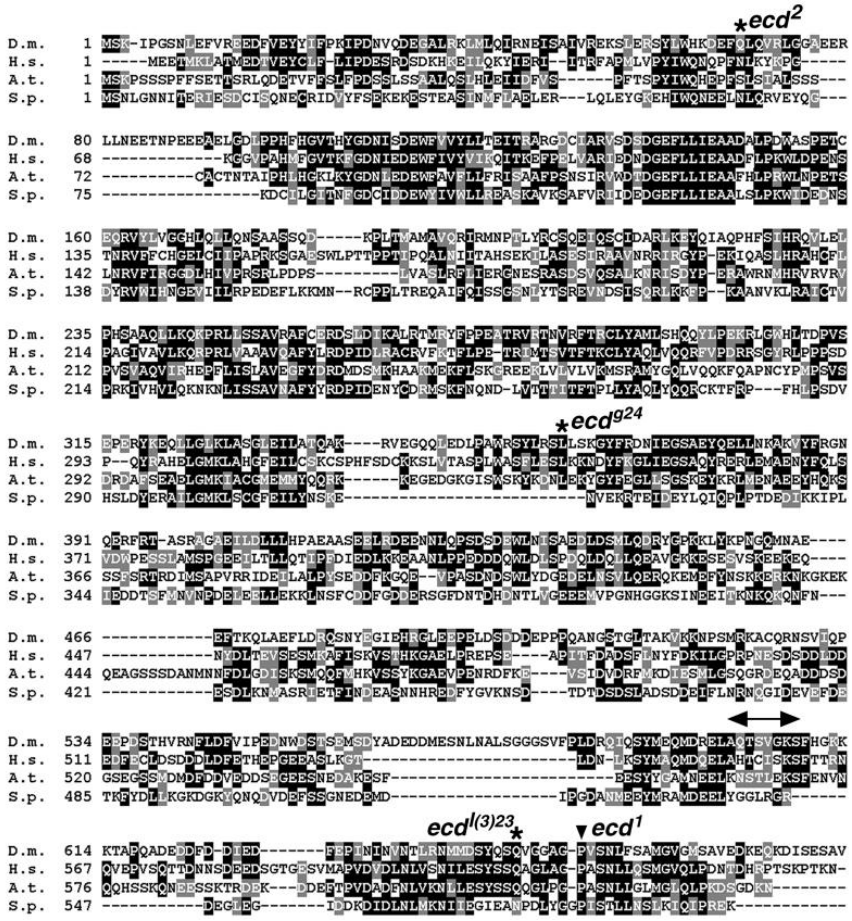

Figure 29: **Ecdysoneless is conserved throughout eukaryotes.** Alignment of the *Drosophila* Ecd protein with human SGT1 and its closest relatives from *A. thaliana* (At; Q9LSM5) and *S. pombe* (Sp; Q9US49), using Clustal W. Black shading indicates amino acid identity, and gray shading indicates similarity if present in two or more of the aligned sequences. The putative ATP/GTP-binding site (P-loop) is marked by horizontal arrow. Asterisks indicate the positions of the premature termination codons in alleles ecd^{2}, ecd^{g24} and ecd^{l23}. The arrowhead indicates the conserved proline 656, which is mutated to serine in ecd^{1} (*Gaziova et al.*, 2004).

Northern blot analysis of whole animals showed a single *ecd* transcript, present throughout development in steroidogenic as well as non-steroidogenic tissues (*Gaziova et al.*, 2004).

The mRNA was more abundant towards the end of the final larval instar and during metamorphosis; the strongest expression was observed in mature, egg-laying females. *In situ* hybridization showed that this increase probably resulted from strong *ecd* expression in the ovarian nurse cells.

The continuous *ecd* expression was confirmed at the protein level using a specific antibody that detected Ecd from early embryogenesis to adulthood (*Gaziova et al.*,

2004). Staining of late-third instar larvae revealed Ecd expression in the steroidogenic lateral lobes of the ring gland. Also the rest of the body displayed only a diffuse signal without a restricted pattern. Ecd expression was found in the nervous system, in the imaginal discs and in developing gonads of third instar larvae. In all cases the Ecd protein predominantly resided in the cytoplasm.

Four *ecd* mutations have been identified and characterized (*Gaziova et al.,* 2004): *ecd* ^{1}, *ecd* ^{2}, *ecd* ^{g24} and *ecd* ^{l23} (Figure 29, see asterisks and arrowhead). The *ecd* ^{1} mutation is a recessive, temperature-sensitive allele that contains a substitution of the conserved proline 656 to serine resulting from a C to T transition. It has been demonstrated that this mutation reduces whole-body ecdysone titers and causes larval arrest at restrictive temperature, 29°C (*Garen et al.,* 1977). The *ecd* ^{2} allele contains a C to T transition that converts Q67 to a stop codon. In the γ-ray induced *ecd* ^{g24}, a four-base-pair deletion causes a frameshift of four aminoacids followed by a stop codon. In *ecd* ^{l23}, the premature termination codon results from a C to T transition at Q650.

4.10 The human and yeast orthologue of *Drosophila ecdysoneless* gene

ecd gene shows a strong evolutionary conservation throughout eukaryotes from fission yeast to humans suggesting a conserved biochemical role. At present, however, no specific structural domains or motifs linked to Ecd function have been identified in any species. The first potential role of Ecd was suggested in yeast where human Ecd was able to substitute for the coactivator function of GCR2, which encodes a general regulatory factor of glycolytic gene expression in *Saccharomyces cerevisiae* (*Sato et al.,* 1999) and deletion of *ecd* in *S. pombe* showed that Ecd is important for cell growth and expression of many genes involved in cellular processes including various metabolic pathways (*Kainou et al.,* 2006). Futhermore, *S. pombe* Ecd appears to be localized to the nucleus and to be required for cell survival. Moreover, previous studies showed that human Ecd (hEcd) interacts with and stabilizes p53 and its overexpression in mammalian cells increases the transcription of p53 target genes (*Zhang et al.,* 2006).

It has also been reported that hEcd directly interacts with three Rb protein family members (p105, p107 and p130), that have emerged as key controllers of cell cycle progression, and competes with E2F transcription factor for association with hypo-phosphorylated Rb, and regulates E2F target gene expression and cell cycle progression, indicating that mammalian Ecd plays a role in cell cycle progression via the Rb-E2F pathway (*Kim et al.*, 2009).

Kim et al., (2010) demonstrated that human Ecd possesses transcriptional activity even though its DNA-binding motif is unknown. Mutational analyses presented by the authors showed that the C-terminal region of Ecd is crucial for its function as a transcriptional regulator. In particular, Asp484 and Leu489 are critical for transactivation, as each single point mutation was able to abolish the transactivation activity. These point mutations in the acidic region might cause a slight structural change in the activation domain, which might result in the reduced transactivation activity of these mutants.

Further evidence to support the observation that Ecd functions as a transcriptional regulator is provided by its cooperation with p300, a histone acetyltransferase (HAT). It is well documented that transcriptional factors directly interact with HAT proteins, such as p300, to perform a role in transcriptional regulation (*Imhof et al.,* 1997; *Vo and Goodman,* 2001).

4.11 *ecd* ^{l23} loss of function clones in eye imaginal disc fail to proliferate

To date, the precise biochemical function of *Drosophila* Ecd in ecdysone pathway, such as an enzyme function or other regulatory role, has not been elucidated.

It has been demonstrated that Ecd clearly plays a role in oogenesis, as the restrictive temperature prevents development of egg chambers beyond stage 8 in *ecd* ^{1} flies. Ovaries with *ecd* $^{-/-}$ clones displayed defective egg chambers with extranumerary nurse cells, often double the normal 15. Moreover, defective egg chambers that had probably fused from several cysts early in their development showed multiple oocyte precursors (*Gaziova et al.,* 2004).

During the 5 months spent in Prof. Marek Jindra's lab, I've been involved in a project directed towards understanding ecd function in non-steroidogenic tissues. In particular, I focused my analyses on exploring *ecd* function in imaginal disc morphogenesis.

To examine whether *ecd* plays a role in imaginal disc development, I analyzed the eye imaginal disc phenotype produced by loss of *ecd* through clonal analysis. To this purpose I generated clones by using a loss-of-function *ecd* mutation. The mutant line used in my analysis was *ecd* ^{l23} (*Gaziova et al.,* 2004). Homozygous *ecd* ^{l23} clones were obtained through somatic recombination using the Flp/FRT system coupled with the UAS/Gal4 system (*Golic,* 1991; *Xu and Rubin,* 1993; *Brand and Perrimon,* 1993). Recombination between FRT sites was induced by driving the Flp enzyme under the control of the *eyeless* promoter (*ey-Flp*). In addition, I used the Flp-out cassette *Act>y*$^{+}$*>Gal4* (*Pignoni and Zipursky,* 1997) to induce *UAS-GFP* expression useful to positively mark the *ecd* mutant clones. Larvae of the correct genotype were kept at 25°C and then, when they reached the L3 instar, were dissected and imaginal eye disc extracted.

As shown in the Figure 30, cells homozygous for *ecd* ^{l23} mutation positively marked by GFP (Figure 30A) are very few. In addition, clones are very small, suggesting that they fail to proliferate (Figure 30B and C). Homozygous *ecd* ^{l23} clones also seem to survive better when located posterior to the morphogenetic furrow and this finding could be due to the fact that these cells do not divide anymore but differentiate into photoreceptors.

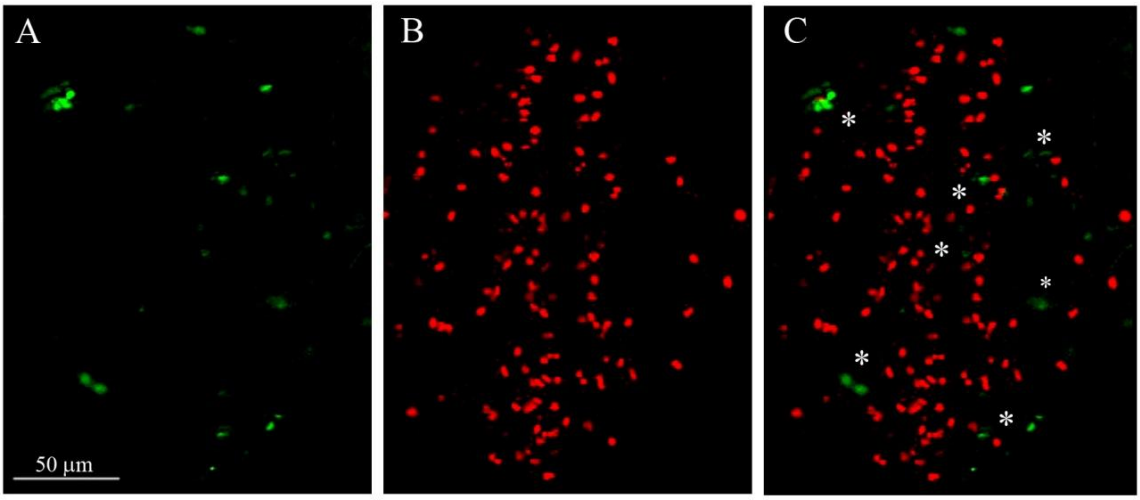

Figure 30: ***ecd*** ^{l23} **loss-of-function clones in eye imaginal disc fail to proliferate. (**A-C) Confocal image of imaginal eye disc where *ecd* mutant clones positively marked by GFP (A; green) are induced using *ey-Flp*. Clones are small and very few (A) and PH3 staining (B; red) shows that *ecd* mutant clones do not proliferate and subsequently do not grow (C, see asterisks). Scale bar represents 50 µm in this figure.

4.12 During imaginal disc development e*cd* depletion through RNA interference promotes apoptosis-induced compensatory proliferation through caspase-3 and JNK activation

In parallel to the analysis made with *ecd* ^{l23}, I investigated the role of *ecd* in the development of imaginal tissues using an RNA interference approach. The transgene used, *UAS-ecdRNAi*, containing a region of 473 bp of the *ecd* gene (position 3048-3521), was generated in M. Uhlirova's laboratory (Figure 20).

First, I performed a clonal analysis of *ecd* in order to knock down its function in imaginal wing disc development. Using the Flp-out/Gal4 technique, I randomly expressed the *UAS-ecdRNAi* transgene under the *actin* promoter in clonal patches of cells by using the Flp-out cassette driver *Act>y*$^{+}$*>Gal4, UAS-GFP* and a *heat-shock-Flp-recombinase* (*hs-Flp*). Clones were induced at 48 hours after egg laying (AEL) and the locations of *ecd* loss of function clones were mapped by the presence of GFP signal. After clones induction, larvae of the correct genotype were kept at 25°C and then, when they reached the L3 instar, were dissected and imaginal wing discs extracted.

Extensive analyses of these imaginal wing discs reveal that clonal cells are visible 24 or 48 hours post induction, but at 72 hours they disappear. Only small islands of round, likely apoptotic, cells may be found at the later time.

The mosaic discs were stained with an antibody against phospho-histone H3 (PH3) (Figure 31B) and I found that cells expressing *ecd* RNAi transgene (Figure 31A) do not possess PH3 signal suggesting that they cannot go through mitosis (Figure 31C). Deep confocal analysis of these discs show that PH3-positive cells mainly surround the clones and this result suggests that wild type cells close to the clones may undergo compensatory proliferation (Figure 31C).

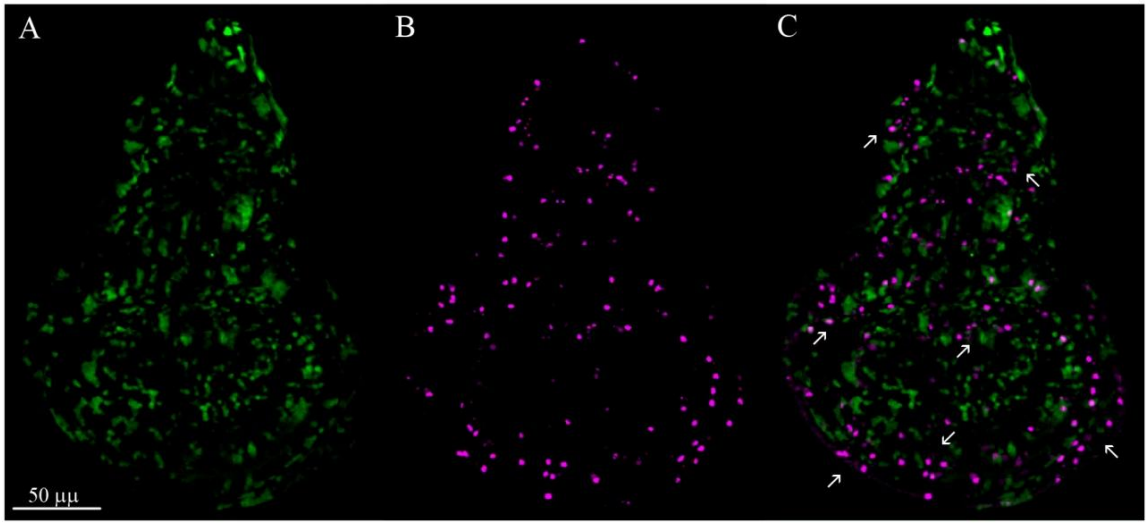

Figure 31: **Clonal e*cd* depletion through RNA interference in wing discs promotes compensatory proliferation of surrounding wild type cells. (**A-C) Confocal image of wing disc where *ecd* RNAi-mediated knockdown is induced in clonal patches of cells using *hs-Flp*. Staining with PH3 antibody (B; magenta) revealed that ecdRNAi clones positively marked by GFP (A; green) fail to proliferate (C). In particular, PH3 signal is detected around clonal cells, indicating that wild type neighboring cells undergo compensatory proliferation (C, see arrows). Scale bar is 50 µm in this panel.

To further investigate if *ecd* knockdown promotes compensatory proliferation in imaginal wing discs, I genetically depleted *ecd* in the posterior compartment of the wing disc by expressing RNA interference transgene previously described under the control of the *engrailed* promoter using the UAS/Gal4 system.

engrailed-Gal4 (*en-gal4*) enhancer trap line leads *UAS*-linked gene expression only in the posterior compartment of the wing disc. Moreover, because of the presence of the anterior/posterior boundary restriction, anterior compartment represents an internal control.

Larvae of the correct genotype were kept at 25°C and then, when they reached the L3 instar, were dissected and imaginal wing discs extracted.

Despite *ecd* depletion was driven only in the posterior compartment, the morphology of the whole disc results altered. Moreover, in the majority of the L3 larvae dissected I could not find wing discs, and larvae *en-Gal4,UAS-GFP/+;UAS-ecdRNAi* failed to complete development arresting at prepupal stage.

Immunostaining with specific antibody for ecd that specifically recognize a region of Ecd protein (aa 270-429, *Gaziova et al.*, 2004) (Figure 32), confirmed that expression of the RNA interfering transgene driven in the posterior compartment (Figure 32B) was effective in reducing Ecd levels (Figure 32A). Moreover, by analyzing the *ecd* knockdown discs, I found that wing pouch is more sensitive to loss of *ecd* than the hinge and notum regions (Figure 32C, see arrows).

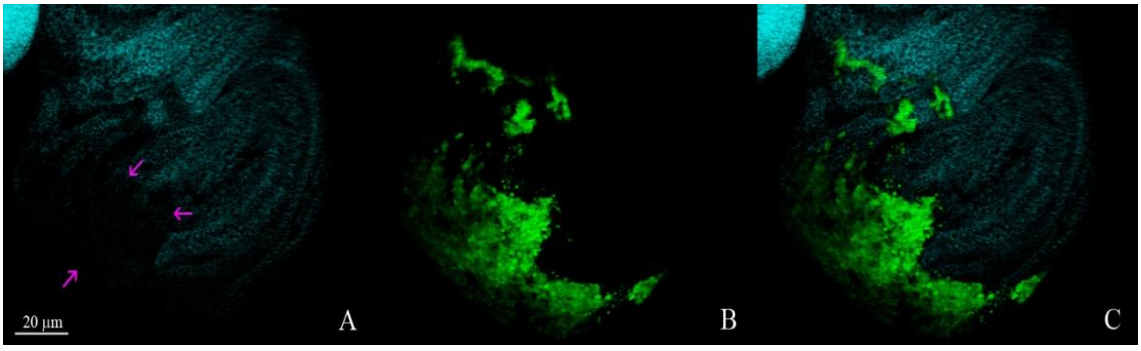

Figure 32: ***ecd* silencing in imaginal wing discs effectively reduces ecd protein level.** Confocal image of wing disc where *ecd* silencing through RNAi is driven by *en-gal4* line. Staining with ecd antibody (A; cyan) reveals that ecd protein is absent or barely detected in the posterior compartment, where *en-Gal4* drives *ecd* knockdown and GFP expression (B and C). As shown in this figure, wing pouch results more sensitive to *ecd* depletion than notum and hinge regions, as ecd antibody staining shows (A, see arrows). Scale bar represents 20 µm.

Staining with PH3 antibody (Figure 33B) shows that the posterior compartment cells overexpressing the *ecd* RNAi transgene (Figure 33A) present a higher number of PH3 positive spots than the ones detected in the anterior compartment. In addition, more PH3 spots are detected in the wing pouch (Figure 33B, see arrows and legend). This result indicates that *ecd* knockdown induces non-autonomous cell proliferation.

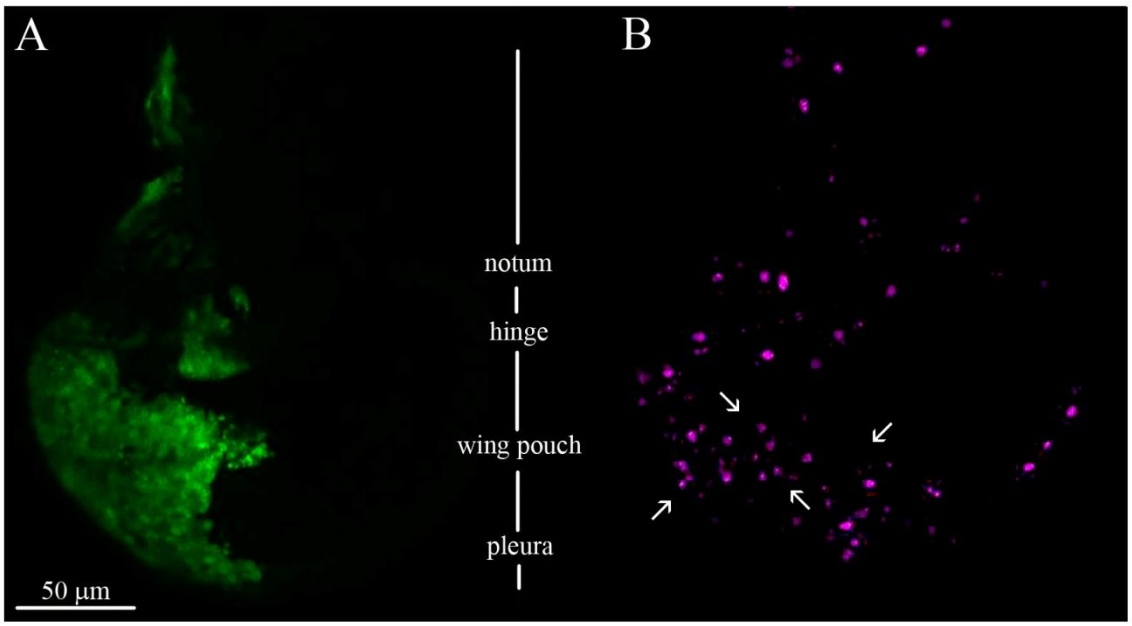

Figure 33: ***ecd* silencing in wing imaginal discs promotes compensatory proliferation.** (A-B) Confocal image of wing disc expressing *UAS-ecd-RNAi* with *en-Gal4* enhancer trap line. Cells overexpressing RNAi transgene are positively marked by GFP (A; green). Staining with PH3 antibody (B; magenta) reveals that in the wing pouch are detected more PH3 positive spots than in other region of the posterior compartment (see legends and arrows). Scale bar represents 50 µm in this figure.

Looking at the morphology of the whole disc, it is clear that the tissue is completely altered. To determine if *ecd* knockdown induces programmed cell death program in particular in the wing pouch region, I checked if there is activation of Caspase-3 protein. Staining with active caspase-3 antibody (Figure 34) shows that *ecd* knockdown cells, positively marked by GFP (Figure 34A), undergo apoptosis (Figure 34B). In particular, programmed cell death mostly occurs at the border of the posterior compartment, where mutant and normal tissues are in close contact (Figure 34B).

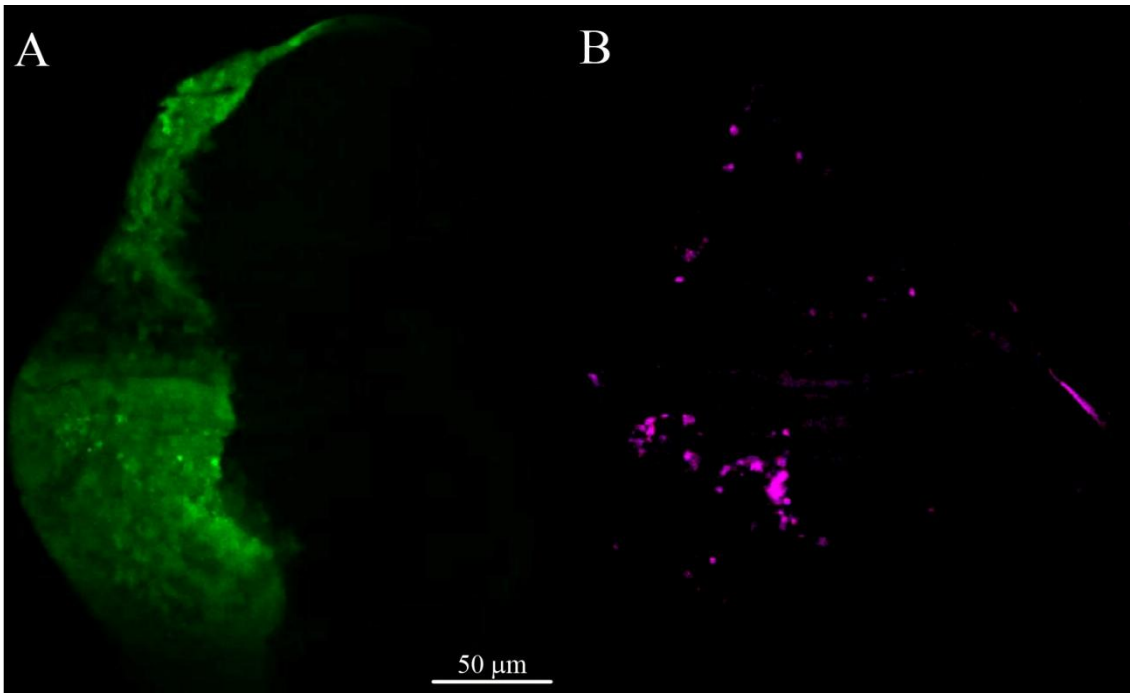

Figure 34: ***ecd* silencing in imaginal wing disc induces apoptosis.** Confocal image of imaginal disc stained with active caspase-3 antibody (B; magenta). Caspse-3 signal is detected in *ecd* RNAi cells, positively marked by GFP (A; green) indicating that these cells undergo apoptosis. In particular, apoptosis is mostly detected at the border suggesting that programmed cell death mostly occurs where mutant and normal tissues are in close contact. Scale bar in this figure represents 50 µm.

It has been demonstrated that during development, epithelia replenish those cells that are damaged and shed during normal physiological conditions. When epithelia are exposed to insults, either environmental or genetic, that lead to increased cell death, they have a remarkable capacity to compensate for this cell loss (*Haynie and Bryant*, 1976).

In general, this model states that when apoptosis is initiated in epithelial cells, these dying cells secrete morphogens to promote proliferation of the surrounding cells, which leads to replacement of the dying cells and maintenance of tissue size. In proliferating epithelial cells, activation of the proapoptotic genes *reaper* (*rpr*) and *head involution defective* (*hid*) leads to degradation of Diap1, thereby releasing the initiator caspase Dronc, and ultimately upregulation and secretion of the morphogens Dpp and Wingless (Wg) via c-Jun N-terminal kinase (JNK) (Figure 35).

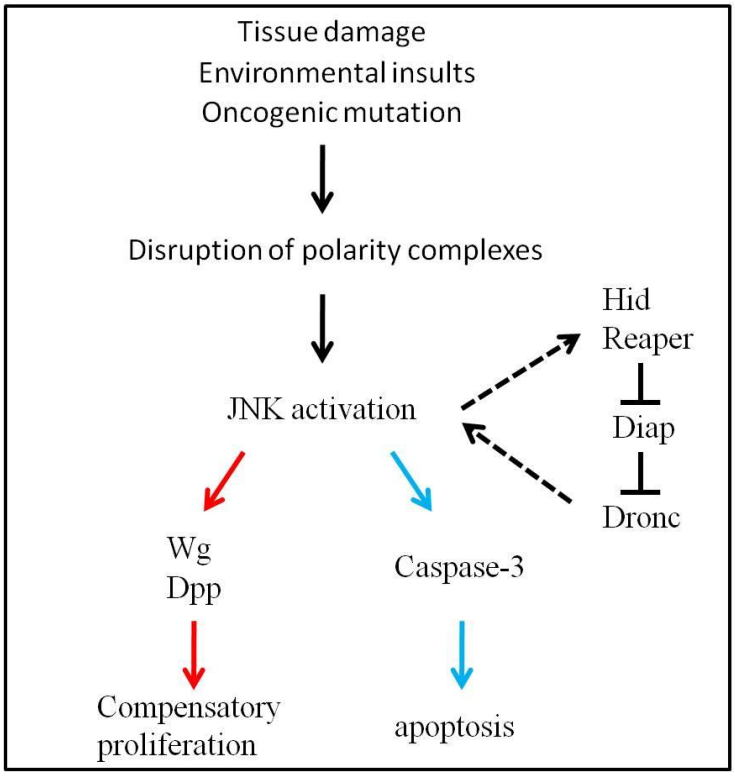

Figure 35: **A working model for regulation of apoptosis-induced compensatory proliferation.** Tissue damage, irradiation or oncogenic mutations that disrupt epithelial polarity activate a JNK cascade, resulting in apoptosis and compensatory proliferation (Modified from *Werner et al.*, 2010).

Hence a key component in the apoptosis-induced compensatory proliferation pathway is JNK. Therefore, I tested whether *ecd* knockdown promotes JNK activation through immunostaining on imaginal discs depleted of *ecd* function using JNK (anti-Phospho-SAPK/JNK, G9, Cell Signaling Technology; *Whitmarsh and Davis*, 1998) and ecd antibodies (Figure 36). I found that in the posterior compartment where *ecd* silencing occurs, as shown by GFP signal (Figure 36A) and ecd labeling (Figure 36C), high JNK activity is detected (Figure 36B and D). This result indicates that cells lacking *ecd* function promotes apoptosis-induced compensatory proliferation through JNK activation.

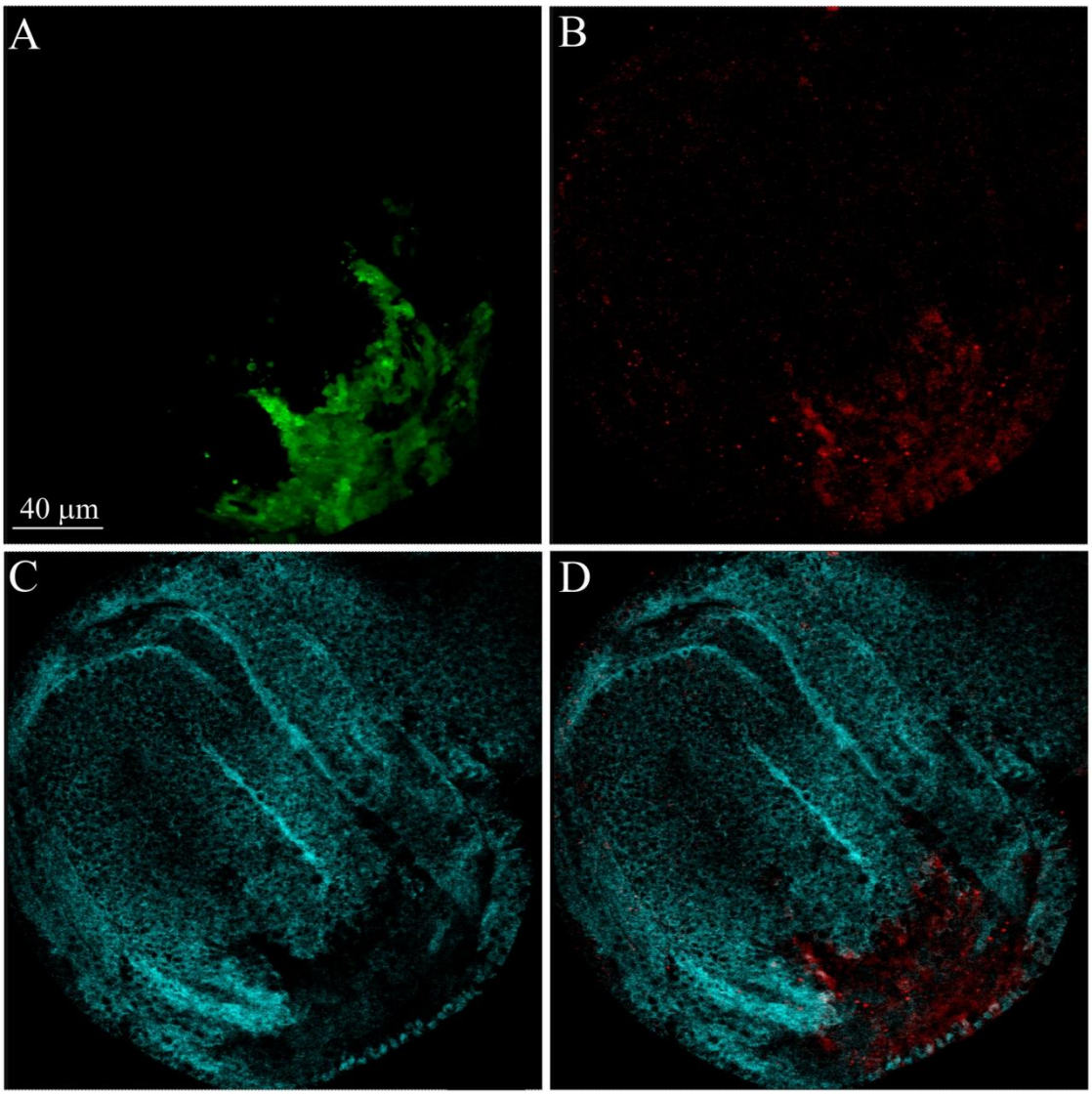

Figure 36: ***ecd* silencing promotes apoptosis-induced compensatory proliferation via JNK activation.** Confocal image of wing disc expressing *UAS-ecdRNAi* transgene in the posterior compartment (A; green) stained with JNK (B; red) and ecd (D; cyan) antibodies. In this picture the strong activation of JNK is detected in cells lacking of *ecd*, as ecd staining shows (D), indicating that *ecd* RNAi cells that are undergoing apoptosis induce JNK activation to promote compensatory proliferation of the tissue. Scale bar in this figure represents 50 µm.

The secreted morphogen Wingless (Wg) has been demonstrated to be upregulated downstream of JNK in the apoptosis-induced compensatory proliferation response in proliferating epithelium (*Ryoo et al.*, 2004; *Perez-Garijo et al.*, 2009) (Figure 37).

To establish if in imaginal wing discs lacking *ecd* function Wg protein is upregulated, I performed an immunostaining with a specific antibody against Wg protein (4D4, DSHB; *Brook and Cohen,* 1996) (Figure 37). By analyzing the wing discs, it results

evident that there is an increment of Wg protein levels in cells depleted of *ecd* (Figure 37C).

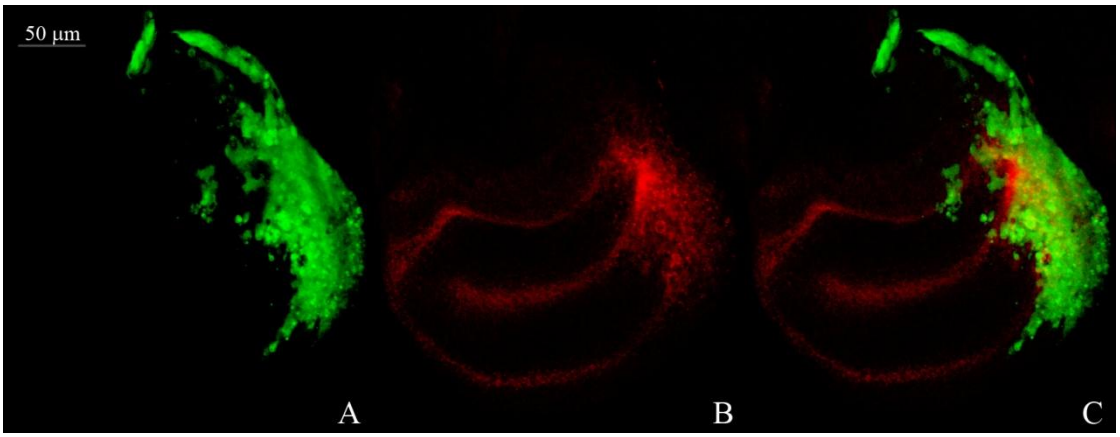

Figure 37: ***ecd* silencing promotes apoptosis-induced compensatory proliferation increasing wg levels.** Confocal image of wing discs where *ecd* knockdown was induced in the posterior compartment (A; green). Staining with an antibody that recognizes Wg protein (B; red) indicates that this protein is strongly upregulated in cells lacking ecd function (C). Sale bar is 50 µm.

These results strongly support that *ecd* silencing in imaginal discs promotes apoptosis-induced compensatory proliferation through activation of caspase-3 and JNK signaling. Moreover, *ecd* RNAi cells that are undergoing apoptosis increase levels of Wg protein, that subsequently promotes proliferation of the surrounding cells, which leads to replacement of the dying cells and maintenance of tissue size.

It is extensively reported that dMyc plays a fundamental role in regulating basic cellular growth machinery. Indeed dMyc regulates both cell growth and cell cycle in imaginal wing discs (*Johnston et al.,* 1999).

Recently, *Smith-Bolton et al.,* (2009) have shown that regeneration in response to surgical or apoptotic tissue damage that occurs via JNK activation and the upregulation of Wg, involves also Myc action. In particular, the increment of Wg levels induces elevated Myc expression in the surrounding cells promoting regenerative growth in order to save tissue size and integrity.

The ability of Myc to potentiate regenerative growth may relate to Myc's role in promoting cell plasticity, which was observed when the overexpresion of *c-myc*

together with other genes that promotes reprogramming of cell fate (*oct-4*, *sox2* and *klf4*) converted cultured adult fibroblast into pluripotent stem cells (*Takahashi and Yamanaka*, 2006).

To determine if surrounding cells increase their ability to growth in response to secretion of Wg morphogen by *ecd* RNAi cells, I performed a co-immunostaining with dMyc (kindly provided by P. Gallant; *Gallant et al.*, 1996) (Figure 38B, red) and Ecd (Figure 38D, cyan) antibodies. As shown in Figure 38, in *ecd* knockdown compartment (A, green) Ecd protein is absent or barely detected (D, cyan) and dMyc signal is strongly reduced (B and C, red), while in the wild type neighboring cells Ecd levels are normal (Figure 38D) and dMyc expression results upregulated (Figure 38B and C). In particular, an increment of dMyc protein is detected at the border of the compartment (Figure 38C, see arrows), suggesting that wild type cells increased their proliferation rate in order to replenish damaged tissue causes by *ecd* silencing (Figure 38E).

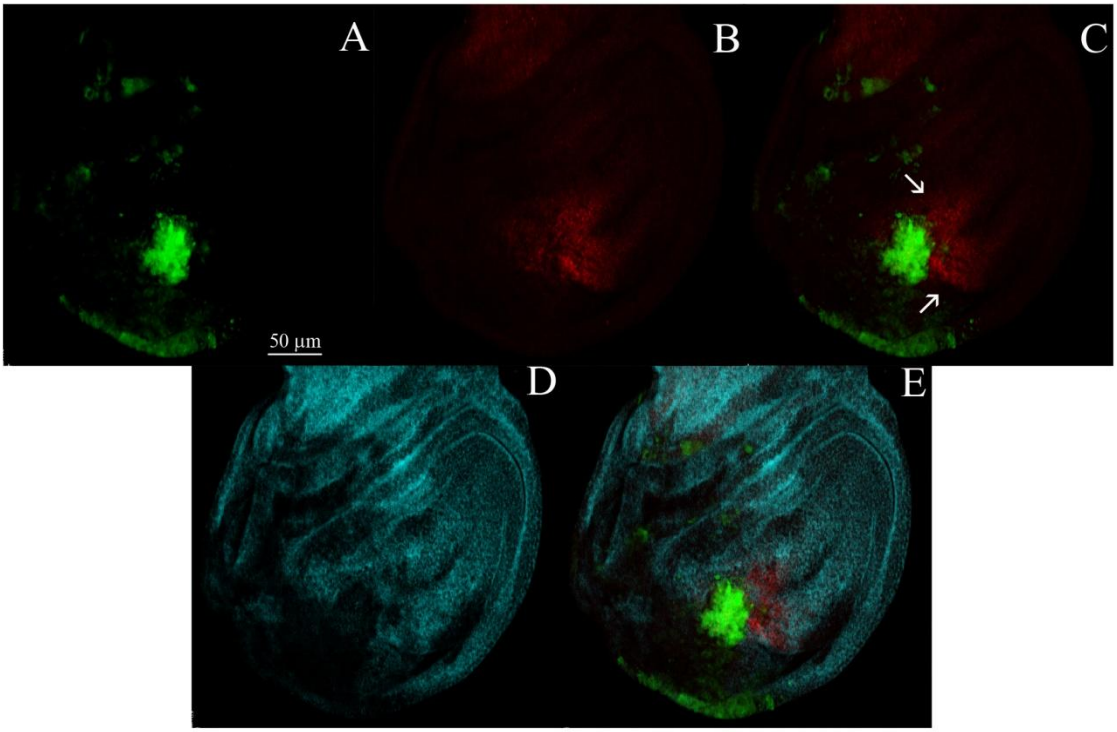

Figure 38: ***ecd* silencing induces an increment of dMyc protein levels in the neighboring cells.** Confocal image of wing disc expressing *UAS-ecdRNAi* in the posterior compartment (A; green). Staining with Ecd antibody (D and E; cyan) and an antibody directed to the whole dMyc protein (B; red) reveals that dMyc is downregulated in the *ecd* knockdown cells (C), while its levels are upregulated in the surrounding cells closer to the border of the compartment (C, see arrows).

5-Discussion

In *Drosophila*, a single steroid hormone, ecdysone, appears to be responsible for directing the major developmental transitions. Pulses of ecdysteroids are produced at various times during fly life cycle and ecdysone acts as a critical spatial and temporal signal to trigger specific hormone-responses in different developmental stages.

To understand the molecular mechanisms that allow ecdysone to accomplish different and sometimes antagonistic functions in the same developmental process, I examined the effects of disruption of ecdysone-dependent cascade in two different stages of *Drosophila* life cycle, the oogenesis and the imaginal disc morphogenesis. In particular, using reverse genetic approaches, I analyzed the effects of blocking hormone signaling at two different steps. On the one hand, I knocked down *EcR* gene function during oogenesis inhibiting ecdysone signaling after hormone production and release, and on the other hand, I depleted during imaginal disc development the function of *ecd*, a gene involved in ecdysone pathway whose mutation affects hormone levels.

EcR signaling affects egg chamber development: Ubiquitous expression in follicle cells (FCs) of a dominant negative form of EcR, EcR-DNF645A, causes early degeneration of the egg chambers. Degeneration occurs at multiple steps inside the ovariole indicating that EcR plays a fundamental role in the maintenance of egg chamber integrity.

Moreover, stage-specific expression of this mutant receptor using *Cy2-Gal4* enhancer trap line also results in degeneration of the egg chambers, supporting for EcR an important role during oogenesis. Furthermore, the analysis of stage 10B egg chambers with DAPI and TRITC-Phalloidin staining shows that EcR-DNF645A expression in main body follicle cells affects the distribution of these cells on the surface of the egg chambers and alters actin cytoskeleton. FCs accumulate at the posterior end of the egg chamber leading the swelling oocyte uncovered. In addition, in the most anterior follicle cells the phosphorylated form of Mad factor is undetectable, indicating that this cell population does not acquire the proper fate.

The clonal analysis shows that at stage 10B patches of FCs expressing EcR-DNF645A

are incorrectly located at the anterior region of the egg chamber instead of being part of the main body follicle cells.

During oogenesis, follicle cells undergo events of differentiation and migration to favor the increase in size of the oocyte. At stage 10B, FCs complete their migration and their differentiation in different subpopulations.

Given this consideration, the data I obtained suggest that overexpression of the mutant EcR hampers proper migration of FCs.

In addition, follicle cell clones overexpressing the EcR mutant receptor exhibit a reduced nuclear size compared with the neighboring wild type cell size. This result may be explained hypothesizing that EcR-DNF645A overexpression affects endoreplication of follicle cells. It has been previously shown that EcR pathways in combination with Notch activity regulates Tramtrack (Ttk69) expression, which in turn triggers the switch from endoreplication to gene amplification in follicle cells. High levels of Ttk69 stop endoreplication and allow the cells to enter the synchronous gene amplification stage (*Sun et al.,* 2008). In the light of that, it is likely to presume that EcR could be involved also in endoreplication process through which the follicle cells become polyploid and increase their size.

Tissue-specific silencing of *EcR-B1* at early and mid-stages of oogenesis results in delamination of follicle cells and loss of follicular monolayer integrity. The analysis of different cell polarity markers shows that targeting *EcR-B1* at stage 7 of oogenesis causes complete loss of follicle cell polarity. The AJs components DE-Cad and Arm fail to localize properly and the F-actin cytoskeleton is strongly affected in multilayered follicle cells. Cadherin-mediated adhesive junctions play a major role in epithelial polarization and are integral to the proper assembly of the lateral surface domain. Accordingly, my analysis of Dlg and Scrib distribution, that are components of the BLJ, shows that baso-lateral polarity is altered in follicle cells in which EcR-B1 function was silenced. Moreover, the analysis of aPKC localization established that apical membrane identity is also compromised.

I observed that multilayering of follicle cells is not due to loss of proliferative control. It has been shown that induction of follicle cell apoptosis by expression of the *reaper* gene causes a decline of Arm levels that is coincident with nuclear condensation (*Chao and Nagoshi,* 1999). The quite undetectable Arm levels I detected in *EcR-B1* knockdown follicle cells were not associated with nuclear pycnosis, suggesting that the decrease in Arm signal does not arise from proteolytic cleavage driven by the apoptotic machinery. In support of this, *EcR-B1* mutant cells are negative to TUNEL assay. Hence the reported abnormalities of polarity markers following late *EcR-B1* knockdown do not arise from cytological events associated with apoptosis.

The ecdysone pathway is involved in the control of turnover of cadherin-containing cell adhesion complexes in border cells. As reported in previous works, loss of *usp* function in border cells blocks their migration and the coactivator of the EcR/USP complex, Taiman, stimulates turnover of adhesion complexes to allow forward movement of border cells (*Bai et al.,* 2000). Thus it is possible to hypothesize that the EcR-B1-mediated ecdysone signaling controls the turnover of AJs components in the follicle cells surrounding the egg chamber.

The clonal analysis performed shows that targeted *EcR-B1* RNAi at early stages of oogenesis, when follicle cells are still actively proliferating, induces apoptotic cell death beside loss of monolayer integrity. The EcR-B1 isoform is required in a cell-autonomous manner, since mutant phenotypes do not extend to the surrounding wild type tissue. *EcR-B1* silencing causes a strong downregulation of Diap1, that holds a key role in preventing apoptosis.

During oogenesis, two developmental checkpoints, in the 2A region of the germarium and at mid-oogenesis (stage 8-9), monitor egg chamber to determine development continuation or apoptosis onset (*McCall,* 2004; *Terashima and Bownes,* 2005). In particular, the ecdysone pathway is involved in the developmental checkpoint at stage 8 of oogenesis and in the apoptotic death of nurse cells occurring during nutritional shortage at stages 8 and 9 of oogenesis. It has been shown that starvation leads to a rapid increase of ecdysteroids levels in the ovaries and that this high concentration

results in apoptotic death of nurse cells (*Bownes*, 1989; *Terashima and Bownes*, 2004; *Terashima et al.*, 2005). Interestingly, it has been reported that Diap1 expression in nurse cells is downregulated at stages 7-8 when mid-oogenesis checkpoint acts, and again at stage 11 when developmentally programmed cell death (PCD) occurs (*Baum et al.*, 2007). In addition, degenerating mid-oogenesis egg chambers exhibit low levels of Diap1 in nurse cells that are coincident with intense activity of caspase-3. Of interest, in *EcR-B1* knockdown follicle clones downregulation of Diap1 and activation of caspase-3 have been detected. Moreover these follicle cells exhibit strong nuclear condensation and DNA fragmentation that are considered strong evidences of cells undergoing apoptosis. In fact, I found TUNEL positivity in correspondence of pycnotic nuclei in *EcR-B1* knockdown follicle cell clones.

Taken together these considerations, it is reasonable to hypothesize that in the follicle cells the EcR regulates the same molecular machinery acting in nurse cells to execute PCD.

Loss of EcR-B1 function at early stages of oogenesis causes piling up of follicle cells. The presence of delaminating follicle cell stretches in early egg chambers could represent a defect that is recognized by the mid-oogenesis checkpoint. This checkpoint could then trigger apoptosis to eliminate these defective egg chambers. Since the mid-oogenesis checkpoint acts at stage 7-8, *EcR-B1* silencing at later stages results in multilayered phenotype without follicle cell death.

The three EcR isoforms are hypothesized to have unique functions triggering distinct responses to ecdysone stimuli in the same developmental process. It has been proposed that this specificity is mostly due to their distinct temporal and spatial expression patterns (*Kim et al.*, 1999; *Robinow et al.*, 1993; *Sung and Robinow*, 2000; *Talbot et al.*, 1993; *Truman et al.*, 1994).

Consistent with this, I found that *EcR-A* knockdown throughout oogenesis using an RNAi approach does not affect egg chamber development. The function of EcR-A in this process seems to be required after mid-oogenesis, when the formation of eggshell

appendages starts. This consideration arises from the finding that *EcR-A* knockdown stages 14 exhibit dorsal appendages shorter and flattened compared to wild type ones.

In light of these data, it is reasonable to hypothesize that also during oogenesis EcR-A and EcR-B1 have distinct functions. It has been shown that the expression profile of these two proteins is similar throughout oogenesis, being present in both germline and somatic cells (*Carney and Bender*, 2000). This raises the possibility that in this process the unique function of the different EcR isoforms is dependent on the distinct biochemical properties of their isoform-specific amino terminal domains containing different AF domains that afterward regulate the transcription of different target genes.

***ecd* knock down causes apoptosis-induced compensatory proliferation in imaginal discs:** *ecd* ^{l23} loss-of-function and *ecd* RNAi clonal analysis in eye and wing imaginal discs shows that in both cases clones are few and very small and, as PH3 staining revealed, these cells fail to proliferate. Moreover, *ecd* RNAi clones disappeared within 72 hours after induction. These data suggest that cells lacking *ecd* cannot go through mitosis and thus *ecd* function in wing and eye imaginal disc cells could be required in cell cycle and proliferation control.

An *ecd* RNAi clonal analysis in wing discs showed that PH3-positive cells are found mainly at the outer border of the clones, hinting that wild type cells close to the clones undergo compensatory proliferation.

This activity is a fundamental property of epithelia that allows to compensate for cell loss resulting from any kind of injury. Indeed, in response to tissue damage unaffected epithelial cells are stimulated to proliferate to maintain the integrity of the epithelium and the final organ size (*Haynie and Bryant*, 1977).

Caspase-3 activity is detected in *ecd* knockdown wing discs. Moreover, cell death mostly occurs in the wing pouch in the proximity of the anterior/posterior border, where mutant and normal tissues are in close contact. In light of that, it is likely to presume that *ecd* silencing causes cell death which in turn induces compensatory proliferation of neighboring cells.

Moreover, the phenomenon of apoptosis-induced compensatory proliferation implies additional divisions of surviving cells after the apoptotic stimulus, in order to restore the normal tissue size. Hence at the same time the stress event eliminates a large number of cells and also generates a stimulus to proliferate (*Perez-Garijo et al.,* 2004; *Ryoo et al.,* 2004).

In agreement with this consideration, PH3 staining of *ecd* depleted wing discs reveals that cells in the wing pouch increase their proliferation rate, as the higher number of PH3 positive spots showed, compared to the other regions of the tissue.

Immunostaining analyses with JNK and Wg antibodies show that strong JNK activity and increased levels of Wg protein are detected in these discs. These findings are in agreement with previous studies on compensatory proliferation in imaginal discs (*Ryoo et al.,* 2004; *Werner et al.,* 2010) confirming the key role in this process of the JNK pathway in promoting the induction of pro-apoptotic genes. Moreover, surrounding wild type neighboring cells express high levels of Myc protein, as immunostaining with a Myc specific antibody shows.

Altogether these data indicate that *ecd* plays a key role in imaginal disc development. A possible model that could explain *ecd* function states that its depletion in wing disc cells, especially in the wing pouch, causes strong JNK activation (Figure 39). The increased activity of JNK induces on the one hand caspase-3 activation leading apoptosis of *ecd* knock down cells. On the other hand promotes the upregulation of Wg protein levels and the subsequent secretion of this morphogen in unaffected cells. Wg high levels induce elevated Myc expression in the surrounding cells promoting regenerative growth in order to save tissue size and integrity.

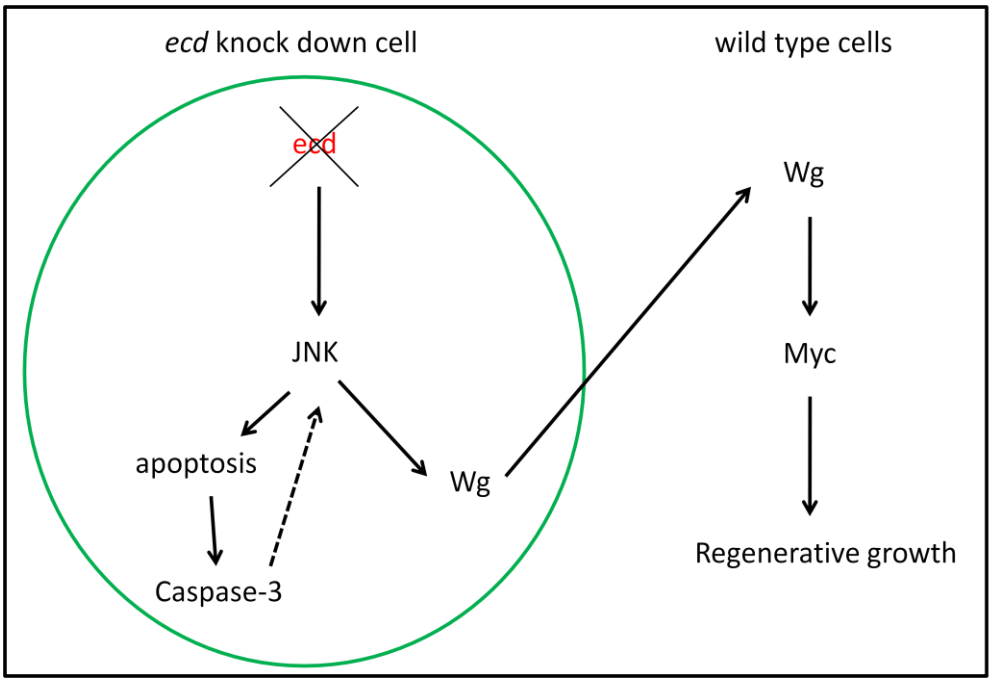

Figure 39: **Proposed model of ecd mechanism for the induction of compensatory proliferation and regenerative growth of wing disc cells.**

In summary, my analyses show that disruption of ecdysone-dependent pathway in imaginal disc morphogenesis and during oogenesis causes apoptotic cell death indicating that in these processes the hormone plays a key role in cell survival and in maintenance of tissue integrity. In imaginal wing discs, ecdysone-dependent cascade inhibition through *ecd* function depletion triggers the non-autonomous mechanism of compensatory proliferation.

6-Bibliografy

Abdelilah-Seyfried S., Cox D.N. and Jan Y.N., 2003 Bazooka is a permissive factor for the invasive behavior of discs large tumor cells in *Drosophila* ovarian follicular epithelia. *Development,* 130(9):1927-1935;

Affolter M. and Basler K., 2007 The Decapentaplegic morphogen gradient: from pattern formation to growth regulation. *Nat. Rev. Genet.,* 8:663-674;

Agrawal N., Kango M., Mishra A. and Sinha P., 1995 Neoplastic transformation and aberrant cell-cell interactions in genetic mosaics of lethal(2)giant larvae (lgl), a tumor suppressor gene of Drosophila. *Dev. Biol.*, 172(1):218-229;

Albertson R. and Doe C.Q., 2003 Dlg, Scrib and Lgl regulate neuroblast cell size and mitotic spindle asymmetry. *Nat. Cell Biol.*, 5(2):166-170;

Baker N.E. and Zitron A.E., 1995 *Drosophila* eye development: Notch and Delta amplify a neurogenic pattern conferred on the morphogenetic furrow by Scabrous. *Mech. Dev., 4*9:173-189;

Bai J., Uehara Y. and Montell D.J., 2000 Regulation of invasive cell behavior by Taiman, a *Drosophila* protein related to AIB1, a steroid receptor coactivator amplified in breast cancer. *Cell,* 103:1047-1058;

Bate M. and Martinez-Arias A., 1991 The embryonic origin of imaginal discs in *Drosophila*. *Development*, 112:755-761;

Baum J.S., Arama E., Steller H. and McCall K., 2007 The *Drosophila* caspases Strica and Dronc function redundantly in programmed cell death during oogenesis. *Cell Death Differ.,* 14:1508-1517;

Beccari S., Teixeira L. and Rørth P., 2002 The JAK/STAT pathway is required for border cell migration during *Drosophila* oogenesis. *Mech. Dev*., 111(1-2):115-123;

Bender M., Imam F.B., Talbot W.S., Ganetzky B. and Hogness D.S., 1997 *Drosophila* ecdysone receptor mutations reveal functional differences among receptor isoforms. *Cell,* 91:777-788;

Bernardi F., Romani P., Tzertzinis G., Gargiulo G. and Cavaliere V., 2009 EcR-B1 and Usp nuclear hormone receptors regulate expression of the *VM32E* eggshell gene during *Drosophila* oogenesis. *Dev. Biol.*, 328(2):541-551;

Bilder D., 2004 Epithelial polarity and proliferation control: links from the *Drosophila* neoplastic tumor suppressors. *Genes Dev.,* 18(16):1909-1925;

Bilder D., Schober M. and Perrimon N., 2003 Integrated activity of PDZ protein complexes regulates epithelial polarity. *Nat. Cell. Biol.*, 5(1):53-58;

Bilder D. and Perrimon N., 2000 Cooperative regulation of cell polarity and growth by *Drosophila* tumor suppressors. *Science,* 7;289(5476):113-116;

Bilder D., Li M. and Perrimon N., 2000 Cooperative regulation of cell polarity and growth by *Drosophila* tumor suppressors. *Science*, 289:113-116;

Blair S.S. and Ralston A., 1997 Smoothened-mediated Hedgehog signaling is required for the maintenance of the anterior-posterior lineage restriction in the developing wing of *Drosophila*. *Development*, 124:4053-4063;

Borg JP., 2004 hScrib: a potential novel tumor suppressor. *Pathol. Biol. (Paris)*, 52(6):328-331;

Bownes M., Ronaldson E. and Mauchline D., 1996 20-Hydroxyecdysone, but not juvenile hormone, regulation of yolk protein gene expression can be mapped to cis-acting DNA sequences. *Dev. Biol.*, 173(2):475-489;

Bownes M., 1989 The roles of juvenile hormone, ecdysone and the ovary in the control of *Drosophila* vitellogenesis. *J. Insect Physiol.*, 34:409-413;

Brand A.H. and Perrimon N., 1993 Targeted gene expression as a means of altering cell fates and generating dominant phenotypes. *Development*, 118:401-415;

Brook W.J. and Cohen S.M., 1996 Antagonistic interaction between Wingless and Decapentaplegic responsible for dorsal-ventral pattern in the *Drosophila* leg. *Science*, 273(5280), 1373-1377;

Brown N.H., 2000 Cell-cell adhesion via the ECM: integrin genetics in fly and worm. *Matrix Biol.*, 19(3):191-201;

Brown H.L.D., Cherbas L., Cherbas P. and Truman J., 2006 Use of time-lapse imaging and dominant negative receptors to dissect the steroid receptor control of neuronal remodelling in *Drosophila*. *Development*, 133(2), 275-285;

Burke R. and Basler K., 1996 Hedgehog-dependent patterning in the *Drosophila* eye can occur in the absence of Dpp signaling. *Dev. Biol.*, 179:360-368;

Buszczak M., Freeman M.R., Carlson J.R., Bender M., Cooley L. and Segraves W.A., 1999 Ecdysone response genes govern egg chamber development during mid-oogenesis in *Drosophila*. *Development*, 126(20):4581-4589;

Calvi B.R., Lilly M. A. and Spradling A.C., 1998 Cell cycle control of chorion gene amplification. *Genes Dev.*, *12*:734-744;

Carney G.E. and Bender M., 2000 The *Drosophila ecdysone receptor* (*EcR*) gene is required maternally for normal oogenesis. *Genetics*, 154:1203-1211;

Casares F. and Mann R.S., 1998 Control of antennal versus leg development in *Drosophila*. *Nature*., 392(6677):723-726;

Cavaliere V., Bernardi F., Romani P., Duchi S., and Gargiulo G., 2008 Building up the *Drosophila* eggshell: first of all the eggshell genes must be transcribed. Dev. Dyn., 237:2061-2072;

Cavaliere V., Taddei C. and Gargiulo G., 1998 Apoptosis of nurse cells at the late stages of oogenesis of *Drosophila melanogaster*. *Dev. Genes Evol.*, 208:106-112;

Cavodeassi F., Rodriguez I. and Modolell J., 2002 Dpp signaling is a key effector of the wing-body wall subdivision of the *Drosophila* mesothorax. *Development*, 117:597-608;

Chao S. and Nagoshi R.N., 1999 Induction of apoptosis in the germline and follicle layer of *Drosophila* egg chambers. *Mech. Dev.*, 88:159-172;

Cherbas L., Hu X., Zhimulev I., Belyaeva E. and Cherbas P., 2003 EcR isoforms in *Drosophila*: testing tissue-specific requirements by targeted blockade and rescue. *Development*, 130:271-284;

Cohen S.M., 1993 Imaginal disc development. 747-843. In: The development of Drosophila melanogaster. Bate M. And Hartenstein V., (editors). *Cold Spring Harbor Laboratories: Long Island NY*;

Colombani J., Bianchini L., Layalle S., Pondeville E., Dauphin-Villemant C., Antoniewski C., Carrè C., Noselli S. and Leopold P., 2005 Antagonistic actions of ecdysone and insulins determine final size in *Drosophila*. *Science*, 310:667-670;

Couso J.P., Bate M. and Martínez-Arias A., 1993 A wingless-dependent polar coordinate system in *Drosophila* imaginal discs. *Science*, 259(5094):484-489;

Cox D.N., Abdelilah-Seyfried S., Jan L.Y. and Jan Y.N., 2001 Bazooka and atypical protein kinase C are required to regulate oocyte differentiation in the *Drosophila* ovary. *Proc. Natl. Acad. Sci. USA*, 98:14475-14480;

Curtiss J. and Mlodzik M., 2000 Morphogenetic furrow initiation and progression during eye development in *Drosophila*: The roles of *decapentaplegic*, *hedgehog* and *eyes absent*. *Development*, 127:1325-1336;

Czerny T., Halder G., Kloter U., Souabni A., Gehring W.J. and Busslinger M., 1999 *twin of eyeless*, a second Pax-6 gene of *Drosophila*, acts upstream of eyeless in the control of eye development. *Mol. Cell*, 3(3):297-307;

Dai J.D. and Gilbert L.I., 1991 Metamorphosis of the corpus allatum and degeneration of the prothoracic glands during the larval-pupal-adult transformation of *Drosophila melanogaster*: a cytophysiological analysis of the ring gland. *Dev. Biol.*, 144(2):309-326;

Danial N.N., and Korsmeyer S.J., 2004 Cell death: critical control points. *Cell*, 116:205-219;

Davis M.B., Carney G.E., Robertson A.E. and Bender M., 2005 Phenotypic analysis of *EcR-A* mutants suggests that EcR isoforms have unique functions during *Drosophila* development. *Dev. Biol.,* 282(2):385-396;

Davis R.J., Tavsanli B.C., Dittrich C., Walldorf U. and Mardon G., 2003 *Drosophila* retinal homeobox (drx) is not required for establishment of the visual system, but is required for brain and clypeus development. *Dev. Biol.,* 259(2):272-287;

deCuevas M., Lilly M. and Mahowald A.P., 1990 Genetic analysis of two female-sterile loci affecting eggshell integrity and embryonic pattern formation in *Drosophila melanogaster*. *Genetics,* 126:427-434;

Deng W.M., Althauser C. and Ruohola-Baker H., 2001 Notch-Delta signaling induces a transition from mitotic cell cycle to endocycle in *Drosophila* follicle cells. *Development,* 128:4737-4746;

Deng W.M. and Bownes M., 1997 Two signalling pathways specify localised expression of the Broad-Complex in *Drosophila* eggshell patterning and morphogenesis. *Development,* 124(22):4639-4647;

Dobens L.L. and Raftery L.A. 2000 Integration of epithelial patterning and morphogenesis in *Drosophila* ovarian follicle cells. *Dev. Dynamics*, *218*:80-93;

Diaz-Benjumea F.J. and Cohen S.M., 1993 Interaction between dorsal and ventral cells in the imaginal disc directs wing development in *Drosophila*. *Cell,* 75:741-752;

DiNardo S., Kuner J.M., Theis J., O'Farrell P.H., 1985 Development of embryonic pattern in *D. melanogaster* as revealed by accumulation of the nuclear engrailed protein. *Cell,* 43(1):59-69;

Fernandes-Alnemri T., Litwack G. and Alnemri E.S., 1994 CPP32, a novel human apoptotic protein with homology to *Caenorhabditis elegans* cell death protein Ced-3 and mammalian interleukin-1 beta-converting enzyme. *J. Biol. Chem.,* 269(49):30761-30764;

Fernández-Miñán A., Martín-Bermudo M.D. and González-Reyes A., 2007 Integrin signaling regulates spindle orientation in Drosophila to preserve the follicular epithelium monolayer. *Curr. Biol.,* 17(8):683-688;

Fernández-Miñán A., Cobreros L., González-Reyes A. and Martín-Bermudo M.D., 2008 Integrins contribute to the establishment and maintenance of cell polarity in the follicular epithelium of the Drosophila ovary. *Int. J. Dev. Biol.,* 52(7):925-932;

Fessler J.H. and Fessler L.I., 1989 Drosophila extracellular matrix. *Annu. Rev. Cell Biol*, 5:309-339;

Flores G.V., Duan H., Yan H., Nagaraj R., Fu W., Zou Y., Noll M. and Banerjee U., 2000 Combinatorial signaling in the specification of unique cell fates. *Cell,* 103:75-85;

Foley K. and Cooley L., 1998 Apoptosis in late stage *Drosophila* nurse cells does not require genes within the H99 deficiency. *Development*, 125:1075-1082;

Freeman M., 1996 Reiterative use of the EGF receptor triggers differentiation of all cell types in the *Drosophila* eye. *Cell,* 87:651-660;

Fristrom D. and Fristrom J.W., 1993 The metamorphic development of the adult epidermis. 842-898. In: The development of *Drosophila melanogaster*. Bate M. And Martinez-Arias A., (editors). *Cold Spring Harbor Laboratory Press*;

Fuller M.T. and Spradling A.C., 2007 Male and female *Drosophila* germline stem cells: two versions of immortality. *Science*, 316, 402–404;

Gallant P., Shiio Y., Cheng P.F., Parkhurst S.M. and Eisenman R.N., 1996 Myc and Max homologs in *Drosophila*. *Science,* 274(5292):1523-1527;

Garcia-Bellido A. And Merriam J.R., 1971 Parameters of the wing imaginal disc development of *Drosophila melanogaster*. *Dev. Biol.,* 24:251-253;

Garen A., Kauvar L. and Lepesant J.A., 1977 Roles of ecdisone in *Drosophila* development. *Proc. Natl. Acad. Sci. USA,* 74(11):5099-5103;

Gavrieli Y., Sherman Y. and Ben-Sasson B.A., 1992 Identification of programmed cell death in situ via specific labeling of nuclear DNA fragmentation. *J. Cell Biol.,* 119(3):493-501;

Gaziova I., Bonnette P.C., Henrich V.C. and Jindra M., 2004 Cell-autonomous roles of the *ecdysoneless* gene in *Drosophila* development and oogenesis. *Development,* 131(11):2715-2725;

Gehring W.J., 2002 The genetic control of eye development and its implications for the evolution of the various eye-types. *Int. J. Dev. Biol.,* 46(1):65-73;

Geisbrecht E.R. and Montell D.J., 2004 A role for *Drosophila* IAP1- mediated caspase inhibition in Rac-dependent cell migration. *Cell,* 118:111-125;

Gilbert L.I., 2004 *Halloween* genes encode P450 enzymes that mediate steroid hormone biosynthesis in *Drosophila melanogaster*. *Mol. Cell Endocrinol.,* 27;215(1-2):1-10;

Gilbert L.I., Rybczynski R. and Warren J.T., 2002 Control and biochemical nature of the ecdysteroidogenic pathway. *Annu. Rev. Entomol.,* 47:883-916;

Glover J.C., 1991 Inductive events in the neural tube. *Trends Neurosci.,* 14(10):424-427;

Godt D. and Tepass U., 1998 *Drosophila* oocyte localization is mediated by differential cadherin-based adhesion. *Nature,* 395:387-391;

Golic K.G., 1991 Site-specific recombination between homologous chromosomes in *Drosophila*. *Science*, 252(5008):958-961;

Gómez-Skarmeta J.L., Campuzano S. and Modolell J., 2003 Half a century of neural prepatterning: the story of a few bristles and many genes. *Nat. Rev. Neuroscience*, 4:587-598;

Gonzalez-Reyes A. and St. Johnston D., 1998 The *Drosophila* AP axis is polarised by the cadherin-mediated positioning of the oocyte. *Development*, 125:3635-3644;

Goode S., Melnick M., Chou T.B. and Perrimon N., 1996 The neurogenic genes *egghead* and *brainiac* define a novel signaling pathway essential for epithelial morphogenesis during *Drosophila* oogenesis. *Development*, 122(12):3863-3879;

Goyal L., McCall K., Agapite J., Hartwieg E. and Steller H., 2000 Induction of apoptosis by *Drosophila reaper*, *hid* and *grim* through inhibition of IAP function. *Embo J.*, 19:589-597;

Grammont M. and Irvine K.D., 2002 Organizer activity of the polar cells during *Drosophila* oogenesis. *Development*, 129(22):5131-5140;

Hackney J.F., Pucci C., Naes E. and Dobens L., 2007 Ras signaling modulates activity of the Ecdysone Receptor EcR during cell migration in the *Drosophila* ovary. *Dev. Dyn.*, 236:1213-1226;

Hagedorn H.H., 1985 The role of ecdysteroids in reproduction. *Comprehensive Insect Physiology, Biochemistry and Pharmacology*, 8, 205-261;

Haynie J.L. and Bryant P.J., 1976 Intercalary regeneration in imaginal wing disk of *Drosophila melanogaster*. *Nature*, 259(5545):659-662;

Heberlein U., Hariharan I.K. and Rubin G.M., 1993 *Star* is required for neuronal differentiation in the *Drosophila* retina and displays dosage-sensitive interactions with *ras1*. *Dev. Biol.*, 160:51-63;

Heberlein U., Singh C.M., Luk A.Y. and Donohoe T.J., 1995 Growth and differentiation in the *Drosophila* eye coordinated by *hedgehog*. *Nature*, 373:709-711;

Heberlein U. and Moses K., Mechanisms of *Drosophila* retinal morphogenesis: The virtues of being progressive. *Cell*, 81:987-990;

Henrich V.C., Szekely A.A., Kim S.J., Brown N.E., Antoniewski C., Hayden M.A., Lepesant J.A. and Gilbert L.I., 1994 Expression and function of the *ultraspiracle (usp)* gene during development of *Drosophila melanogaster*. *Dev. Biol.*, 165(1):38-52;

Henrich V.C., Livingston L., Gilbert L.I., 1993 Developmental requirements for the ecdysoneless (ecd) locus in *Drosophila melanogaster*. *Dev. Genet.*, 14(5):369-377;

Henrich V.C., Sliter T.J., Lubahn D.B., MacIntyre A. and Gilbert L.I., 1990 A steroid/thyroid hormone receptor superfamily member in *Drosophila melanogaster* that

shares extensive sequence similarity with a mammalian homologue. *Nucleic Acids Res.*, 18(14):4143-4148;

Horne-Badovinac S. and Bilder D., 2005 Mass transit: epithelial morphogenesis in the Drosophila egg chamber. *Dev. Dyn.*, 232:559-574;

Hou Y.C., Chittaranjan S., Barbosa S.G., McCall K. and Gorski S.M., 2008 Effector caspase Dcp-1 and IAP protein Bruce regulate starvation-induced autophagy during Drosophila melanogaster oogenesis. J. Cell Biol., 182(6):1127-1139;

Hu Z., Cherbas L. and Cherbas P., 2003 Transcription activation by the ecdysone receptor (EcR/USP): identification of activation functions. *Molecular Endocrinology*, 17(4):716-731;

Huang Z. and Kunes S., 1996 Hedgehog, transmitted along retinal axons, triggers neurogenesis in the developing visual centers of the *Drosophila* brain. Cell, 86:411-422;

Hutterer A., Betschinger J., Petronczki M. and Knoblich J.A., 2004 Sequential roles od Cdc42, Par-6, aPKC and Lgl in the establishment of epithelial polarity during *Drosophila* embryogenesis. *Dev. Cell*, 6:845-854;

Imhof A., Yang X.J., Ogryzko V.V., Nakatani Y., Wolffe A.P. and Ge H., 1997 Acetylation of general transcription factors by histone acetyltransferases. *Curr. Biol.*, 7:689-692;

Jarman A.P., Sun Y., Jan L.Y. and Jan Y.N., 1995 Role of the proneural gene, *atonal*, in formation of *Drosophila* chordotonal organs and photoreceptors. *Development*, 121:2019-2030;

Kainou T., Shinzato T., Sasaki K., Mitsui Y., Giga-Hama Y., Kumagai H. and Uemura H., 2006 *Spsgt1*, a new essential gene of *Schizosaccharomyces pombe*, is involved in carbohydrate metabolism. *Yeast*, 23:35-53;

Keller Larkin M., Deng W.M., Holder K., Tworoger M., Clegg N. and Ruohola-Baker H., 1999 Role of Notch pathway in terminal follicle cell differentiation during Drosophila oogenesis. *Dev. Genes Evol.*, 209(5):301-311;

Kennerdell J.R. and Carthew R.W., 2000 Heritable gene silencing in *Drosophila* using double-stranded RNA. *Nat. Biotechnol.*, 18:896-898;

Kenyon K.L., Ranade S.S., Curtiss J., Mlodzik M. and PIGNONI F., 2003 Coordinating proliferation and tissue specification to promote regional identity in the *Drosophila* head. *Dev. Cell*, 5:403-414;

Kim J.H., Gurumurthy C.B., Band H. and Band V., 2010 Biochemical characterization of human Ecdysoneless reveals a role in transcriptional regulation. *Biol. Chem.*, 391(1):9-19;

Kim J.H., Gurumurthy C.B., Naramura M., Zhang Y., Dudley A.T., Doglio L., Band H. and Band V., 2009 Role of mammalian Ecdysoneless in cell cycle regulation. *J. Biol. Chem.,* 284(39):26402-26410;

King R.C., 1970 Ovarian development in *Drosophila melanogaster*. *Academic Press, New York, London and San Francisco*;

Knust E., 2002 Regulation of epithelial cell shape and polarity by cell-cell adhesion. *Mol. Membr. Biol.,* 19:113-120;

Knust E. and Bossinger O., 2002 Composition and formation of intercellular junctions in epithelial cells. *Science,* 298(5600):1955-1959;

Koelle M.R., 1992 Molecular analysis of the *Drosophila* ecdysone receptor complex. Ph.D. thesis, Stanford University, Stanford, CA;

Koelle M.R., Talbot W.S., Segraves W.A., Bender M.T., Cherbas P. and Hogness D.S., 1991 The *Drosophila EcR* gene encodes an ecdysone receptor, a new member of the steroid receptor superfamily. *Cell,* 4;67(1):59-77;

Kozlova T. and Thummel C.S., 2000 Steroid regulation of postembryonic development and reproduction in Drosophila. *Trends Endocrinol. Metab.,* 11(7):276-280;

Kumar J.P. and Moses K., 2001 The EGF receptor and Notch signaling pathways control the initiation of the morphogenetic furrow during *Drosophila* eye development. *Development,* 128:2689-2697;

Lee J.K., Brandin E., Branton D. and Goldstein L.S., 1997 Alpha-Spectrin is required for ovarian follicle monolayer integrity in *Drosophila melanogaster*. *Development*., 124(2):353-362;

Lee T. and Luo L., 1999 Mosaic analysis with a repressible cell marker for studies of gene function in neuronal morphogenesis. *Neuron.,* 22:451–461;

Lin H. and Spradling A., 1993 Germ line stem cell division and egg chamber development in transplanted *Drosophila* germaria. *Dev. Biol.,* 159:140-152;

López-Schier H., 2003 The polarisation of the anteroposterior axis in *Drosophila*. *Bioessays,* 25(8):781-791;

Ma C., Zhou Y., Beachy P.A. and Moses K., 1993 The segment polarity gene *hedgehog* is required for progression of the morphogenetic furrow in the developing *Drosophila* eye. *Cell,* 75:927-938;

McCall K., 2004 Eggs over easy: cell death in the *Drosophila* ovary. *Dev. Biol.,* 274:3-14;

McGuire S.E., Le P.T., Osborn A.J., Matsumoto K. and Davis R.L., 2003 Spatiotemporal rescue of memory dysfunction in *Drosophila*. *Science,* 302:1765-1768;

Mahadevan L.C., Willis A.C. and Barratt M.J., 1991 Rapid histone H3 phosphorylation in response to growth factors, phorbol esters, okadaic acid, and protein synthesis inhibitors. *Cell*, 65(5):775-783;

Mangelsdorf D.J., Thummel C., Beato M., Herrlich P., Schütz G., Umesono K., Blumberg B., Kastner P., Mark M., Chambon P. and Evans R.M., 1995 The nuclear receptor superfamily: the second decade. *Cell*, 83(6):835-839;

Mazumdar A. and Mazumdar M., 2002 How one becomes many: blastoderm cellularization in *Drosophila melanogaster*. *Bioessays*, 24:1012-1022;

Miller D.T. and Cagan R.L.,1998 Local induction of patterning and programmed cell death in the developing *Drosophila* retina. *Development*, 125:2327-2335;

Morata G. and Lawrence P.A., 1975 Control of compartment development by the engrailed gene in *Drosophila*. *Nature*, 255:614-617;

Morrison S.J. and Spradling A.C., 2008 Stem cells and niches: mechanisms that promote stem cell maintenance throughout life. *Cell*, 132, 598–611;

Mouillet J.F., Henrich V.C., Lezzi M. and Vögtli M., 2001 Differential control of gene activity by isoforms A, B1 and B2 of the *Drosophila* ecdysone receptor. *Eur. J. Biochem.*, 268(6):1811-9;

Müller H.A. and Bossinger O., 2003 Molecular networks controlling epithelial cell polarity in development. *Mech. Dev.*, 120:1231-1256;

Müller H.A., 2000 Genetic control of epithelial cell polarity: lessons from *Drosophila*. *Dev. Dyn.*, 218(1):52-67;

Nagaraj R. and Banerjee U., 2007 Combinatorial signaling in the specification of primary pigment cells in the *Drosophila* eye. *Development*, 134:825-831;

Neubueser D., Warren J.T., Gilbert L.I. and Cohen S.M., 2005 *molting defective* is required for ecdysone biosynthesis. *Developmental Biology*, 280:362-372;

Neumann C.J. and Cohen S.M., 1996 A hierarchy of cross-regulation involving Notch, wingless, vestigial and cut organizes the dorsal/ventral axis of the *Drosophila* wing. *Development*, 122(11):3477-3485;

Nezis I.P., Stravopodis D.J., Papassideri I.S., Robert-Nicoud M. and Margaritis L.H., 2002 Dynamics of apoptosis in the ovarian follicle cells during the late stages of *Drosophila* oogenesis. *Cell Tissue Res.*, 307:401-409;

Nijhout H.F., 1994 Genes on the wing. *Science*, 265(5168):44-45;

Niwa N., Hiromi Y. and Okabe M., 2004 A conserved developmental program for sensory organ formation in *Drosophila melanogaster*. *Nat. Genet.*, 36:293-297;

Oda H., Uemura T. and Takeichi M., 1997 Phenotypic analysis of null mutants for DEcadherin and Armadillo in *Drosophila* ovaries reveals distinct aspects of their functions in cell adhesion and cytoskeletal organization. *Genes Cells*, 2(1):29-40;

Oda H., Uemura T., Harada Y., Iwai Y. and Takeichi M. 1994 A *Drosophila* homolog of cadherin associated with armadillo and essential for embryonic cell-cell adhesion. *Dev. Biol.,* 165(2):716-726;

Ohno S., 2001 Intercellular junctions and cellular polarity: the PAR-aPKC complex, a conserved core cassette playing fundamental roles in cell polarity. *Curr. Opin. Cell Biol*., 13(5):641-648;

Ohshiro T., Yagami T., Zhang C. and Matsuzaki F., 2000 Role of cortical tumoursuppressor proteins in asymmetric division of *Drosophila* neuroblast. *Nature*, 408(6812):593-596;

O'Donnell K.H., Chen C.T. and Wensink P.C., 1994 Insulating DNA directs ubiquitous transcription of the *Drosophila melanogaster α1-tubulin* gene. *Molecular and Cellular Biology,* 14(9):6398-6408;

Oro A.E., McKeown M. and Evans R.M., 1990 Relationship between the product of the *Drosophila* ultraspiracle locus and the vertebrate retinoid X receptor. *Nature*, 347(6290):298-301;

Panin V.M., Papayannoupolos V., Wilson R. and Irvine K.D., 1997 Fringe modulates Notch-ligand interactions. *Nature*, 387:908-912;

Parnas D., Haghighi A.P., Fetter R.D., Kim S.W. and Goodman C.S., 2001 Regulation of postsynaptic structure and protein localization by the Rho-type guanine nucleotide exchange factor dPix. *Neuron,* 32(3):415-424;

Peifer M., Orsulic S., Sweeton D. and Wieschaus E., 1993 A role for the *Drosophila* segment polarity gene *armadillo* in cell adhesion and cytoskeletal integrity during oogenesis. *Development,* 118:1191-1207;

Peng C.Y., Manning L., Albertson R. and Doe C.Q., 2000 The tumour-suppressor genes *lgl* and *dlg* regulate basal protein targeting in *Drosophila* neuroblasts. *Nature*, 408(6812):596-600;

Perez-Garijo A., Shlevkov E. and Morata G., 2009. The role of Dpp and Wg in compensatory proliferation and in the formation of hyperplastic overgrowths caused by apoptotic cells in the *Drosophila* wing disc. *Development,* 136, 1169-1177;

Persson U., Izumi H., Souchelnytskyi S., Itoh S., Grimsby S., Engstrom U., Heldin C.H., Funa K. and ten Dijke P., 1998. The L45 loop in type I receptors for TGF-beta family members is a critical determinant in specifying Smad isoform activation. *FEBS Lett.,* 434, 83–87;

Peterson J.S., Barkett M. and McCall K., 2003 Stage-specific regulation of caspase activity in *Drosophila* oogenesis. *Dev. Biol.,* 260:113-123;

Pignoni F. and Zipursky S.L., 1997 Induction of *Drosophila* eye development by Decapentaplegic. *Development,* 124:271-278;

Pritchett T.L., Tanner E.A. and McCall K., 2009 Cracking open cell death in the *Drosophila* ovary. *Apoptosis,* 14(8):969-979;

Queenan A.M., Ghabrial A. and Schupbach T., 1997 Ectopic activation of torpedo/Egfr, a *Drosophila* receptor tyrosine kinase, dorsalizes both the eggshell and the embryo. *Development,* 124:3871-3880;

Quondamatteo F., 2002 Assembly, stability and integrity of basement membranes *in vivo*. *Histochem. J.,* 34(8-9):369-381;

Ray R.P. and Schüpbach T., 1996 Intercellular signalling and the polarization of body axes during *Drosophila* oogenesis. *Genes Dev.,* 10:1711-1723;

Riddiford L.M., Cherbas P. and Truman J.W., 2000 Ecdysone receptors and their biological actions. *Vitam. Horm.,* 60:1-73;

Riddiford L.M., 1993 Hormones and Drosophila development. In The Development of *Drosophila melanogaster* (Bate M. and Martinez-Arias A.), pp. 899–939;

Riddihough G. and Pelham H.R., 1987 An ecdysone response element in the *Drosophila hsp27* promoter. *EMBO J.,* 6(12):3729-3734;

Riddihough G. and Pelham H.R., 1986 Activation of the *Drosophila hsp27* promoter by heat shock and by ecdysone involves independent and remote regulatory sequences. *EMBO J.,* 5(7):1653-1658;

Riggleman B., Schedl P. and Wieschaus E., 1990 Spatial expression of the *Drosophila* segment polarity gene armadillo is posttranscriptionally regulated by wingless. *Cell,* 63(3):549-560;

Robertson K., Mergliano J., Minden J.S., 2003 Dissecting *Drosophila* embryonic brain development using photoactivated gene expression. *Dev. Biol.,* 260(1):124-137;

Robinow S., Talbot W.S., Hogness D.S. and Truman J.W., 1993 Programmed cell death in the *Drosophila* CNS is ecdysone-regulated and coupled with a specific ecdysone receptor isoform. *Development,* 119(4):1251-1259;

Roignant J.Y., Carrè C., Mugat B., Szymczak D., Lepesant J.A. and Antoniewski C., 2003 Absence of transitive and systemic pathways allows cell-specific and isoform-specific RNAi in *Drosophila. RNA,* 9:299-308;

Roignant J.Y. and Treisman J.E., 2009 Pattern formation in the *Drosophila* eye disc. *Int. J. Dev. Biol.,* 53(5-6):795-804;

Roman G., 2004 The genetics of *Drosophila* transgenics. *BioEssays,* 26:1243–1253;

Romani P., Bernardi F., Hackney J., Dobens L., Gargiulo G. and Cavaliere V., 2009 Cell survival and polarity of *Drosophila* follicle cells require the activity of ecdysone receptor B1 isoform. *Genetics*, 181(1):165-175;

Rübsam R., Hollmann M., Simmerl E., Lammermann U., Schäfer M.A., Büning J. and Schäfer U., 1998 The *egghead* gene product influences oocyte differentiation by follicle cell-germ cell interactions in *Drosophila melanogaster*. *Mech. Dev.*, 7:131-140;

Ruohola H., Bremer K.A., Baker D., Swedlow J.R., Jan L.Y. and Jan Y.N., 1991 Role of neurogenic genes in establishment of follicle cell fate and oocyte polarity during oogenesis in *Drosophila*. *Cell*, 66(3):433-449;

Ryoo H.D., Gorenc T. and Steller H., 2004. Apoptotic cells can induce compensatory cell proliferation through the JNK and the Wingless signaling pathways. *Dev. Cell*, 7, 491–501;

Sato T., Jigami Y., Suzuki T. and Uemura H., 1999 A human gene, *hSGT1*, can substitute for GCR2, which encodes a general regulatory factor of glycolitic gene expression in *Saccharomyces cerevisiae*. *Mol. Gen. Genet.*, 260:535-540;

Scherer L.J., Harris D.H. and Petri W.H., 1988 *Drosophila* vitelline membrane genes contain a 114 bp region of highly conserved coding sequence. *Dev. Biol.*, 130:786-788;

Schober M., Rebay I. and Perrimon N., 2005 Function of the ETS transcription factor Yan in border cell migration. *Development*, 132(15):3493-3504;

Schubiger M., Wade A.A., Carney G.E., Truman J.W. and Bender M., 1998 *Drosophila* EcR-B ecdysone receptor isoforms are required for larval molting and for neuron remodelling during metamorphosis. *Development*, 125:2053-2062;

Schubiger M., Carrè C., Antoniewski C. and Truman J.W., 2005 Ligand-dependent de-repression via EcR/USP acts as a gate to coordinate the differentiation of sensory neurons in the *Drosophila* wing. *Development*, 132:5239-5248;

Shea M.J., King D.L., Conboy M.J., Mariani B.D. and Kafatos F.C., 1990 Proteins that bind to *Drosophila* chorion *cis*-regulatory elements: a new C2H2 zinc finger protein and a C2C2 steroid receptor-like component. *Genes Dev.*, 4(7):1128-1140;

Silver S.J. and Rebay I., 2005 Signaling circuitries in development: Insights from the retinal determination gene network. *Development*, 132:3-13;

Sliter T.J., Henrich V.C., Tucker R.L. and Gilbert L.I., 1989 The genetics of the Dras3-Roughened-ecdysoneless chromosomal region (62B3-4 to 62D3-4) in *Drosophila melanogaster*: analysis of recessive lethal mutations. *Genetics*, 123(2):327-336;

Sotillos S., Díaz-Meco M.T., Caminero E., Moscat J. and Campuzano S., 2004 DaPKC dependent phosphorylation of Crumbs is required for epithelial cell polarity in *Drosophila*. *J. Cell Biol.*, 166(4):549-557;

Spradling A.C., 1993 Developmental genetics of oogenesis. In the development of

Drosophila melanogaster. Volume 1 (M. Bate and A. Martinez Arias, eds.). *Cold Spring Harbor, New York: Cold Spring Harbor Laboratory Press*, pp. 1-70;

Steller H., 2008 Regulation of apoptosis in *Drosophila*. *Cell Death Differ.,* 15:1132-1138;

Sun J, Smith L, Armento A, Deng WM., 2008 Regulation of the endocycle/gene amplification switch by Notch and ecdysone signaling. *J. Cell Biol.,* 182(5):885-896;

Sung C. and Robinow S., 2000 Characterization of the regulatory elements controlling neuronal expression of the A-isoform of the *ecdysone receptor* gene of *Drosophila* melanogaster. *Mech. Dev.,* 91(1-2):237-248;

Szafranski P. and Goode S., 2007 Basolateral junctions are sufficient to suppress epithelial invasion during *Drosophila* oogenesis. *Dev. Dyn.,* 236(2):364-373;

Takai, Y., Kishimoto A., Iwasa Y., Kawahara Y., Mori T., Nishizuka Y., 1979 Calcium-dependent activation of a multifunctional protein kinase by membrane phospholipids. *J. Biol. Chem.,* 254: 3692-3695;

Talbot W.S., Swyryd E.A. and Hogness D.S., 1993 *Drosophila* tissues with different metamorphic responses to ecdysone express different ecdysone receptor isoforms. *Cell*, 2;73(7):1323-37;

Tanentzapf G. and Tepass U., 2003 Interactions between the crumbs, lethal giant larvae and bazooka pathways in epithelial polarization. *Nat. Cell. Biol*., 5(1):46-52;

Tanentzapf G., Smith C., McGlade J. and Tepass U., 2000 Apical, lateral, and basal polarization cues contribute to the development of the follicular epithelium during *Drosophila* oogenesis. *J. Cell Biol*., 151(4):891-904;

Tepass U., Tanentzapf G., Ward R. and Fehon R., 2001 Epithelial cell polarity and cell junctions in *Drosophila*. *Annu. Rev. Genet.,* 35:747-784;

Tepass U., 1999 Genetic analysis of cadherin function in animal morphogenesis. *Curr. Opin. Cell Biol*., 11(5):540-548;

Tepass U., 1997 Epithelial differentiation in Drosophila. *Bioessays*, 19(8):673-682;

Tepass U., Theres C. and Knust E., 1990 Crumbs encodes an EGF-like protein expressed on apical membranes of *Drosophila* epithelial cells and required for organization of epithelia. *Cell*, 61(5):787-799;

Terashima J. and Bownes M., 2005(a) E75A and E75B have opposite effects on the apoptosis/development choise of the *Drosophila* egg chamber. *Cell Death and Differentiation*;

Terashima J. and Bownes M., 2005 (b) A microarray analysis of genes involved in relating egg production to nutritional intake in *Drosophila*. *Cell Death and Differentiantion*, 12:429-440;

Terashima J., Takaki K. and Bownes M., 2005 (c) Nutritional status 20-hydroxyecdysone concentration and progression of oogenesis in *Drosophila melanogaster*. *J. Endocrinology*, 187:69-79;

Terashima J. and Bownes M., 2004 Translating available food into the number of eggs laid by *Drosophila melanogaster*. *Genetics*, 167:1711-1719;

Thummel C.S., 1996 Files on steroids: *Drosophila* metamorphosis and the mechanisms of steroid hormone action. *Trends Genet*, 12(8):306-310;

Tomlinson A. and Ready D.F., 1987 Neuronal differentiation in the *Drosophila* ommatidium. *Dev. Biol.*, 120:366-376;

Tzolovsky G., Deng W.M., Schlitt T. and Bownes M., 1999 The function of the Broad-Complex during *Drosophila melanogaster* oogenesis. *Genetics*, 153(3):1371-1383;

Truman J.W., 1994 Ecdysone receptor expression in the CNS correlates with stage-specific responses to ecdysteroids during *Drosophila* and *Manduca* development. *Development*, 120(1):219-34;

Vasioukhin V., 2006 Lethal giant puzzle of Lgl. *Dev. Neurosci.*, 28(1-2):13-24;

Vo N. and Goodman R.H., 2001 CREB-binding protein and p300 in transcriptional regulation. *J. Biol. Chem.*, 276:13505-13508;

Wang S.L., Hawkins C.J., Yoo S.J., Muller H.A. and Hay B.A., 1999 The *Drosophila* caspase inhibitor DIAP1 is essential for cell survival and is negatively regulated by HID. *Cell*, 98:453-463;

Waring G.L., 2000 Morphogenesis of the eggshell in *Drosophila*. *Int. Rev. Cytol.*, 198:67-108;

Warren J.T., Yerushalmi Y., Shimell M.J., O'Connor M.B., Restifo L.L. and Gilbert L.I., 2006 Discrete pulses of molting hormone 20-hydroxyecdysone, during late larval development of *Drosophila melenogaster*: correlations with changes in gene activity. *Developmental Dynamics*, 235:315-326;

Warren J.T., Petryk A., Marqués G., Parvy J.P., Shinoda T., Itoyama K., Kobayashi J., Jarcho M., Li Y., O'Connor M.B., Dauphin-Villemant C. and Gilbert L.I., 2004 *Phantom* encodes the 25-hydroxylase of *Drosophila melanogaster* and Bombyx mori: a P450 enzyme critical in ecdysone biosynthesis. *Insect Biochem. Mol. Biol.*, 34(9):991-1010;

Warren J.T., Bachmann J.S., Dai J.D. and Gilbert L.I., 1996 Differential incorporation of cholesterol and cholesterol derivatives into ecdysteroids by the larval ring glands and adult ovaries of *Drosophila melanogaster*: a putative explanation for the *l(3)ecd1* mutation. *Insect Biochem. Mol. Biol.*, 26(8-9):931-493;

Warner S.J., Yashiro H. and Longmore G.D., 2010 The Cdc42/Par6/aPKC polarity complex regulates apoptosis-induced compensatory proliferation in epithelia. *Curr. Biol.,* 20:1-10;

Whiteland J.L., Nicholls S.M., Shimeld C., Easty D.L., Williams N.A. and Hill T.J., 1995 Immunohistochemical detection of T-cell subsets and other leukocytes in paraffin-embedded rat and mouse tissues with monoclonal antibodies. *J. Histochem. Cytochem.,* 43(3):313-320;

Whitmarsh A.J. and Davis R.J., 1998 Structural organization of MAP-kinase signaling modules by scaffold proteins in yeast and mammals. *Trends Biochem. Sci.,* 23(12):481-485;

Wirtz-Peitz F. and Knoblich J.A., 2006 Lethal giant larvae take on a life of their own. *Trends Cell Biol.,* 16(5):234-241;

Wodarz A., Ramrath A., Grimm A. and Knust E., 2000 *Drosophila* atypical protein kinase C associates with Bazooka and controls polarity of epithelia and neuroblasts. *J. Cell Biol*., 150(6):1361-1374;

Wolff T. and Ready D.F., 1991 The beginning of pattern formation in the *Drosophila* compound eye: The morphogenetic furrow and the second mitotic wave. *Development,* 113:841-850;

Wu J., and Cohen S.M., 2002 Repression of Teashirt marks the initiation of wing development. *Development*, 129:2411-2418;

Wu X., Tanwar P.S. and Raftery L.A., 2008 *Drosophila* follicle cells:morphogenesis in an eggshell. *Semin. Cell Dev. Biol.,* 19:271-282;

Wu P.S., Egger B. and Brand A.H., 2008 Asymmetric stem cell division: lessons from *Drosophila*. *Semin. Cell Dev. Biol.,* 19(3):283-293;

Xi R., McGregor J.R. and Harrison D.A., 2003 A gradient of JAK pathway activity patterns the anterior-posterior axis of the follicular epithelium. *Dev. Cell.*, 4(2):167-177;

Xu D., Li Y., Arcaro M., Lackey M. and Bergmann A., 2005 The CARD carrying caspase Dronc is essential for most, but not all, developmental cell death in *Drosophila*. *Development,* 132:2125-2134;

Xu T. and Rubin G.M., 1993 Analysis of genetic mosaics in developing and adult *Drosophila* tissues. *Development,* 117:1223-1237;

Yamanaka T. and Ohno S., 2008 Role of Lgl/Dlg/Scribble in the regulation of epithelial junction, polarity and growth. *Front. Biosci*., 13:6693-6707;

Yap A.S., Brieher W.M., Pruschy M. and Gumbiner B.M., 1997 Lateral clustering of the adhesive ectodomain: a fundamental determinant of cadherin function. *Curr. Biol.,* 7(5):308-315;

Yin V.P. and Thummel C.S., 2005 Mechanisms of steroid-triggered programmed cell death in *Drosophila*. Semin. *Cell Dev. Biol.,* 16:237-243;

Zhang Y., Chen J., Gurumurthy C.B., Kim J., Bhat I., Gao Q., Dimri G., Lee S.W., Band H. and Band V., 2006 The human orthologue of *Drosophila* ecdysoneless protein interacts with p53 and regulates its function. *Cancer Res.,* 66(14):7167-7175.

7-Summary

During my PhD research program I've been involved in a project focused on understanding the role of ecdysone signaling during *Drosophila melanogaster* development.

Ecdysone is a steroid hormone and its activity is mediated by a heterodimeric receptor composed of the Ecdysone Receptor, EcR (*Koelle et al.,* 1991; *Koelle,* 1992) and Ultraspiracle, USP (*Shea et al.,* 1990; *Oro et al.,* 1990) nuclear receptor proteins. *USP* encodes a single product, while *EcR* locus encodes three different isoforms, named EcR-A, EcR-B1 and EcR-B2. It has been proposed that EcR isoforms distinct temporal and spatial expression pattern is responsible of the different cellular responses to hormone stimuli. The EcR/USP heterodimer directly controls expression of early ecdysone response genes, which coordinate the subsequent transcription of tissue-specific late genes (*Ashburner et al.,* 1974; *Thummel,* 1996).

Ecdysone is responsible to regulate the major developmental transitions and understand how this single hormone can control different processes such as differentiation and programmed cell death in distinct tissues is a fascinating challenge.

In order to investigate the molecular mechanisms that allow this hormone to accomplish different and sometimes antagonistic functions in the same developmental process, I explored the effects of blocking ecdysone signaling during oogenesis and during imaginal disc development.

I analyzed the effect of ecdysone-cascade inhibition in follicular epithelium morphogenesis through silencing of its nuclear receptor gene, *EcR* taking advantage of a dominant negative form of this receptor (EcR-DN).

From my analysis, results evident that ecdysone signaling plays a key role in follicular epithelium maintenance throughout oogenesis. I found that disruption of hormone signaling overexpressing EcR-DN causes degeneration of the egg chambers at multiple steps. Furthermore, stage-specific and clonal expression of EcR-DN hampers proper migration of follicle cells causing an altered distribution of these cells on the surface of the egg chamber. In addition, I found that cells lacking EcR function exhibit reduced size and this finding may suggest an involvement of EcR in endoreplication control.

In the light of the results obtained expressing EcR-DN, in order to gain insight into the role of the different EcR isoforms during oogenesis, I specifically knock down EcR-B1 and EcR-A using an RNA interference approach.

I determined that *EcR-B1* specific knockdown at mid-oogenesis results in delamination of follicle cells and loss of follicular monolayer integrity (*Romani et al.,* 2009). Accordingly, polarity complex protein distribution results affected in cells lacking EcR-B1 function. The clonal analysis performed shows that targeted *EcR-B1* RNAi at early stages of oogenesis induces, beside loss of monolayer integrity, apoptotic cell death through caspase-3 activation. Altogether these results indicate that EcR-B1 function is required during oogenesis for cell survival and for maintenance of epithelial integrity.

Specific knockdown of *EcR-A* indicates that this isoform does not affect egg chamber development but its function is required in dorsal appendages formation.

These findings support the hypothesis that also during oogenesis ecdysone pleiotropic functions are ensured by the unique functions of EcR isoforms that trigger different responses to hormone stimuli. It has been shown that the expression profile of these two proteins is similar throughout oogenesis, being present in both germline and somatic cells (*Carney and Bender,* 2000). This may suggest that in this process the unique function of EcR-A and EcR-B1 is dependent on the biochemical properties of their isoform-specific amino terminal domains containing different AF domains that afterward regulate the transcription of distinct target genes.

In addition, during the period that I spent in Prof. Jindra's lab, I explored in imaginal discs morphogenesis the function of *ecd,* a gene involved in ecdysone signaling whose mutation affects ecdysone hormone production (*Garen et al.,* 1977).

In particular, I analyzed the effect of an *ecd* loss-of-function mutation in eye imaginal discs and the effect of *ecd* silencing through transgenic RNA interference in wing disc development.

ecd loss-of-function and *ecd* RNAi in clones of eye and wing imaginal discs affects proliferation of these cells.

In addition, specific *ecd* knockdown in the wing disc posterior compartment results in strong activation of caspase-3 and c-Jun terminal kinase (JNK) indicating that ecd is necessary for cell survival. Interestingly, I found elevated levels of Wg morphogen and Myc protein in the neighboring wild type cells indicating that these cells undergo compensatory proliferation to save tissue size and integrity.

In summary, my analyses on ecdysone signaling pathway function during follicular epithelium morphogenesis and in imaginal disc development show that the hormone plays a key role in cell survival and in maintenance of tissue integrity.